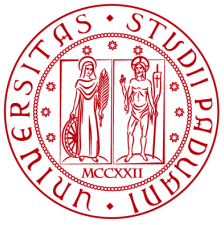

UNIVERSITÀ DEGLI STUDI DI PADOVA

DIPARTIMENTO DI INGEGNERIA DELL'INFORMAZIONE

Dipartimento di Ingegneria dell'Informazione

Corso di Laurea magistrale in Bioingegneria

Closed-loop control of anesthetic drugs administration: a comparison between PID and MPC

Relatore: Prof. Simone Del Favero

Correlatrice: Dott. ssa Eleonora Manzoni

Laureanda: Anastasia Borghi

Anno accademico: 2021-2022

Data di laurea: 14/07/2022

Contents

Sommario

Il controllo automatico dell'anestesia è una questione rilevante nella pratica clinica in quanto provvede ad una somministrazione sicura e personalizzata di farmaci anestetici, fornendo al tempo stesso vantaggi per gli anestesisti, come ad esempio la riduzione del carico di lavoro e la conseguente possibilità di focalizzarsi su compiti di alto livello e la gestione delle emergenze, e per i pazienti stessi, in quanto si minimizzerebbe la possibilità di errore umano, come il sottodosaggio o sovradosaggio accidentale. L'obiettivo di questa tesi è il confronto di due controllori per la somministrazione in closed-loop di farmaci anestetici. Questo lavoro beneficia dell'esistenza di un simulatore del paziente, implementato in Matlab&Simulink [1], che riceve in ingresso le dosi di farmaci anestetici e fornisce in uscita variabili anestetiche ed emodinamiche, tramite le quali è possibile monitorare gli effetti dell'anestesia nel paziente. Per l'implementazione del controllo automatico dell'anestesia sono stati progettati un controllore Proporzionale-Integrale-Derivativo (PID) ed un controllore Model Predictive Control (MPC). Questo problema di controllo è un problema multivariabile, in quanto sono stati considerati tre farmaci da controllare. Per questo motivo sono stati progettati tre controllori PID, applicandoli direttamente al suddetto simulatore. Con la strategia MPC è invece possibile gestire casi multivariabili. Preventivamente all'applicazione del controllore MPC, vista la presenza di non linearità nel simulatore, il modello del paziente è stato estratto dal simulatore e linearizzato. Le performance dei due controllori sono state testate e confrontate in diversi scenari simulativi su una popolazione di 24 pazienti.

[1] C. Ionescu, M. Neckebroek, M. Ghita and D. Copot. An Open Source Patient Simulator for Design and Evaluation of Computer Based Multiple Drug Dosing Control for Anesthetic and Hemodynamic Variables. IEEE Access, 2021.

Abstract

The automated control of anesthesia is a relevant issue in clinical practice since it provides a safe and individualized administration of anesthetic drugs, providing at the same time advantages for the anesthesiologists, such as the workload reduction and the consequent possibility of focusing on high level tasks and emergency management, and for the patients themselves, since the possibility of human error, such as under- or over-dosing, would be minimized. The aim of this thesis is to compare two controllers for the implementation of the closed-loop anesthetic drugs delivery. This work benefits from the existence of a patient simulator, implemented in Matlab&Simulink [2], which receives in input the doses of the anesthetic drugs and outputs the anesthetic and hemodynamic variables, through which is possible to monitor the effects of anesthesia in the patient. For the implementation of the automated control of anesthesia, a Proportional-Integral-Derivative (PID) controller and a Model Predictive Control (MPC) controller have been design. This control problem is a multivariable problem, since three drugs have been considered. For this reason three PID controllers have been designed, applying them directly to the above mentioned simulator. Previously to the application of the MPC controller, the patient model has been extracted form the simulator and linearized. The performance of the two controllers have been tested and compared in several simulative scenarios on a population of 24 patients.

[2] C. Ionescu, M. Neckebroek, M. Ghita and D. Copot. An Open Source Patient Simulator for Design and Evaluation of Computer Based Multiple Drug Dosing Control for Anesthetic and Hemodynamic Variables. IEEE Access, 2021.

Introduction

Effective control of the total intravenous anesthesia (TIVA) is one of the most important issues in the field of surgery, because millions of people worldwide undergo operations daily. Indeed, inadequate intraoperative anesthesia can cause several complications, such as [11], [12]:

- unintended intraoperative awareness, caused by underdosing of anesthetic drugs;
- deep hypnotic levels, caused by overdosing of anesthetic drugs, that are associated with postoperative mortality. A cumulative time with Bispectral Index (BIS, an hypnotic level index that will be considered in this thesis) <45 has been associated with poor outcomes in the elderly, in patients with cancer and during cardiac surgery;
- changes in the hemodynamic system, for example low mean arterial pressure;

Indeed, patient safety is the motivation of the use of automation in clinical anesthesia delivey. Nowadays, computer-controlled drug administration is implemented by open-loop target-controlled infusion (TCI) systems, the first step toward automation of drug delivery. TCIs maintain a constant infusion rate of the anesthetic, modeled using pharmacokinetics principles for the target effect-site or plasma concentrations dictated by the clinicians. However, the anesthesiologist is implied in the control loop by selecting the initial target doses and adjusting them accordingly to the peri-operative evaluation of the patient's state. The effect of the drugs on each patient is assumed by the clinicians based on monitoring devices and clinical expertise. While this strategy is manually closed by the anesthesiologist, closed-loop control systems use direct measurements from the patient monitoring in order to automatically adapt the drugs infusion rates. The measured responses of the patient are used as feedback for the controller [12]. Several studies claim that automated administration outperform manual control of anesthetic drugs. For instance, the results of a meta-analysis of randomized controlled trials to evaluate the safety and accuracy of closed-loop systems for anesthesia regulation, compared with manual control, have been published in [4]. In particular, to assess the clinical significance of the control aspect of closed-loop systems, it has been investigated from this meta-analysis if there is a significant improvement in the percentage of time of "desired" control (the variable of interest to control in the predefined range of target control) with respect to manual control. Regarding anesthesia, the improvement has been assessed to 17% for

maintenance of a target level of anesthesia. Moreover, unershooting and overshooting have been chosen as parameters of safety evaluation: the improvement was 12% for avoidance of undershooting or overshooting a given level of anesthesia.
An important aspect to consider in the introduction of automated drug delivery systems is the workload reduction and vigilance increase of clinicians. The anesthesiologists would be released from repetitive trivial tasks, allowing them to focus on decisions that require human cognitive processes, emergency clinical decisions or medical staff cooperation. The workload reduction can also avoid human distractions or bias introduced by possible burnout of the anesthesiologists, thus resulting in the minimization of accidental over- or under-dosing of anesthetic drugs [12]. Another feature to deal with is cost-effectiveness: through the quantification of the performance of closed-loop control of drugs administration it is possible to analyze the cost-savings with respect to the manual infusion control. In fact, the reduction of the workload of the anesthesiologists and the reduction of the amount of drug used are important issues to assess the socio-economic benefits of the automation of anesthesia [26]. Another advantage of the automated drug dosing is that it allows a better personalized approach and knowledge-based precision therapy with higher reproductibility. Indeed, a decrease in variation in clinical practice is a key goal in quality improvement, and only feedback has the ability to reduce the effect of uncertainty, in this case mainly due to interpatient variability. Thus, appropriately designed and implemented closed-loop control systems in anesthesia will provide less variability in desired clinical effects than manual adjustments performed by the anesthesiologists [11]. Over the past decades, research groups have focused on multiple control strategies, patients states monitors, adaptive optimization algorithms, drugs interactions, modelling approaches, and more other components of the complex process towards the control of anesthesia. The new technologies and methodologies brought by control systems could change the way people receive anesthesia. It would enable personalized services that are more responsive to patient's state, offering optimized drug doses and preventive surgical approaches that ultimately create a more sustainable patient peri- and post-anesthesia care [12].
This thesis is organized as follows. Chapter 1 provides the description of the anesthesia paradigm, with the introduction of the drugs and monitoring variables, and the report of the patient simulator, with the mathematical formulation of the patient model. Moreover, the control objectives and the indices for the performance assessment are examined. Finally, the open-loop simulation results are reported. Chapter 2 contains the PID control design, with the tuning description, and the results of the simulations of the induction and maintenance phases of anesthesia. Chapter 3 reports the MPC strategy, with the patient model linearization, the design description of the controller, and the results of the simulation of the induction phase of anesthesia. Ultimately, the comparison between the PID and the MPC control has been performed.

Chapter 1

Patient modeling and simulation

1.1 Anesthesia paradigm

The term anesthesia refers to a drug-induced reversible pharmacological state, based on three main effects induced on the patient: hypnosis, analgesia and areflexia. In this thesis, the total intravenous anesthesia (TIVA) has been considered. The TIVA uses the continuous infusion or repeated boluses of short-acting hypnotic drugs, opioids and muscle relaxants. The presentation of this material is mainly inspired by the treatment proposed in [28].

Hypnosis

Hypnosis is defined as the level of unconsciousness or amnesia required to prevent intraoperative awareness and memorization. Several parameters computed using the raw data from the electroencephalogram (EEG) have been used to monitor the level of hypnosis, for example the spectral edge frequency, the auditory evoked potentials and the approximate entropy. Recently, the Bispectral Index (BIS) has taken the lead, being the index most widely used by anesthesiologists and researchers in the field to infer hypnosis. The BIS is an EEG-based index system. A sensor, placed on the forehead of the patient, transmits EEG signals to a digital signal converter, which sends the information to the monitor for processing and analysis. The BIS uses a proprietary algorithm that elaborates the EEG signal in real time and computes the BIS index, which is a natural number. This index is dimensionless and ranges from 0 to 100, and indicates the patient's level of consciousness. A value of 100 corresponds to a complete awake and conscious state, whereas 0 corresponds to a profound state of coma or unconsciousness that is reflected by an isoelectric EEG. This system measures specific features of the spectrogram, the bispectrum, and the level of burst suppression and uses a predetermined weighting scheme to convert these features into the BIS index value. From a clinical point of view, a patient is considered to be appropriately anesthetized when the BIS value ranges from 40 to 60 [28]. Table 1.1 reports the level of hypnosis related to the BIS scores [29].

In this simulation, the drug administered to induce hypnosis is Propofol. Propofol, a phenolic derivate, is a fast-acting and fast-recovery drug, the most frequently provided for the TIVA, and it has been broadly acknowledged as most suitable for use with closed-loop control systems. At the neurophysiology level, it is an agonist at the GABA receptors which function is to enhance inhibition. There is usually a balance between excitatory and inhibitory control of pyramidal neurons, and Propofol improves the inhibitory effects. Moreover, it affects the thalamus by increasing inhibition, which decreases excitatory inputs to the cortex. Propofol potential side effects are cardiovascular depression (see Section 1.2.1), respiratory depression, pain during injection and allergic reactions [2], [28].

BIS score	**Level of hypnosis**
[100 - 90]	Awake state
[90 - 70]	Light and moderate sedation
[70 - 60]	Deep sedation
[60 - 40]	General anesthesia
[40 - 1]	Deep hypnotic state
0	Flat EEG

Table 1.1: Bispectral index score

Analgesia

Analgesia is defined as the absence of pain. During anesthetic procedures, this state is necessary for the suppression of the physiological responses to nociceptive stimulations. Monitoring analgesia is considered the most complex task during anesthesia. In recent years, a lot of tools to objectively assess the analgesia component, excepting the doctor's expertise, have been invented and commercialized. They are based on the frontal electroencephalography (EEG) and electromyography (EMG) responses, evaluation of the autonomic state and autonomic reactions, spinal reflex pathways and calculated drug concentrations. However, there are currently no validated objective indexes of nociception recommended for clinical use, so no reliable pain measurement device has yet been introduced in clinical practice. The physiological pathway of pain is a complex process consisting of three main phases:

- The microscopic level consists of phenomena involved in transduction: when a stimulus is applied to the skin, the nociceptors located there trigger action potentials by converting the physical energy from a noxious thermal, mechanical or chemical stimulus into electrochemical energy;
- The mesoscopic level mainly describes the pain transmission phase: the signals are transmitted in the form of action potentials via nerve fibers from the site of transduction (periphery) to the dorsal root ganglion, which then activates the interneurons;

- The macroscopic level includes the action-reaction phase from stimulus to signal modulation and perception: the appreciation of signals arriving in specified areas of the cerebral cortex as pain, based on descending inhibitor and facilitator input from the brainstem that modulates the nociceptive transmission from the spinal cord.

Despite modern techniques, pain remains a highly subjective experience and health care professionals have to rely on patients' ratings. Several factors, such as age, race and gender, seem to modify patients' pain perception and reporting. Identification of the optimal pain scale in noncommunicative (anesthetized) patients is in progress, and no single tool at the present time is universally accepted [7]. In this simulation, the variable used to assess the pain level is the Richmond agitation sedation scale (RASS). RASS, which is a dimensionless variable, is a 10 point scale, with four levels of anxiety or agitation (+1 to +4), one level to denote a calm and alert state (0), and 5 levels of sedation (-1 to -5). The values and descriptions of each level of the scale are listed in Table 1.2. This scale can be used to assess both sedation and analgesia, but in this simulation it is only used to evaluate analgesia. The identification of the RASS score is performed by clinicians through the verbal or motor stimulation of the patient and the observation of its response, and it is considered to be highly reliable in medical and surgical, ventilated and nonventilated, sedated and nonsedated patients [30].
Analgesia is obtained with the infusion of analgesic drugs, in this case Remifentanil has been examined. Remifentanil is an opioid with a unique pharmacokinetic profile. It differs from the other opioids since it possesses an ester linkage, making it susceptible to nonspecific esterases in tissues and blood, thus resulting in a rapid and uniform clearance leading to highly predictable onset and offset of action. Remifentanil has a rapid blood-brain equilibration time of between 1 and 1.5 min. The time for the concentration of Remifentanil at its effect-site to decrease by 50 % is also short: 3 to 5 min. Computer modeling predicts that the time for Remifentanil concentration to decrease by 80 % is less than 15 min. Thus, it has a fast onset and offset, allowing it to be easily titratable in a clinical setting. Although the rapid termination of its effect may reduce problems associated with side effects, it also results in the absence of any analgesic activity in the immediate withdrawal period. Remifentanil side effects include respiratory depression and hemodynamic alterations (see Section 1.2.1), in particular with high doses or when coadministered with other agents that produce vasodilatory effects, such as Propofol [6].

RASS score	Term	Description
+4	Combative	Overly combative/violent, danger to staff
+3	Very agitated	Aggressive behaviour
+2	Agitated	Nonpurposeful movements
+1	Restless	Anxious but not aggressive
0	Alert and calm	
-1	Drowsy	Not fully alert/sustained awakening with eye contact
-2	Light sedation	Briefly awakens with eye contact to voice
-3	Moderate sedation	Movements to voice/no eye contact
-4	Deep sedation	No responce but movements to physical stimulation
-5	Unarousable	No response to any stimulation

Table 1.2: Richmond agitation sedation scale

Areflexia

Areflexia, evaluated through the neuromuscular blockade (NMB), is defined as the lack of movement and it aims to achieve an adequate level of paralysis to perform surgical procedures. NMB is dimensionless and is expressed in [%]. This variable varies from 0% to 100%, where 0% represents the total paralysis and 100% represents the total muscular activity. From a physiological point of view, the principal pharmacological effect of neuromuscular-blocking drugs (NMBD) is to interrupt the transmission of synaptic signaling at the neuromuscular junction (NMJ), a chemical synapse located in the peripheral nervous system, by interacting with the nicotinic acetylcholine receptor (AChR). In this thesis, the neuromuscular-blocking drug considered is Atracurium, a nondepolarizing NMBD. Regarding the duration of the effect, it is classified as an intermediate-acting drug (its effect lasts from 45 to 60 min). The chemical classification is benzylisoquinolines, and it is a mixture of 10 stereoisomers. The drug is cleared by Hofmann elimination, a nonbiologic and spontaneous process independent on renal, hepatic and enzimatic functions, thus it is indicated for patients with severe renal and hepatic diseases. The clearance rate is influenced by pH and body temperature. Atracurium does not have influence on the cardiovascular system, indeed it is recommended when the cardiovascular stability is required [28], [2].
NMB monitoring has three main purposes [28],[7]:

- To ensure appropriate relaxation of vocal cords and neck muscles to allow safe tracheal intubation and mechanical ventilation, and facilitate its timing;
- To assess the muscle tonus during surgery, allowing for adjustment to particular surgical requirements of immobility and muscle relaxation;
- To estimate the level of residual NMB and muscle strength at the end of the surgical procedure, to decide the timing of tracheal extubation and assumption of sponta-

neous autonomous ventilation.

The principle of NMB monitoring consists of the electrical stimulation of a motor nerve and the evaluation of the induced muscle response. Usually the electrodes are applied over the cleaned skin above the ulnar nerve at the wrist. The electrical stimulation can be generated in various ways, including the train-of-four (TOF), which is characterized by a sequence of four pulses (twitches) at 0.5 s intervals. The train of pulses is repeated with a TOF period that can be selected and is typically 20 s, a value that ensures the recovery of the muscle to its unstimulated state. TOF is a useful method for NMB monitoring because it provides a good measure of neuromuscular blockade, it is less painful than other stimulation techniques (for example tetanic stimulation) and it does not affect subsequent recovery [7], [28].

Hemodynamic variables

To complete the anesthesia paradigm the hemodynamic system must be taken into account. The goal of hemodynamic management is to maintain an adequate organ perfusion. Since organ perfusion is difficult to measure in vivo, systemic blood pressure is monitored as an indicator of blood flow and organ perfusion. The relationship between systemic blood pressure and systemic perfusion can be modeled by the the following law:
MAP - CVP = SVR $\times$ CO, where MAP is the mean arterial pressure, CVP is the central venous pressure, SVR is the systemic vascular resistance and CO is the cardiac output. In this simulation, the hemodynamic system is monitored through MAP and CO. Mean arterial pressure can be calculated with the following formula: MAP = CO $\times$ TPR, where TPR is the total peripheral vascular resistance. The measurement unit of MAP is [mmHg]. Cardiac output can be obtained by: CO = HR $\times$ SV, where HR is the heart rate and SV is the stroke volume, which is the volume of blood pumped from the left ventricle per beat and it is influenced by preload, afterload and myocardial compliance and contractility [28]. The measurement unit of CO is [l/min]. Hypnotic and analgesic drugs influence the hemodynamic variables (MAP and CO), as reported in Section 1.2.1

Phases of anesthesia

There are three phases of anesthesia during a standard surgery procedure [7]:

- Induction phase: it is the initial phase of anesthesia, during which the anesthetic variables (BIS, RASS and NMB) are driven from the baseline values to the target values;

- Maintenance phase: at this stage the surgery procedures are performed, once the required levels of the anesthetic variables are achieved. It is important to maintain

an adequate level of hypnosis despite the occurrence of disturbances, mainly due to noxious stimuli;

- Emergency phase: it is the final phase of anesthesia, during which the administation of the drugs is stopped (usually during or at the end of the skin closure). The patient starts to recover from anesthesia after 8-10 min.

1.2 Patient modeling and simulation

1.2.1 PKPD models of the patient

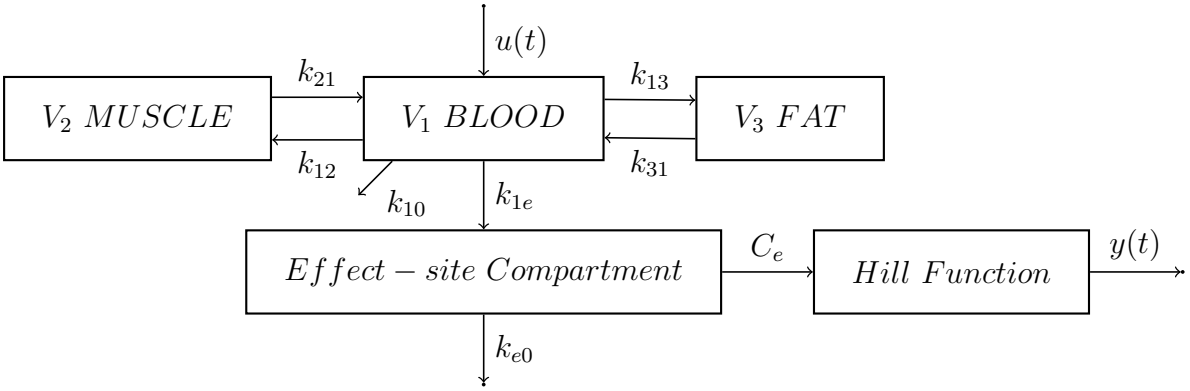

Figure 1.1: PKPD model for one drug

The goal of anesthesia during surgery procedures is to rapidly induce unconsciousness and avoid awareness during the operation, to titrate analgesia to avoid responses to nociceptive stimulations, to induce paralysis, to maintain hemodynamic stability and to facilitate rapid recovery. This cannot be achieved with constant infusion rates of anesthetic drugs: boluses are given to rapidly induce anesthesia, to adjust drug dosing during the procedure and in anticipation or response to stimulations. As an anticipation of the end of the surgery, drug dosing adjustments can be made to ensure rapid recovery. For these reasons and for prediction and model-based control purposes of anesthesia, an appropriate model of the patient is crucial in capturing the complex physiological phenomena of the interaction between drugs and patient responses. The presentation of this material is inspired by the treatment proposed in [7] and [16]. The most popular modeling approach is the PKPD population model [7]. A PKPD model in general consists of a pharmacokinetic (PK) model section in series with a pharmacodynamic (PD) model section. The PK model component provides the concentration of the drug over time in the sampled body fluid (normally blood). The PK compartmental models are the most commonly used for drug kinetics and are based on Gaussian normalized distributions. PK principles refer to the dose-concentration dependency by modeling the processes of absorption, distribution and elimination of the drug in the body. The PD model component relates the concentration of drug obtained by the PK model to the observed effect at the effect-site compartment, i.e. the site of action of the drug [10]. Usually, in biological systems, the PK component

is linear while the PD component is non linear.
In Figure 1.1 it is shown a generic PKPD model of a drug, which is valid for Propofol and, excluding the Hill function, also for Remifentanil. The three compartments of the upper part of Figure 1.1 (Blood, muscle and fat) are the PK model components, while the effect-site compartment and the Hill function are the PD model components. It is common to find in the literature individual compartments associated with tissue types: in the context of the TIVA, the central compartment represents the blood, being the site where the drug is administered. The peripheral compartments (fat and muscles) only exchange drug with each other indirectly through the central compartment. Furthermore, the drug is assumed only to be eliminated from the central compartment; in the intravenous context, such elimination occurs typically through metabolism in the liver, combined with renal excretion. It is straightforward to derive the state space equations for a compartment system of arbitrary order and topology. However, increasing the number of parameters also increases the demand on clinical identification data to avoid over-fitting. For clinical purposes, the three compartmental model generally provides an adequate fit for experimental PK data of most anesthetic drugs. Regarding the linearity of the model, the only non linear part is the Hill function. This type of models, that consist of a linear dynamic followed by a non linear dynamic are called Wiener-Hammerstein models [23].

Models for anesthetic variables

The number of compartments of the PK model required to capture response dynamics vary between drugs: the PK models of Propofol and Remifentanil are three compartmental linear models [16], as presented in Equation 1.1.

$$\begin{cases} \dot{x_1}(t) = -(k_{10} + k_{12} + k_{13})x_1(t) + k_{21}x_2(t) + k_{31}x_3(t) + \dfrac{1}{V_1}u(t) \\ \dot{x_2}(t) = k_{12}x_1(t) - k_{21}x_2(t) \\ \dot{x_3}(t) = k_{13}x_1(t) - k_{31}x_3(t) \end{cases} \tag{1.1}$$

where x_i [mg/ml] (i=1,2,3) is the concentration of the drug in the i-th compartment, k_{ij} $[min^{-1}]$ is the drug transfer rate from the i-th to the j-th compartment, k_{i0} $[min^{-1}]$ is the drug metabolic rate of the i-th compartment, u(t) [mg/min] is the drug infusion rate in the central compartment (blood) and V_1 [l] is the volume of the central compartment [16].
An additional hypothetical effect-site compartment is added to represent the lag between plasma drug concentration and drug response [23]. x_e is the drug concentration in this compartment and it is called effect-site compartment concentration. The effect compartment receives drug from the central compartment by a first-order process and it is

considered as a virtual additional compartment:

$$\dot{x_e}(t) = k_{1e}x_1(t) - k_{e0}x_e(t) \tag{1.2}$$

The differential equation of the effect-site compartment is linear and it is considered as the first part of the PD model. Below the matrices of the state space representation of the PK model and the previously mentioned effect-site compartment are reported:

$$A = \begin{bmatrix} -(k_{10} + k_{12} + k_{13}) & k_{21} & k_{31} & 0 \\ k_{12} & -k_{21} & 0 & 0 \\ k_{13} & 0 & -k_{31} & 0 \\ k_{1e} & 0 & 0 & -k_{e0} \end{bmatrix} \tag{1.3}$$

$$B = \begin{bmatrix} \frac{1}{V_1} \\ 0 \\ 0 \\ 0 \end{bmatrix} \tag{1.4}$$

$$C = \begin{bmatrix} 0 & 0 & 0 & 1 \end{bmatrix} \tag{1.5}$$

$$D = \begin{bmatrix} 0 \end{bmatrix} \tag{1.6}$$

From the matrix representation it is straightforward to notice that the input u(t) acts directly only on the plasma concentration, the output is influenced only by the effect-site concentration and there is no feedforward.

Propofol PK model parameters are calculated using the following set of equations [16]:

$k_{10} = \frac{C_{l1}}{V_1}\,[min^{-1}]$; $k_{12} = \frac{C_{l2}}{V_1}\,[min^{-1}]$; $k_{13} = \frac{C_{l3}}{V_1}\,[min^{-1}]$;

$k_{21} = \frac{C_{l2}}{V_2}\,[min^{-1}]$; $k_{31} = \frac{C_{l3}}{V_3}\,[min^{-1}]$; $k_{e0} = k_{1e} = 0.456\,[min^{-1}]$;

$V_1 = 4.27\,[l]$; $V_2 = 18.9 - 0.39(age - 53)\,[l]$; $V_3 = 238\,[l]$;

$C_{l1} = 1.89 + 0.0456(weight - 77) - 0.0681(lbm - 59) + 0.0264(height - 177)\,[l/min]$;

$C_{l2} = 1.29 - 0.024(age - 53)\,[l/min]$; $C_{l3} = 0.836\,[l/min]$;

where V_i (i = 1,2,3) is the volume of the i-th compartment and C_{li} (i = 1,2,3) is the clearance rate of the i-th compartment. Through these equations, the PK model of Propofol includes the interpatient variability; in fact, the parameters age, weight, height and lbm are patient specific (see Table 1.3).

The Propofol transfer rate from the plasma compartment to the effect-site compartment is considered in clinical practice to be equal to the rate of drug removal from the effect-site compartment: $k_{e0} = k_{1e} = 0.456\ [min^{-1}]$. The second part of the Propofol PD model is the dose-effect response and it is represented by a nonlinear Hill function [23]:

$$E = E_0 - E_{max}\frac{x_e^\gamma}{C_{50}^\gamma + x_e^\gamma} \tag{1.7}$$

where E denotes the effect of Propofol (BIS index) at the effect-site, x_e is the effect-site concentration of Propofol at time t, E_0 is the baseline value, meaning that there is no drug infusion and the patient is awake, E_{max} is the maximum effect that can be achieved by the drug infusion, C_{50} is the Propofol concentration needed to attain 50 % of E_{max} and γ is the Hill coefficient of sigmoidicity, representing the steepness of the curve but also the degree of nonlinearity. γ and C_{50} delineate the patient sensitivity to the drug. These values, reported in Table 1.3, are patient dependent, thus also the Hill function for the BIS index includes the interpatient variability.
The Hill function (closely related to the logistic function) is structurally simple and has the following characteristics, which are observed in clinical practice: it has a linear region around $x_e = C_{50}$ and saturation effects as $x_e \to 0$ and $x_e \to \infty$. For some drugs, the use of the Hill function can be motivated by ligand-binding models from receptor theory [7].

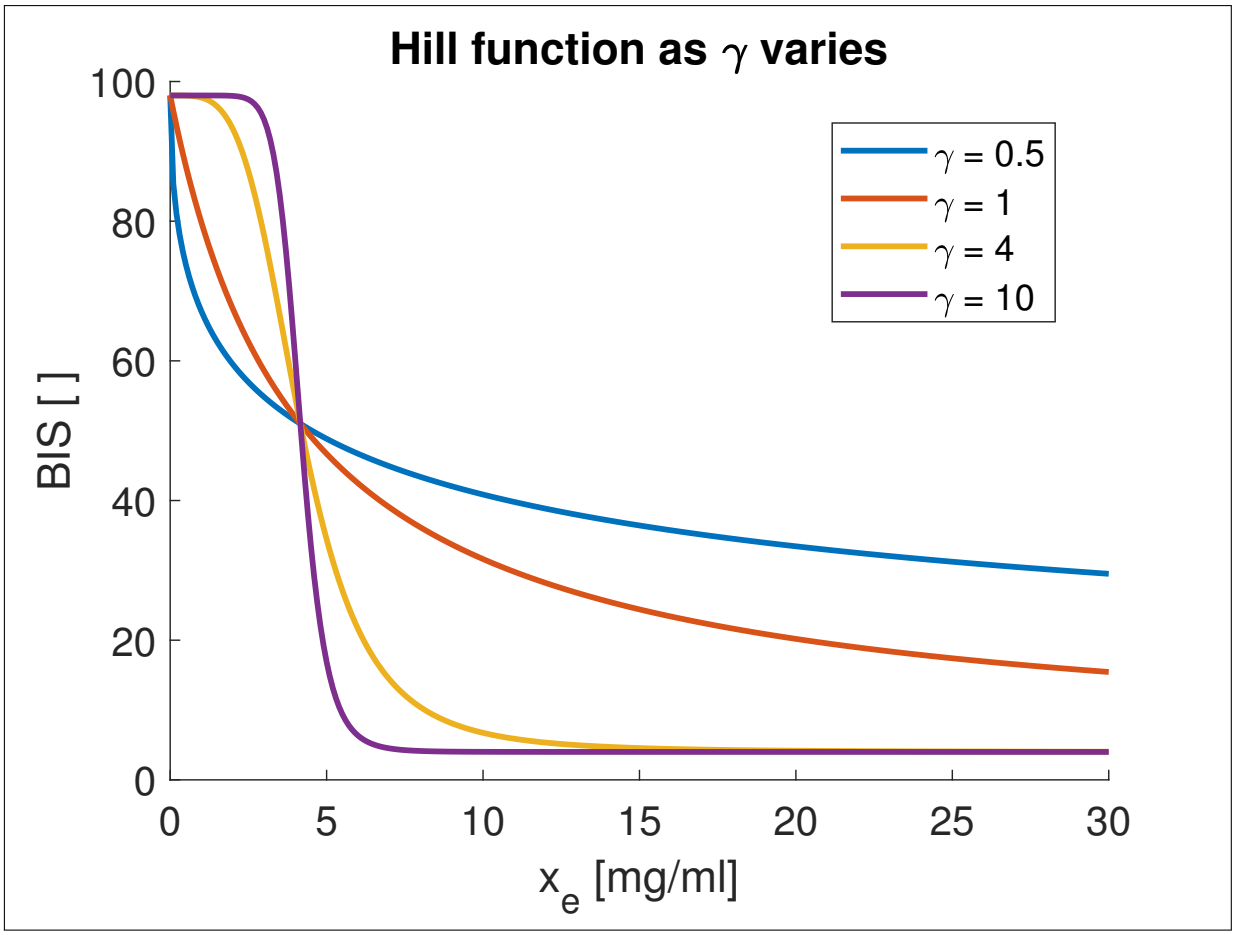

Figure 1.2: Hill functions as γ varies

In Figure 1.2 it is illustrated how the Hill function is affected by changing γ: as γ increases, the steepness of the curve increases and the maximum effect value is achieved quicker.

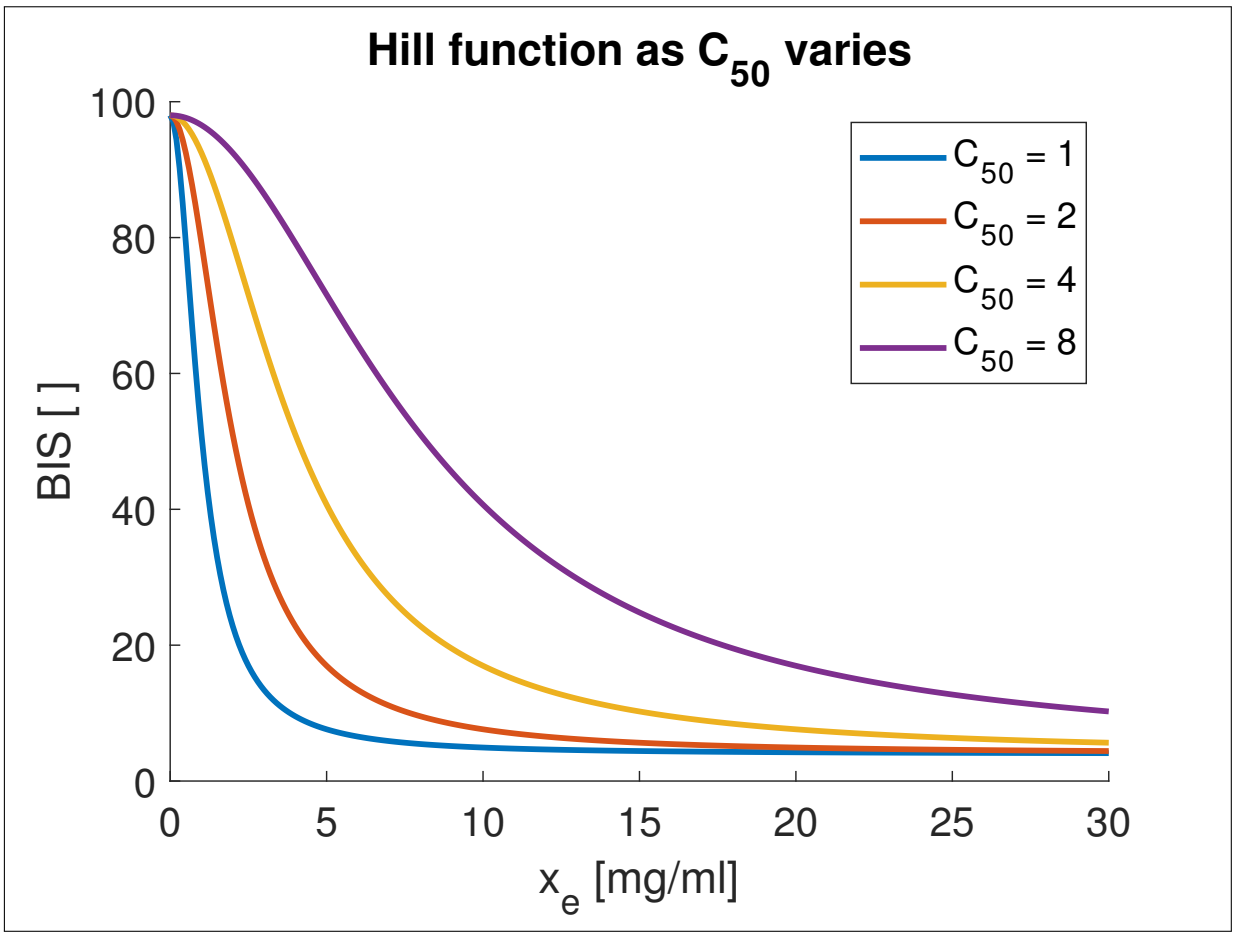

Figure 1.3: Hill functions as C_{50} varies

In Figure 1.3 it is illustrated how the Hill function is affected by changing C_{50}: as C_{50} increases, the steepness of the curve decreases and the maximum effect value is achieved slower.

Regarding Remifentanil, its PK model parameters are calculated using the following set of equations [22]:

$k_{10} = \frac{C_{l1}}{V_1}\,[min^{-1}]$; $k_{12} = \frac{C_{l2}}{V_1}\,[min^{-1}]$; $k_{13} = \frac{C_{l3}}{V_1}\,[min^{-1}]$;

$k_{21} = \frac{C_{l2}}{V_2}\,[min^{-1}]$; $k_{31} = \frac{C_{l3}}{V_3}\,[min^{-1}]$; $k_{e0} = 0.595 - 0.007(age - 40)\,[min^{-1}]$;

$V_1 = 5.1 - 0.0201(age - 40) + 0.072(lbm - 55)\,[l]$;

$V_2 = 9.82 - 0.0811(age - 40) + 0.108(lbm - 55)\,[l]$;

$V_3 = 5.42\,[l]$;

$C_{l1} = 2.6 + 0.0162(age - 40) - 0.0191(lbm - 55)\,[l/min]$;

$C_{l2} = 2.05 - 0.0301(age - 40)\,[l/min]$; $C_{l3} = 0.076 - 0.00113(age - 40)\,[l/min]$;

Through these equations, the PK model of Remifentanil includes the interpatient variability; in fact, the parameters age, weight, height and lbm are patient specific (see Table 1.3).

As for Propofol, the first part of the Remifentanil PD model is the effect-site compartment, whose drug transfer rates are: $k_{e0} = 0.357\,[min^{-1}]$; $k_{1e} = 0.456\,[min^{-1}]$.

The second part of the Remifentanil PD model is the nonlinear dose-effect response [16]:

$$RASS = \frac{1}{k_1 x_e + k_0} \frac{-2}{s+2} \tag{1.8}$$

where $k_1 = k_0 = 0.81$. From the control perspective of the TIVA, no direct opioid-to-analgesia dynamic model is available, also due to the lack of reliable and robust patient-monitoring technology and a systematic analysis of available devices for pain monitoring. For this reason, unlike Propofol, the RASS PD component has been modeled with a first order transfer function, not with an Hill function.

In the case of Atracurium, an alternative model, with a reduced number of parameters, has been introduced [7]. The proposed model has the following transfer function, considered as the PK part:

$$\frac{x_e(s)}{u(s)} = \frac{k_1 k_2 k_3 \alpha^3}{(s + k_1\alpha)(s + k_2\alpha)(s + k_3\alpha)} \tag{1.9}$$

where $k_1 = 1$, $k_2 = 4$ and $k_3 = 10$.

The Atracurium PD model is a nonlinear Hill function:

$$E = E_{max} \frac{C_{50}^{\gamma}}{C_{50}^{\gamma} + x_e^{\gamma}} \tag{1.10}$$

The entire model includes only two parameters to estimate: the parameter α of the linear kynetics and the parameter γ of the nonlinear dynamics. The value of γ is listed in Table 1.4, while $\alpha = 0.0374$. These parameters are not patient dependent, so the NMB variable does not include the interpatient variability.

The Atracurium transfer function can be written in state space form as follows:

$$\begin{cases} \dot{x}(t) = A(\alpha)x(t) + B(\alpha)u(t) \\ x_e(t) = Cx(t) \end{cases} \tag{1.11}$$

where

$$A(\alpha) = \begin{bmatrix} -\alpha & 0 & 0 \\ 4\alpha & -4\alpha & 0 \\ 0 & 10\alpha & -10\alpha \end{bmatrix} \tag{1.12}$$

$$B(\alpha) = \begin{bmatrix} \alpha \\ 0 \\ 0 \end{bmatrix} \tag{1.13}$$

$$C = \begin{bmatrix} 0 & 0 & 1 \end{bmatrix} \tag{1.14}$$

Whereas there is no significant PKPD interaction between commonly employed neuromuscular blocking agents and other anesthetic drugs, it is well known that several hypnotic and analgesic agents interact synergistically both toward loss of awareness and nociception. Notably, Propofol exhibits a synergistic interaction with Remifentanil [7],[15]. In clinical practice, when Remifentanil is coadministered, the synergy results in the sparing

of the Propofol dose necessary to achieve the required level of hypnosis. The PK model of Propofol is not affected by Remifentanil coadministration, and the same applies to the PK model of Remifentanil. Consequently, the synergy is attributed to the PD. This synergy is commonly modeled using a generalization of the Hill curve to a 3D surface (see Figure 1.4), i.e., the hypnotic effect becomes a function of the normalized Propofol and Remifentanil effect-site concentrations:

$$E = E_0 - E_{max}\frac{I^\gamma}{1 + I^\gamma} \tag{1.15}$$

where

$$I = U_P + U_R + \sigma U_P U_R \tag{1.16}$$

denotes the interaction term.
$U_P = \frac{x_{eP}}{C_{50P}}$ and $U_R = \frac{x_{eR}}{C_{50R}}$ are the effect-site concentrations of Propofol and Remifentanil, respectively, normalized to their concentrations at half maximum effect. σ denotes the amount of synergy present between Propofol and Remifentanil, and γ represents the Hill coefficient of sigmoidicity. γ is patient dependent (see Table 1.3), while $\sigma = 8.2$.

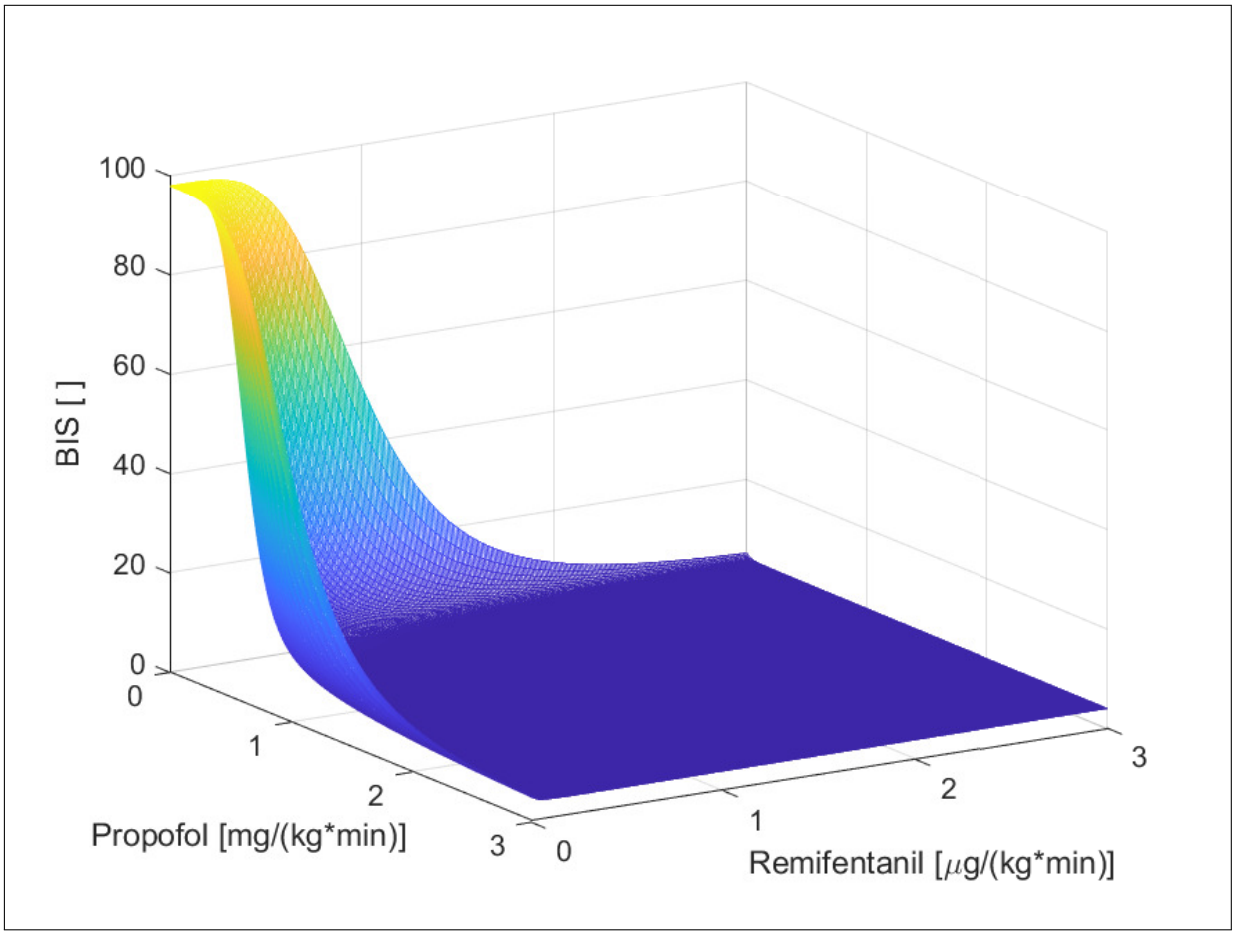

Figure 1.4: BIS surface model: Propofol and Remifentanil interaction

Models for hemodynamic variables

There is evidence to claim that Remifentanil affects negatively the mean arterial pressure (MAP), and this influence is modeled by [16]:

$$MAP = \frac{-1}{k_1 x_e + k_0} \tag{1.17}$$

$$E = E_{max} \frac{MAP^{\gamma}}{MAP^{\gamma} + C_{50}^{\gamma}} \tag{1.18}$$

where $k_1 = k_0 = 0.31$.
Remifentanil has instead a positive influence on cardiac output (CO):

$$CO = \frac{1}{k_1 x_e + k_0} \tag{1.19}$$

$$E = E_{max} \frac{CO^{\gamma}}{CO^{\gamma} + C_{50}^{\gamma}} \tag{1.20}$$

where $k_1 = k_0 = 0.51$.
Propofol causes hypotension, due to vasodilation. Hypotension can be very pronounced (more than 40 %), and it is function of the dosage of the drug (the higher the drug dosage, the higher the hypotension) [2]. The following equations show how MAP is negatively affected by Propofol:

$$MAP = \frac{-1}{k_1 x_e + k_0} \tag{1.21}$$

$$E = E_{max} \frac{MAP^{\gamma}}{MAP^{\gamma} + C_{50}^{\gamma}} \tag{1.22}$$

where $k_1 = 0.61$ and $k_0 = 0.81$.
Finally, Propofol has a slight negative influence even on CO:

$$CO = \frac{-1}{k_1 x_e + k_0} \tag{1.23}$$

$$E = E_{max} \frac{CO^{\gamma}}{CO^{\gamma} + C_{50}^{\gamma}} \tag{1.24}$$

where $k_1 = k_0 = 0.81$.
The values of E_{max}, C_{50} and γ in Equations 1.18, 1.20, 1.22 and 1.24 are reported in Table 1.4.

1.2.2 Simulation

Considering the patient model presented above, it is now possible to describe the simulations of the closed-loop control of anesthetic drugs administration. This simulations have been performed on a population of 24 patients, whose biometric values are reported in Table 1.3. The patient profiles have been artificially created to mimic as close as possible

reality, reflecting the interpatient variability [16]. The 25th patient represents the mean patient.

Index	**Age** [yrs]	**Height** [cm]	**Weight** [kg]	**Gender** [1=male]	**lbm** [kg]
1	74	164	88	1	60
2	67	161	69	1	53
3	75	176	101	1	69
4	69	173	97	1	67
5	45	171	64	1	52
6	57	182	80	1	62
7	74	155	55	1	44
8	71	172	78	1	60
9	65	176	77	1	60
10	72	192	73	1	62
11	69	168	84	1	60
12	60	190	92	1	71
13	61	177	81	1	62
14	54	173	86	1	63
15	71	172	83	1	62
16	53	186	114	1	77
17	72	162	87	1	59
18	61	182	93	1	69
19	70	167	77	1	58
20	69	168	82	1	60
21	69	158	81	1	55
22	60	165	85	1	60
23	70	173	69	1	56
24	56	186	99	1	73
25	65.2	172.9	83.1	1	61.4

Table 1.3: Patients database: PK model biometric values

	$\mathbf{E_0}$	$\mathbf{E_{max}}$	$\mathbf{C_{50}}$	$\boldsymbol{\gamma}$
Propofol → BIS	98	94	4.16	2
Propofol → MAP	5	5	6	4.5
Propofol → CO	5	5	8	4.5
Remifentanil → MAP	70	70	17	4.5
Remifentanil → CO	15	5	12	4.5
Atracurium → NMB	-	94	3.2425	2.6677

Table 1.4: Hill functions parameters

In Table 1.3, lbm is the lean body mass, that is the mass of the body minus the storage lipid. lbm is calculated differently for males and females, and can be obtained by the James equation from the height and the weight of the patient (see Table 1.3) [7]:

$$\begin{cases} lbm_{male} = 1.1weight - 128\dfrac{height^2}{weight^2} \\ lbm_{female} = 1.07weight - 148\dfrac{height^2}{weight^2} \end{cases} \tag{1.25}$$

Table 1.3 reports the biometric data of the patients: age, height, weight, gender and lean body mass are used to individualize the Propofol and Remifentanil PK model components. Table 1.4 lists the Hill functions parameters related to the PD models of Propofol and Atracurium and the Hill functions parameters that model the influence of Propofol and Remifentanil on the hemodynamic variables. This parameters are not patient dependent, but are the mean population values. In particular, Propofol → MAP represents the influence of Propofol on MAP, i.e. the Hill function that relates the effect-site Propofol concentration to the modification of the MAP level. The same concept can be applied to the other variables.

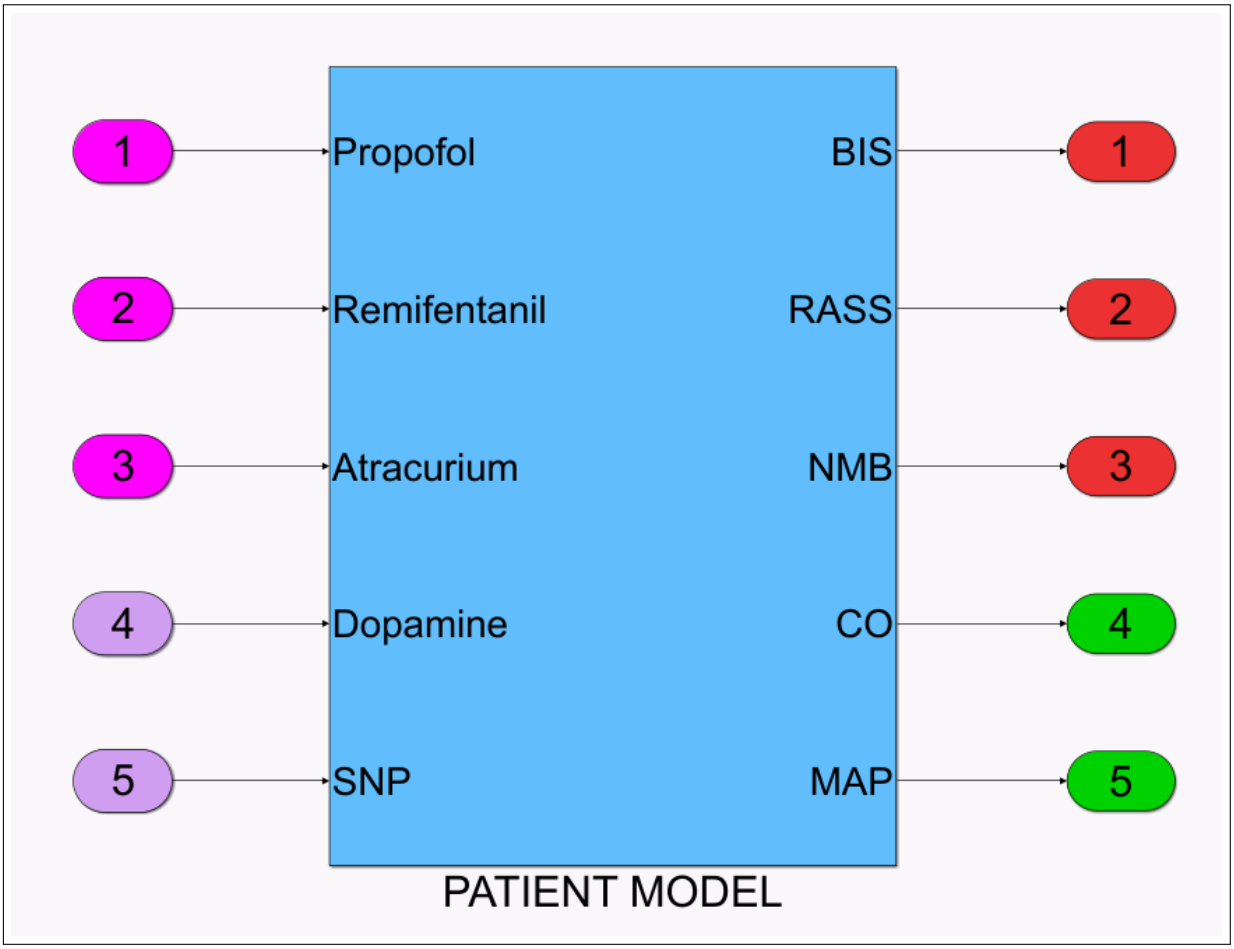

Figure 1.5: General structure of the simulator

The patient simulator employed for this thesis, described in [16], is an open source simulator, programmed in Matlab&Simulink from MathWorks(R) software platform. As shown in Figure 1.5, it includes five inputs and five outputs. The inputs are the infusion rates of the drugs: Propofol, Remifentanil, Atracurium, Dopamine (DP) and Sodium Nitroprusside (SNP). DP and SNP have antagonistic effects on the hemodynamic system, but are not taken into account in this thesis, thus only Propofol, Remifentanil and Atracurium are considered as actual inputs. Regarding the measurement units of the drugs infusion rates, Propofol infusion rate is expressed in [mg/(kg min)], Remifentanil infusion rate in [μg/(kg min)] and Atracurium infusion rate in [mg/(kg min)]. Regarding outputs, as explained above, BIS, RASS and NMB are the anesthetic variables, while CO and MAP are the hemodynamic variables.

I/O	**BIS**	**RASS**	**NMB**	**CO**	**MAP**
Propofol	$\Downarrow$	–	–	$\downarrow$	$\downarrow$
Remifentanil	$\downarrow$	$\Downarrow$	$\downarrow$	$\uparrow$	$\downarrow$
Atracurium	–	–	$\Downarrow$	–	–

Table 1.5: I/O interactions

Table 1.5 describes the interactions between inputs and outputs of the simulator. The direct cause-effect models (indicated in Table 1.5 by the double arrows) include: Propofol to BIS, Remifentanil to RASS and Atracurium to NMB. The interaction models (indicated in Table 1.5 by the single arrows) include: Propofol and Remifentanil synergic effect on BIS, Remifentanil to NMB, MAP and CO, Propofol to CO and MAP [16]. The downward pointing arrow means that by increasing the drug infusion rate, the corresponding variable decreases, whereas the upward pointing arrow means that by increasing the drug infusion rate, the corresponding variable increases. In the patient simulator, the direct cause-effect models and the interaction models are the PKPD models described in Section 1.2.1, implemented through a combination of Matlab tools, as for the state space representation of the PK models, and Simulink blocks, as for the Hill functions.
The sampling time of the simulator is $T_s = 1$ s. In order to include the quantization in the simulation, the function round (round to the nearest integer) has been used for the anesthetic variables, because in their estimation decimal values cannot be considered.

Drug	**Saturation**
Propofol [mg/(kg min)]	[0 - $5V_1$/weight]
Remifentanil [μg/(kg min)]	[0 - $2.5V_1$/weight]
Atracurium [mg/(kg min)]	[0 - 10]

Table 1.6: Drugs saturation values

In order to avoid overdosing and ensure patient safety, constraints on the drugs infusion rates have been included in the simulation. The saturation values are reported in Table 1.6. The minimum values are obviously 0 for all the drugs, since it is not possible to administer negative doses. As reported in Table 1.6, the maximum saturation values of Propofol and Remifentanil depend on the volume of the central compartment of the PK model, V_1 (see Section 1.2.1), and on the weight of the patient (see Table 1.3). The maximum saturation value of Atracurium is instead constant for all the patients.
The patient simulator is designed so that it can include disturbances and anesthesiologist's actions. The most notable disturbances are those caused by surgical and other nociceptive stimulations, acting on the awareness level and entering the system as patient inputs. Events such as incisions or other surgical procedures through out the maintenance phase typically decrease the effect of hypnotic drugs, with a consequent increase in the BIS. A closed-loop controller for the hypnotic component of anesthesia must therefore be designed to attenuate these disturbances sufficiently to avoid adverse effects, such as awareness. A first step in ensuring sufficient disturbance attenuation is to know the characteristics of the expected disturbances [7]. As shown in Figure 1.6, the surgical stimulation is modeled as a step of amplitude 10 [% of BIS] and duration 1000 s (about 15 min). As explained in [26], this step can be considered as a step signal of amplitude 10, followed by another step after 1000 s of amplitude -10.

The model of the nociceptor pathway is described by the following transfer function:

$$NOCI = K\frac{(s^2 + z_1 2 + z_2)(s^2 + z_3 2 + z_4)(s^2 + z_5 2 + z_6)}{(s^2 + p_1 s + p_2)(s^2 + p_3 s + p_4)(s^2 + p_5 s + p_6)} \tag{1.26}$$

with the following values: $z_1 = 90$, $z_2 = 22500$, $z_3 = 26.4$, $z_4 = 27225$, $z_5 = 31$, $z_6 = 24025$, $p_1 = 65.56$, $p_2 = 22201$, $p_3 = 48.9$, $p_4 = 26569$, $p_5 = 31$, $p_6 = 24025$ and $K = 1$. The surgical stimulation profile is filtered through this model and then added to the BIS value given by the PD model of hypnosis [16].

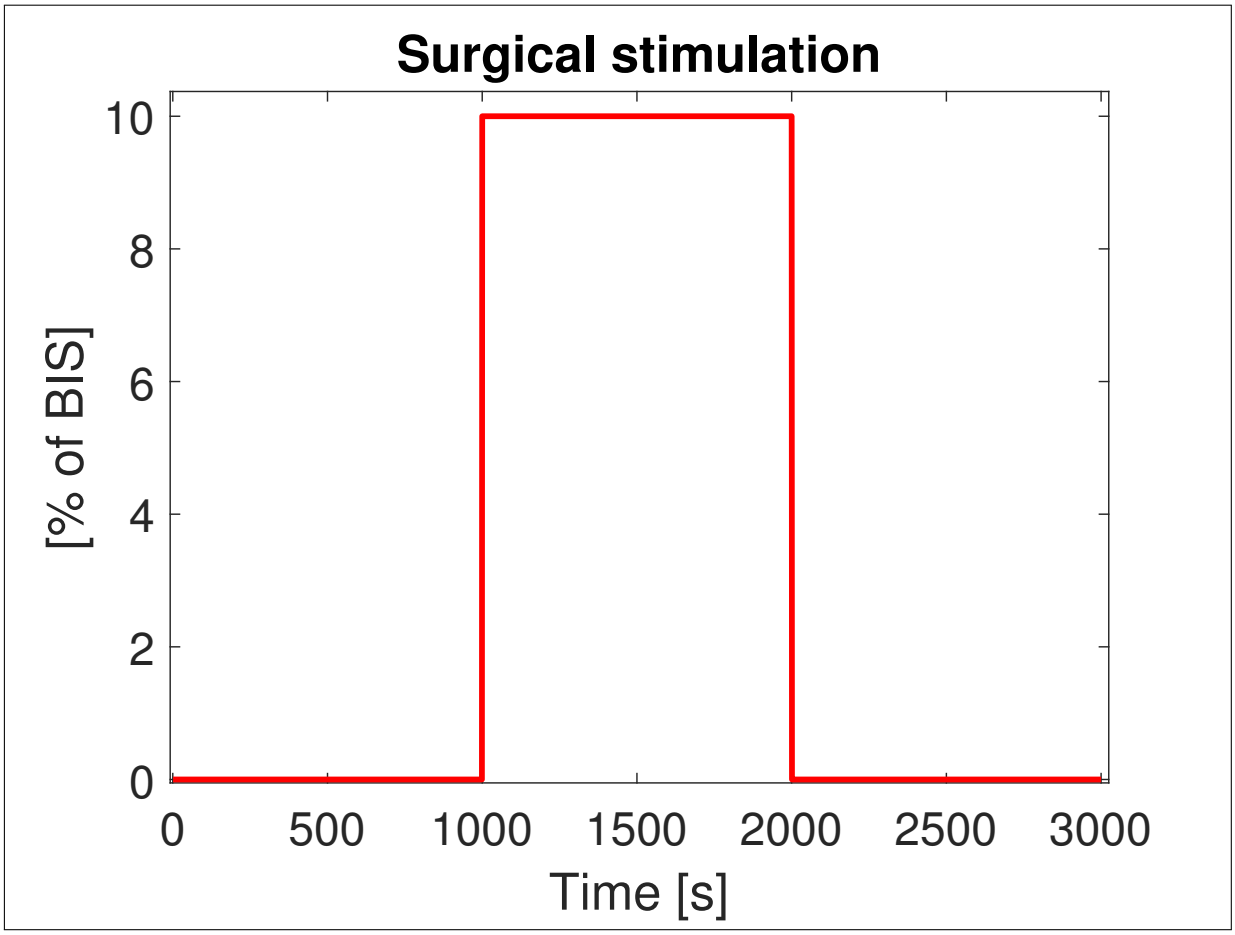

Figure 1.6: Surgical stimulation's profile

If the anesthesiologist is aware that a disturbance will occur, he may administer an additional Propofol dose, through a feedforward action, to assist the controller in the disturbance rejection task. The Propofol dose provided by the anesthesiologist is modeled as a step of the same duration of the surgical simulation, and the amplitude is individualized for each patient through the following formula: $0.05\frac{V_1}{weight}$ [mg/(kg min)], where V_1 is the volume of the central compartment of the Propofol PK model of the patient (see Section 1.2.1) and weight is the weight of the patient (see Table 1.3). Figure 1.7 illustrates the profile of the anesthesiologist's action for patient 1.

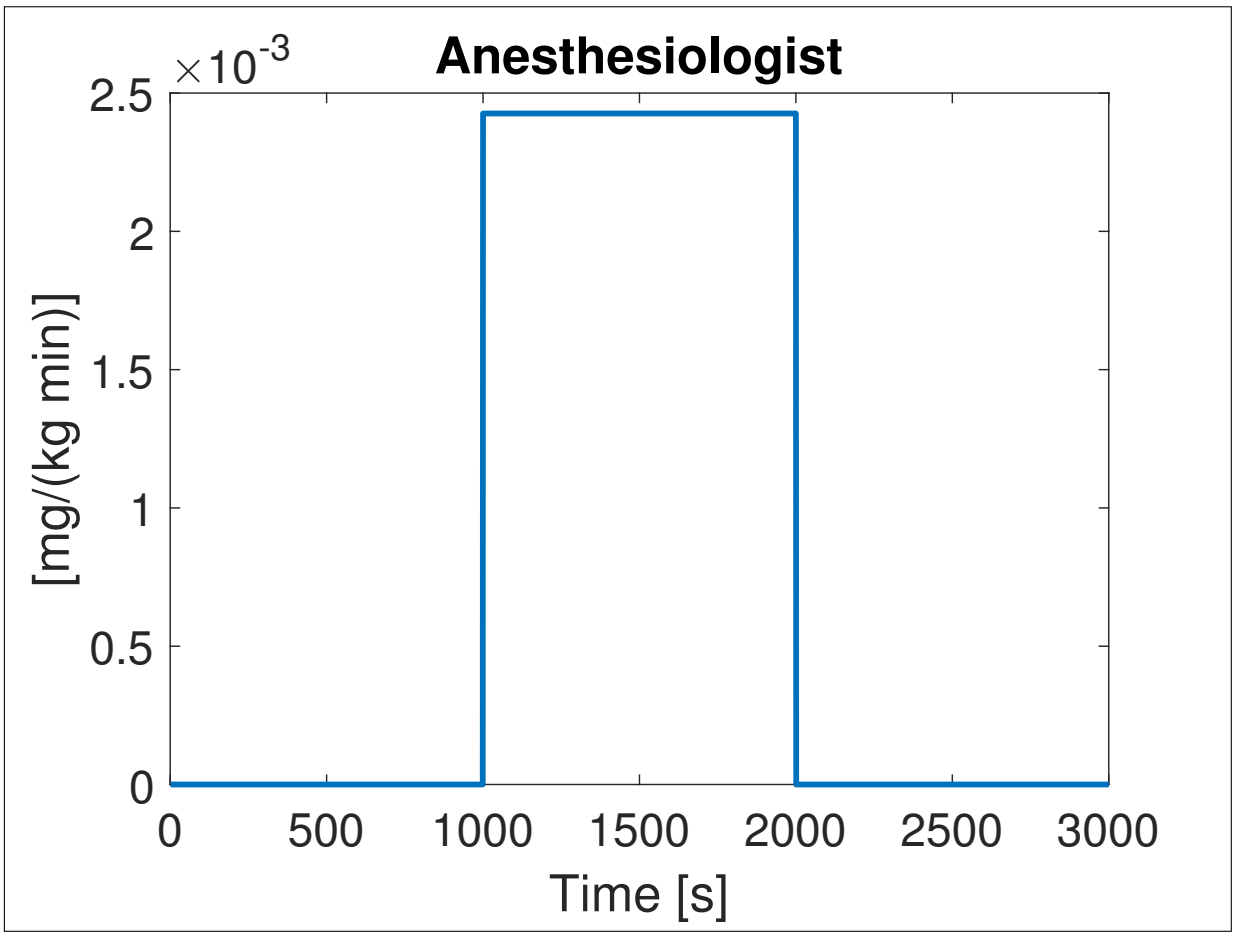

Figure 1.7: Anesthesiologist's drug infusion profile

Finally, measurement noise on the BIS can be included in the simulation, in order to mimick real BIS signals. The noise is a gaussian noise with zero mean and variance equal to 6.2721. The value of the variance has been estimated close to that observed from real BIS data [26].

By means of this simulator, it is possible to successfully reproduce the clinical expected effects of various drugs interacting among the anesthetic and hemodynamic states. The originality of the approach is the inclusion of synergy effects, antagonist effects, patient variability, clinical value intervals, nociceptor stimulation disturbances, drug trapping models and co-simulation of anesthestic and hemodynamic states along with their complex interactions. In this thesis is therefore used a simulator, provided by the Ghent University, which is uniquely defined in current state of the art and first of its kind for this application of dose management problems in anesthesia. This simulator provides the research community with accessible tools to allow a systematic design, evaluation and comparison of various control algorithms for multi-drug dosing optimization objectives in anesthesia [16].

1.3 Control objectives

As explained in Section 1.1, there are three phases of anesthesia during a standard surgery procedure. In this thesis, only the induction phase and the maintenance phase are analyzed. From a control system point of view, the induction phase can be considered as a set-point (SP) following task, while in the maintenance phase a disturbance rejection (DR) task is carried out.

Variable	**Baseline**
BIS [ ]	98
RASS [ ]	0
NMB [%]	94
CO [l/min]	5
MAP [mmHg]	80

Table 1.7: Baseline values of the controlled variables

Variable	**Target**	**Safe interval**
BIS [ ]	50	[45 - 55]
RASS [ ]	-4	[(-5) - (-4)]
NMB [%]	10	[10 - 20]
CO [l/min]	-	[4 - 6.5]
MAP [mmHg]	-	[60 - 110]

Table 1.8: Control objectives

Regarding the objectives of the control of anesthesia, Table 1.7 reports the baseline values of the anesthetic and hemodynamic variables, while Table 1.8 lists the target values and the safe intervals. One can notice that the safe interval of the BIS is different from the interval of [40 - 60] indicated in Table 1.1 regarding the indication for the general anesthesia. This is due to the fact that the manufacturer reports that the BIS has an accuracy of $\pm$ 5 [14]. For this reason, the BIS safe interval has been set to [45 - 55].
Some of the most dangerous side effects of BIS excessive undershooting include hypotension, cognitive impairement and post-operative delirium. For this reason, the BIS reference must be tracked with a settling time of about 4-5 min, which is an acceptable time according to clinical practice [7]. Moreover, it is specified that the cardiovascular side effects of Propofol are reduced if the drug is administered slowly [2].

Performance assessment

In order to evaluate the performance of the open- and closed-loop control of the BIS, RASS and NMB, the following set of performance indices has been used [7], [14]:

- TT [s]: observed time to target, the time required for the controlled variable to reach for the first time the safe interval (see Table 1.8);
- NADIR: the lowest value of the controlled variable observed during the induction phase;
- ST [s]: settling time, defined as the time when the controlled variable enters for the last time in the safe interval (see Table 1.8);
- US [%]: undershoot, defined as the negative amount of which the controlled variable exceeds the lower limit of the safe interval (see Table 1.8).
- PE [%]: performance error. $PE = 100\dfrac{Variable_{measured} - Reference}{Reference}$

Regarding the hemodynamic variables, as reported in Table 1.8, CO must remain in the range [4-6.5 l/min] and MAP in the range [60-110 mmHg].

1.4 Open-loop simulation

In this section, the results of the open-loop simulation of the induction phase of anesthesia are presented. The drugs infusion rates have been modeled as steps, whose amplitudes have been set to the steady-state values reported in Table 1.9.

Drug	**Open-loop infusion rate**
Propofol [mg/(kg min)]	$0.295V_1$/weight
Remifentanil [μg/(kg min)]	$1.85V_1$/weight
Atracurium [mg/(kg min)]	6.9

Table 1.9: Drugs open-loop infusion rates

where V_1 is the volume of the central compartment (blood) and weight is the weight of the patient (see Table 1.3).

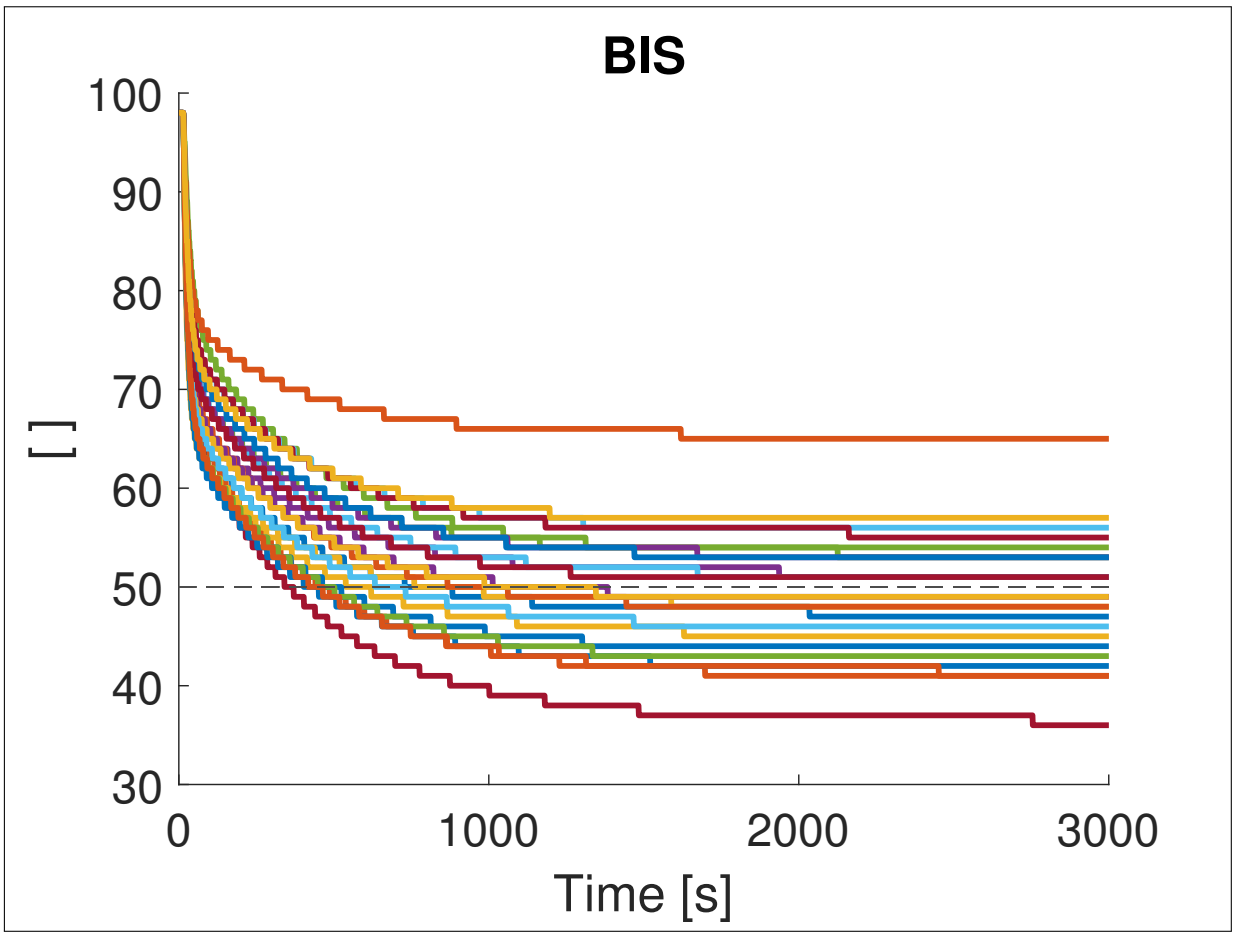

Figure 1.8: Open-loop simulation - Induction phase: BIS

As can be seen in Figure 1.8, the performance of the open-loop administration of Propofol is not acceptable. Indeed, only 15 patients show a BIS index within the desired BIS interval (see Table 1.8). As reported in Table 1.10, the minimum BIS value obtained during the induction phase is 36, while the maximum is 65; this values are not acceptable during a general anesthesia procedure. The time to target indices refer only to those patients whose BIS is in accordance to the control objectives; anyway, the maximum and mean TTs are too high, compared to the required time to target of the induction phase (about 4-5 min). These results confirm the hypothesis that the open-loop administration of Propofol can not properly handle the interpatient variability.

PID performance	
min TT [s]	283
max TT [s]	2162
mean TT [s]	675.6
min BIS-NADIR [ ]	36
max BIS-NADIR [ ]	65
mean BIS-NADIR [ ]	49.4

Table 1.10: Induction phase: performance of Propofol open-loop administration

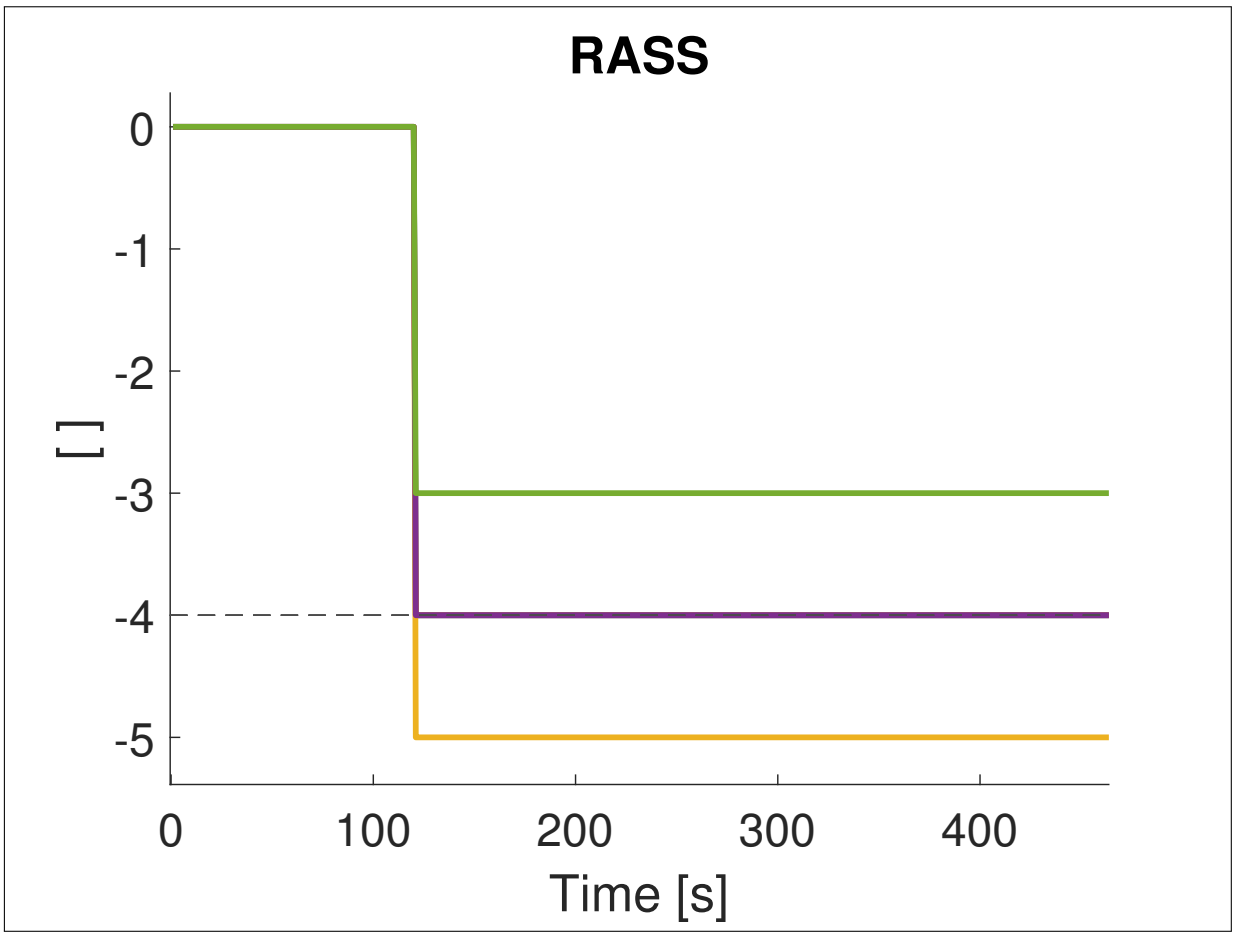

Figure 1.9: Open-loop simulation - Induction phase: RASS

Figure 1.9 shows the RASS in response to the open-loop administration of Remifentanil. The set-point following task performs well for all the patients except two; in fact, the RASS of patient 5 stabilizes at -3, that is not acceptable, while the RASS of patient 3 stabilizes at -5. This last case is acceptable since the RASS remains within the required interval (see Table 1.8). The time to target is the same for all the subjects, with a value of 120 s (i.e. 1 T_s).

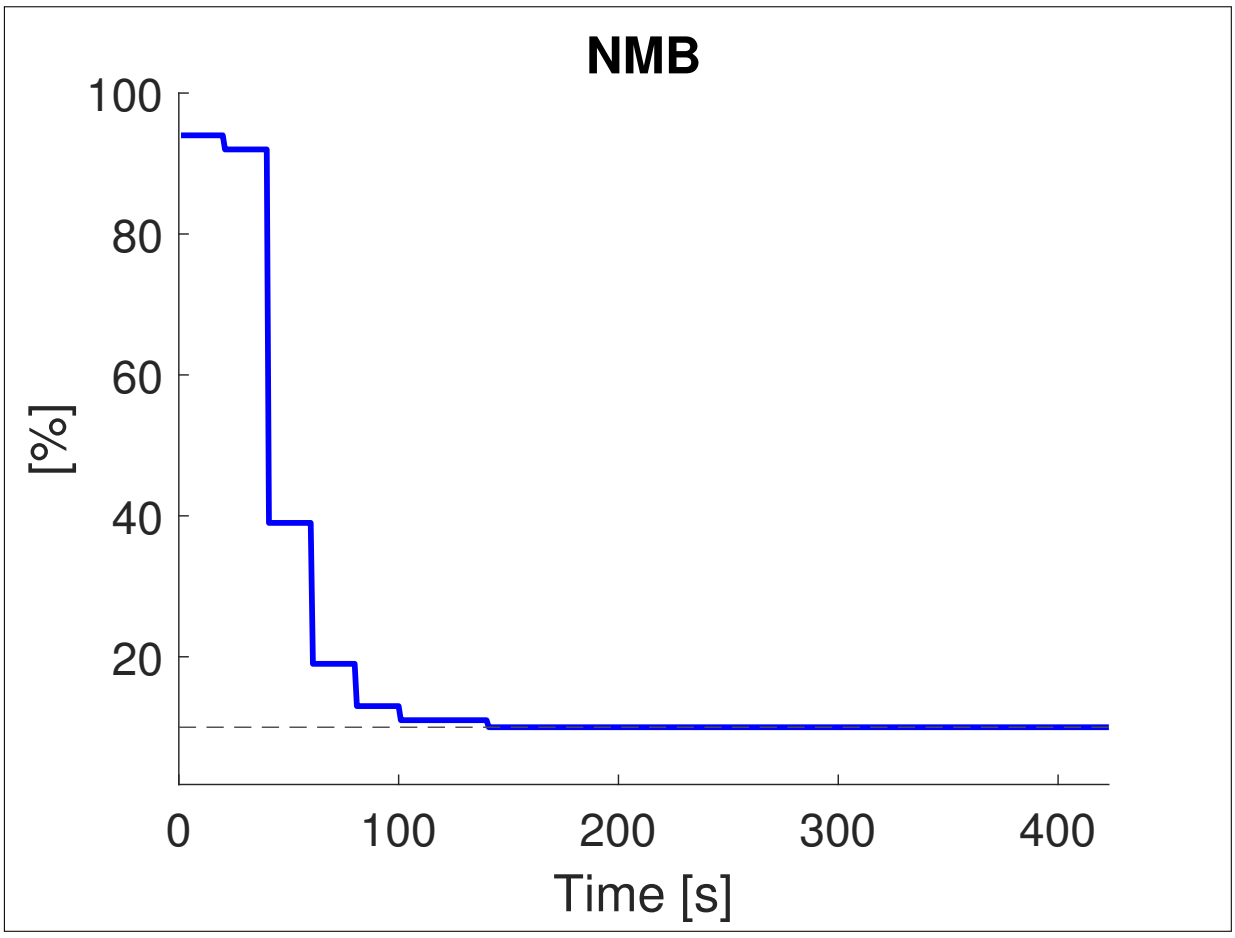

Figure 1.10: Open-loop simulation - Induction phase: NMB

Figure 1.10 shows the NMB response to the open-loop administration of Atracurium. In this case, the performance is acceptable; indeed, since the Atracurium patient model does not include the interpatient variability, the time to target for all the patients is 61 s, and there is no undershoot.

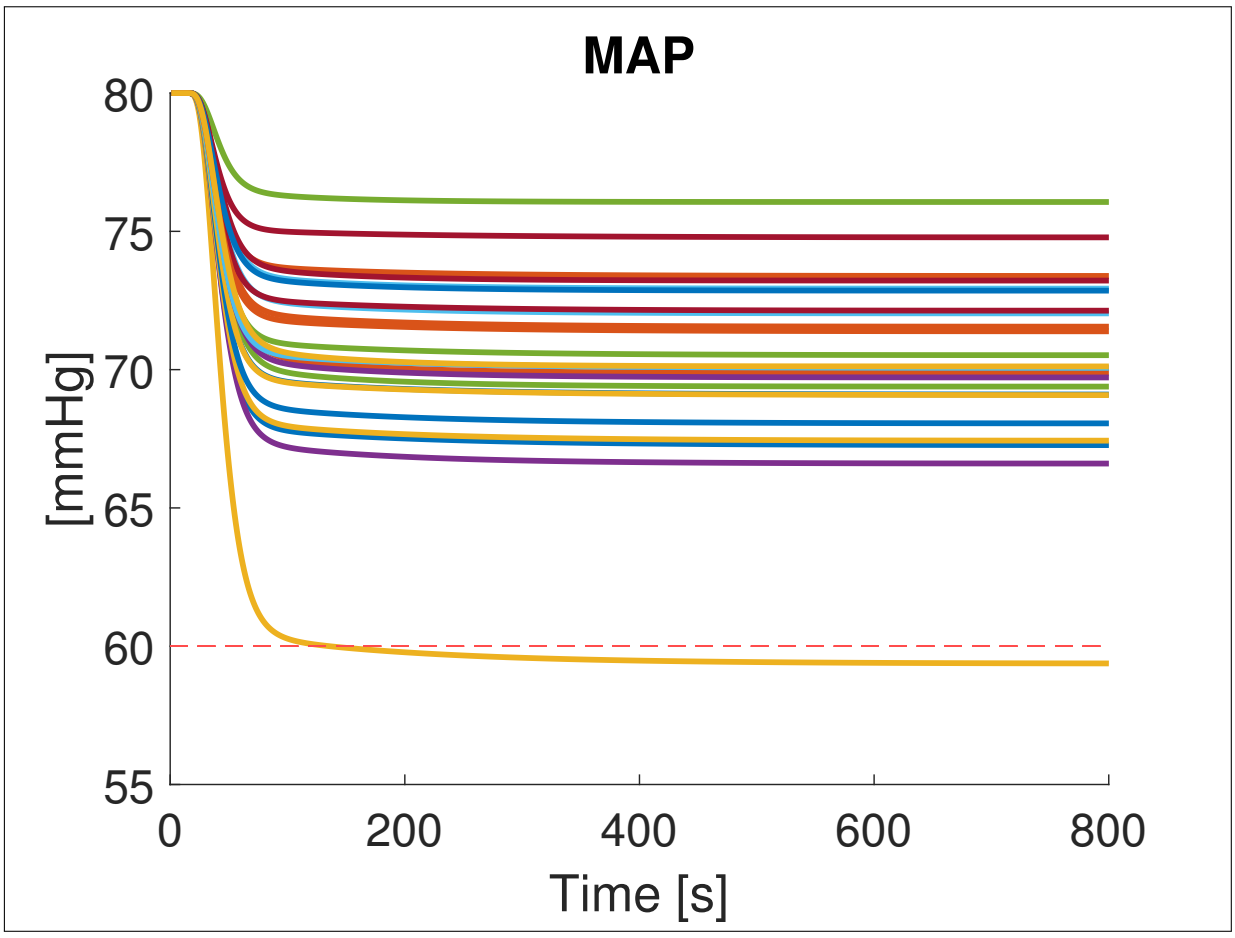

Figure 1.11: Open-loop simulation - Induction phase: MAP

Figure 1.11 illustrates the Mean arterial pressure in response to the open-loop administration of the drugs mentioned above. The dashed red line indicates the lower limit of the safe MAP interval (see Table 1.8). The outcome is acceptable for all the patients except patient 3, whose MAP level drops below the threshold, even if only slightly. This is because patient 3 needs a lower Remifentanil dose, as can be noticed from the fact that its RASS response is too accentuated. Indeed, as explained above, Remifentanil has a negative influence on MAP. Therefore, by reducing the Remifentanil infusion rate, the MAP level would increase. This result confirms that the open-loop strategy can not properly manage the interpatient variability.

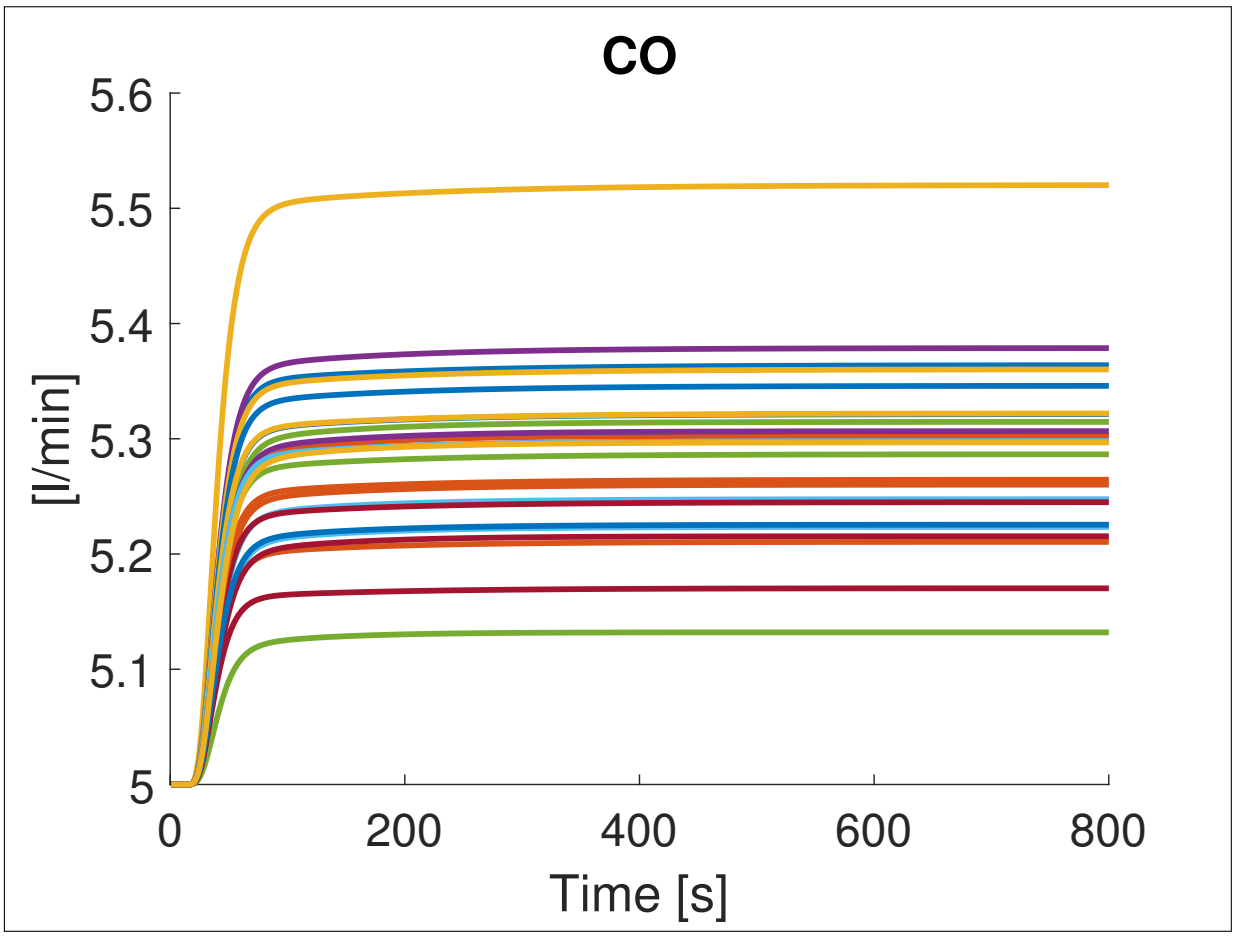

Figure 1.12: Open-loop simulation - Induction phase: CO

Regarding the Cardiac output (CO), as can be seen in Figure 1.12, the signal remains within the safe range (see Table 1.8) for all the subjects.

Chapter 2

PID

2.1 Introduction

Closed-loop systems are made of the following main components: the controlled system (in this simulation, the patient undergoing TIVA), the controlled variables (the output of the controlled system, i.e. BIS, RASS and NMB), the desired target or reference or set-point of the controlled variables (that evaluates the loop), the manipulated variables (the input of the controlled system, i.e. the drugs infusion rates), the actuator (the syringe pumps) and the controller [7]. The presentation of this topic has been mainly ispired by the treatment proposed by [3] and [7].

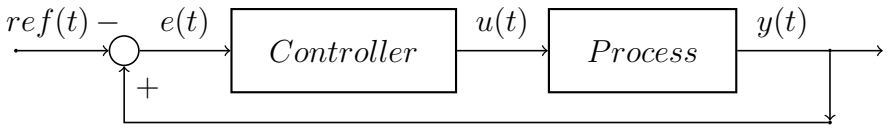

Figure 2.1: Closed-loop control scheme

In Figure 2.1, that shows the closed-loop control scheme, ref(t) is the reference signal, e(t) is the control error, u(t) is the process input signal and y(t) is the process output signal. The block diagram shows that the feedback in this particular case is not a standard negative feedback, because as u(t) increases, y(t) decreases. More precisely, u(t) increases if e(t) is positive, while decreases if e(t) is negative. As a result, e(t) = y(t) - ref(t).
Taking the BIS index as an example, ref(t) is the BIS reference, y(t) is the BIS signal, e(t) is the difference between the BIS signal and the BIS reference, and u(t) is the Propofol dose.
In order to perform a closed-loop control of anesthetic drugs infusion rates, a Proportional-Integral-Derivative (PID) controller has been designed. The PID controller is a simple implementation of feedback, it is by far the most common control algorithm and most feedback loops are controlled by it. The PID controller can be implemented in many different forms, as a stand-alone controller or as part of a direct digital control package or a hierarchical distibuted control system. It can be viewed as a device that can be operated with a few rules of thumb, but it can also be approached analytically [3].

The PID output u(t) is the sum of three actions:
$u(t) = u_p(t) + u_i(t) + u_d(t)$, where $u_p(t)$ is the proportional action, $u_i(t)$ is the integral action and $u_d(t)$ is the derivative action. These three actions are calculated separately and then summed. The proportional action is directly proportional to the control error:

$$u_p(t) = K_p e(t) \tag{2.1}$$

where K_p is the proportional gain. Proportional control has the drawback that the process output often deviates from the set-point, i.e. there is normally a non-zero control error in steady state (e_{ss}). Increasing K_p increases the speed of the response and reduces e_{ss}, but increasing it too much can cause over- or under-shooting. The steady state deviation can be avoided by adding the integral action:

$$u_i(t) = K_i \int_0^t e(\tau) d\tau \tag{2.2}$$

where K_i is the integral gain. Equation 2.2 shows that the control action is proportional to the integral of the error. Assume that there is a steady state with constant error e_{ss} and constant control signal u_{ss}. It follows that $u_{iss} = K_i e_{ss}$. Since u_{ss} is a constant, it follows that e_{ss} must be zero. This proves that if there is a steady state and the integral action is included in the controller, the steady state error is always zero.
The derivative action is proportional to the derivative of the error:

$$u_d(t) = K_d \frac{de(t)}{dt} \tag{2.3}$$

where K_d is the derivative gain. The purpose of the derivative action is to improve the closed-loop stability. The instability mechanism can be described as follows: because of the process dynamics, it will take some time before a change in the controlled variable is noticeable in the process output. Thus, the control system will be late in correcting for an error. Adding the derivative action, the controller is made proportional to the predicted process output, where the prediction is made by extrapolating the error by the tangent to the error curve. The control signal is thus proportional to an estimate of the control error at T_d (see Equation 2.5) times ahead. Increasing K_d increases the stability of the signal, but amplifies the measurement noise.
The controller action is thus a sum of three terms: the integral term represents the past, the proportional term represents the present and the derivative term represents the future [3]. Indeed, as can be seen in Figure 2.2, the integral error corresponds to the past, the proportional error to the present and the derivative error to the future.

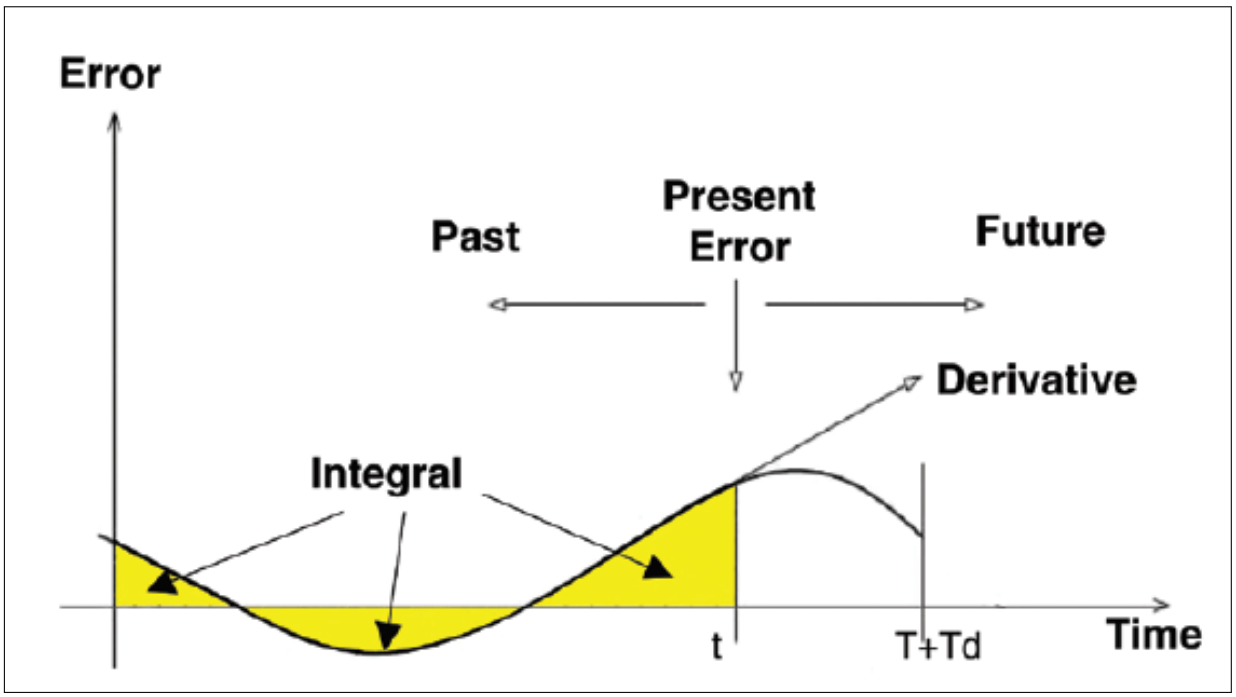

Figure 2.2: PID controller - Error components

The PID algorithm can be represented by the following transfer function:

$$C(s) = K_p(1 + \frac{1}{sT_i} + sT_d) \tag{2.4}$$

where T_i is the integral time constant and T_d is the derivative time constant. T_i and T_d can be derived from the integral gain and the derivative gain through the following relations:

$$T_i = \frac{K_p}{K_i}$$
$$T_d = \frac{K_d}{K_p} \tag{2.5}$$

PID control is the first strategy studied in depth of anesthesia regulation [7]. This control technique applies accurate and responsive correction of the manipulated variables. The practical advantages of this method observed in depth of anesthesia regulation are the fast transient responses until finally reaching a steady-state value of the controlled variables and the high reduction of the steady-state errors. Simulation tests confirm that the PID-based control scheme is also robust in regards to the interpatient variability. On the other hand, PID controllers do not have the ability to anticipate the response of the patient [7]. This problem can be solved through a model-based strategy, that will be discussed in Chapter 3.

2.2 Induction phase

The induction phase and the maintenaince phase are considered separately, since the diversity of the tasks, therefore a gain scheduling technique has been employed. The tuning

of the PID parameters has been optimized independently for the two phases, as reported in Table 2.5. Since the disturbance rejection task only concerns hypnosis (i.e. the BIS), the gain scheduling technique has only been applied for the control of this variable, while for RASS and NMB only the tuning for the set-point following task has been performed. In this section, the results of the PID control over the population during the induction phase are discussed. During the induction phase, the target values of the controlled variables should be rapidly attained, while avoiding, at the same time, an excessive overshoot, as this implies an unnecessary large amount of amdinistered drugs and possible dangerous effects. For this reasons, the reference of the BIS has been designed as a a ramp that goes from the baseline BIS value (see Table 1.3) to the target BIS value (see Table 1.8) in 4 min. The choice of the shape of the reference has been made in accordance to the control objective specifications (see Section 1.3). Regarding RASS and NMB, their references have been delineated as steps from the baseline values (see Table 1.7) to the target values (see Table 1.8).
Since there are three manipulated variables, three PID controllers have been designed. In order to find the optimal PID gains (see Table 2.1), an automatic tuning has been performed for Propofol and Remifentanil infusion control, because of the synergic effect of this drugs, with the following mean squared tracking error cost function:

$$J(Kp_{Propofol}, Kp_{Remifentanil}) = \sum_{i=1}^{N}(|err_{BIS}(iT)|^2 + |err_{RASS}(iT)|^2 + p) \tag{2.6}$$

where N is the simulation time, err_{BIS} is the normalized error of the BIS, i.e. $\text{err}_{\text{BIS}} = \text{y}_{\text{BIS}}$ - ref_{BIS} adjusted with min max normalization, err_{RASS} is the normalized error of the RASS and p is the weight for the constraints on the hemodynamic variables. If MAP and CO are within the safe intervals (see Table 1.8), p = 0, otherwise p = 500. The simulation has been performed with different values of $\text{Kp}_{\text{Propofol}}$ and $\text{Kp}_{\text{Remifentanil}}$, i.e. the proportional gains of the PID controllers for Propofol and Remifentanil, holding fixed the intergral and the derivative time constants, since the integral and the derivative gains depend on the proportial gains and on the time constants (see Equation 2.5). The optimal proportional gains have been selected based on the correspondence with the minimum cost function. The tuning has then been manually adjusted. The tuning of the PID gains for Atracurium infusion control has been performed manually.

SP	$\mathbf{K_p}$	$\mathbf{K_i}$	$\mathbf{K_d}$
Propofol	0.05 [mg/(kg min)]	0.0002 [mg/(kg min^2)]	0.001 [mg/kg]
Remifentanil	0.03 [μg/(kg min)]	0.002 [μg/(kg min^2)]	0.0001 [μg/kg]
Atracurium	0.01 [mg/(kg min)]	0.0011 [mg/(kg min^2)]	0.0001 [mg/kg]

Table 2.1: Tuning of PID parameters for induction phase

In this section, since the surgical stimulation occurs in the maintenance phase, disturbances and anesthesiologist's actions are set to zero.

Simulation results

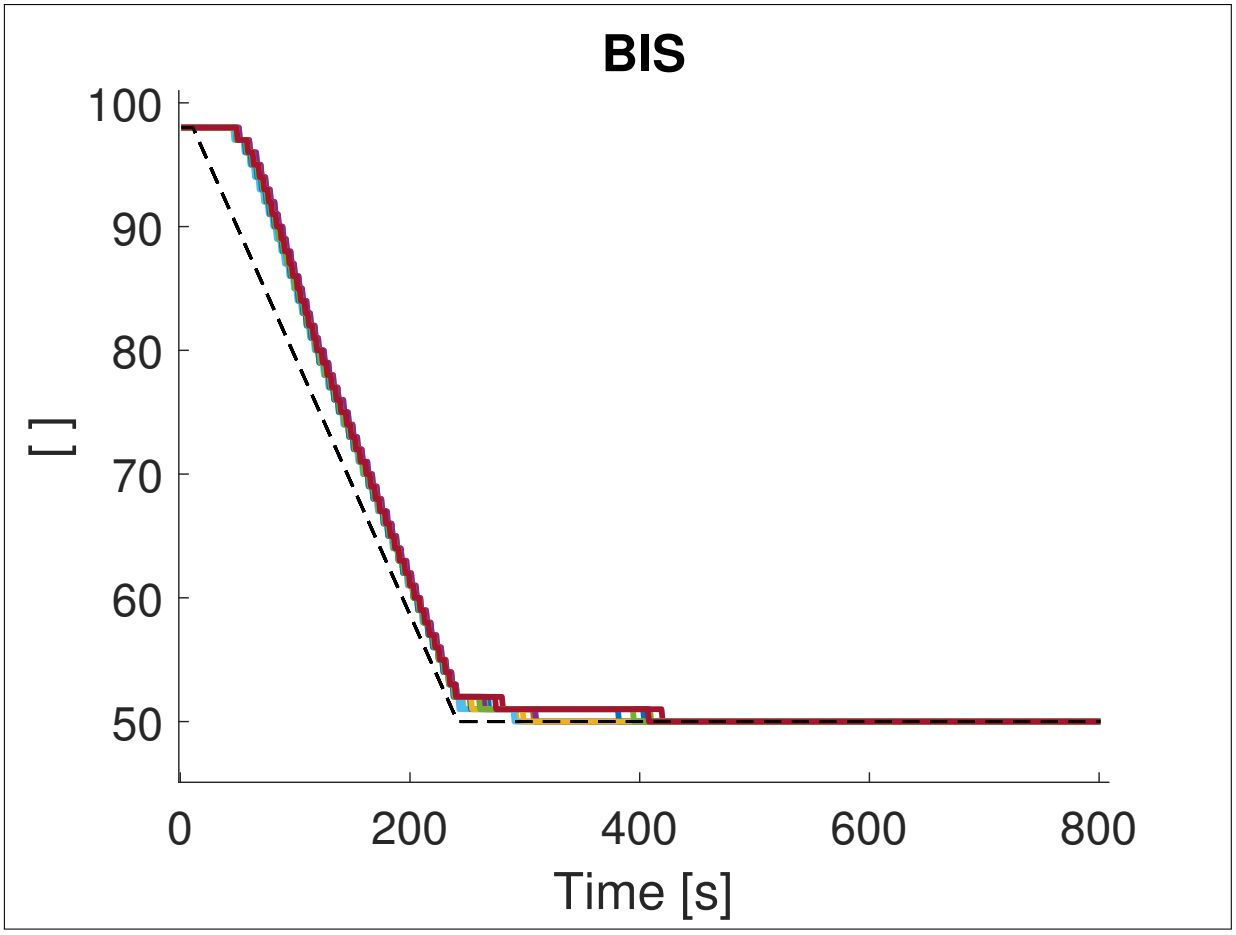

Figure 2.3: PID simulation - Induction phase: BIS

PID performance	
min TT [s]	225
max TT [s]	230
mean TT [s]	225.8
min BIS-NADIR [ ]	50
max BIS-NADIR [ ]	50
mean BIS-NADIR [ ]	50
min ST [s]	225
max ST [s]	230
mean ST [s]	225.8
min US [%]	0
max US [%]	0
mean US [%]	0
min PE [%]	0
max PE [%]	9.96
mean PE [%]	2.15

Table 2.2: Induction phase: PID performance for Propofol administration

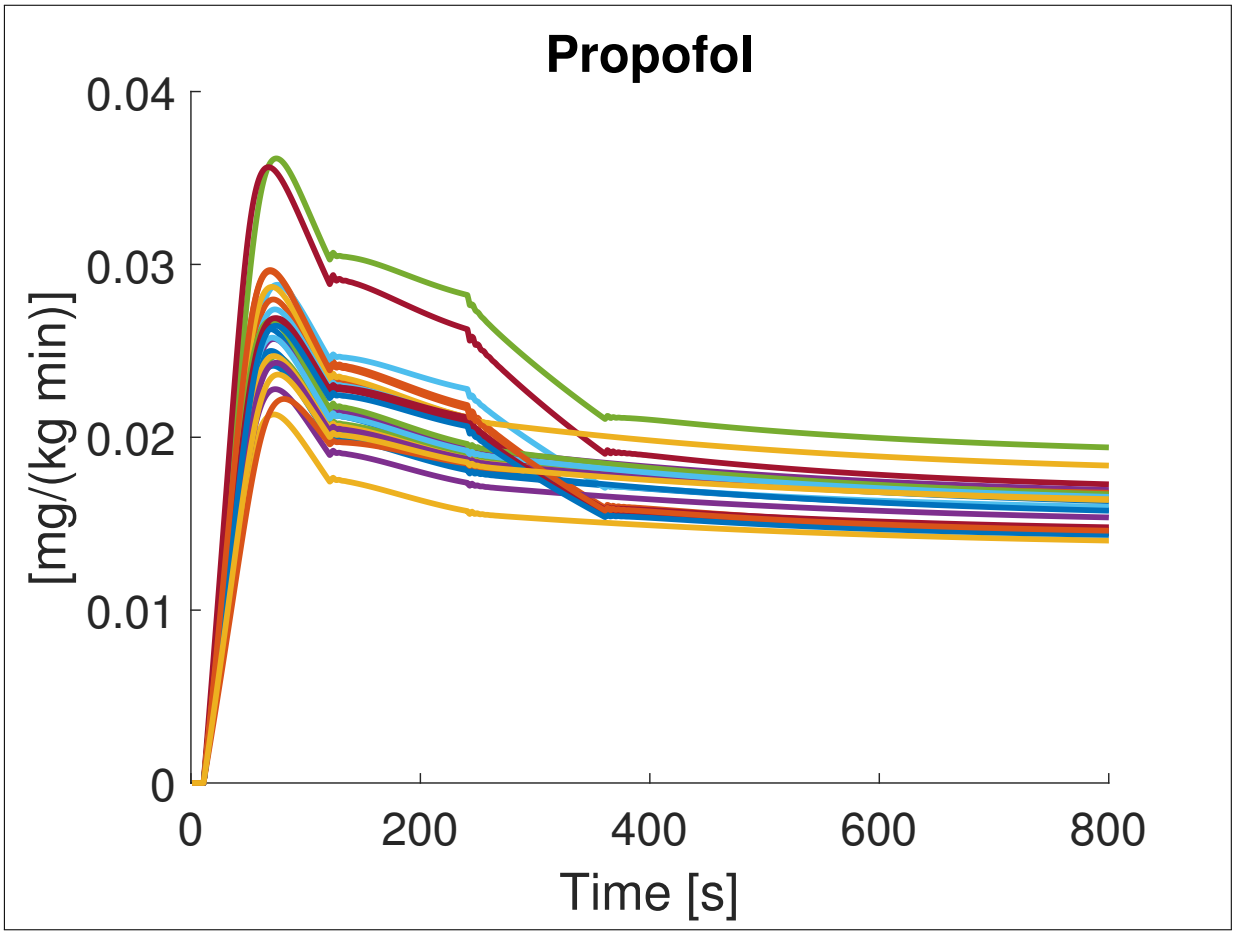

Figure 2.4: PID simulation - Induction phase: Propofol

Table 2.2 reports the performance of the PID controller for Propofol administration during the induction phase: as can also be seen from Figure 2.3, the observed time to target (TT) of the BIS follows the indicated timing (4-5 min) and the settling time (ST) is equal to the TT since there is no undershoot. The Propofol infusion rates are illustrated in Figure 2.4.

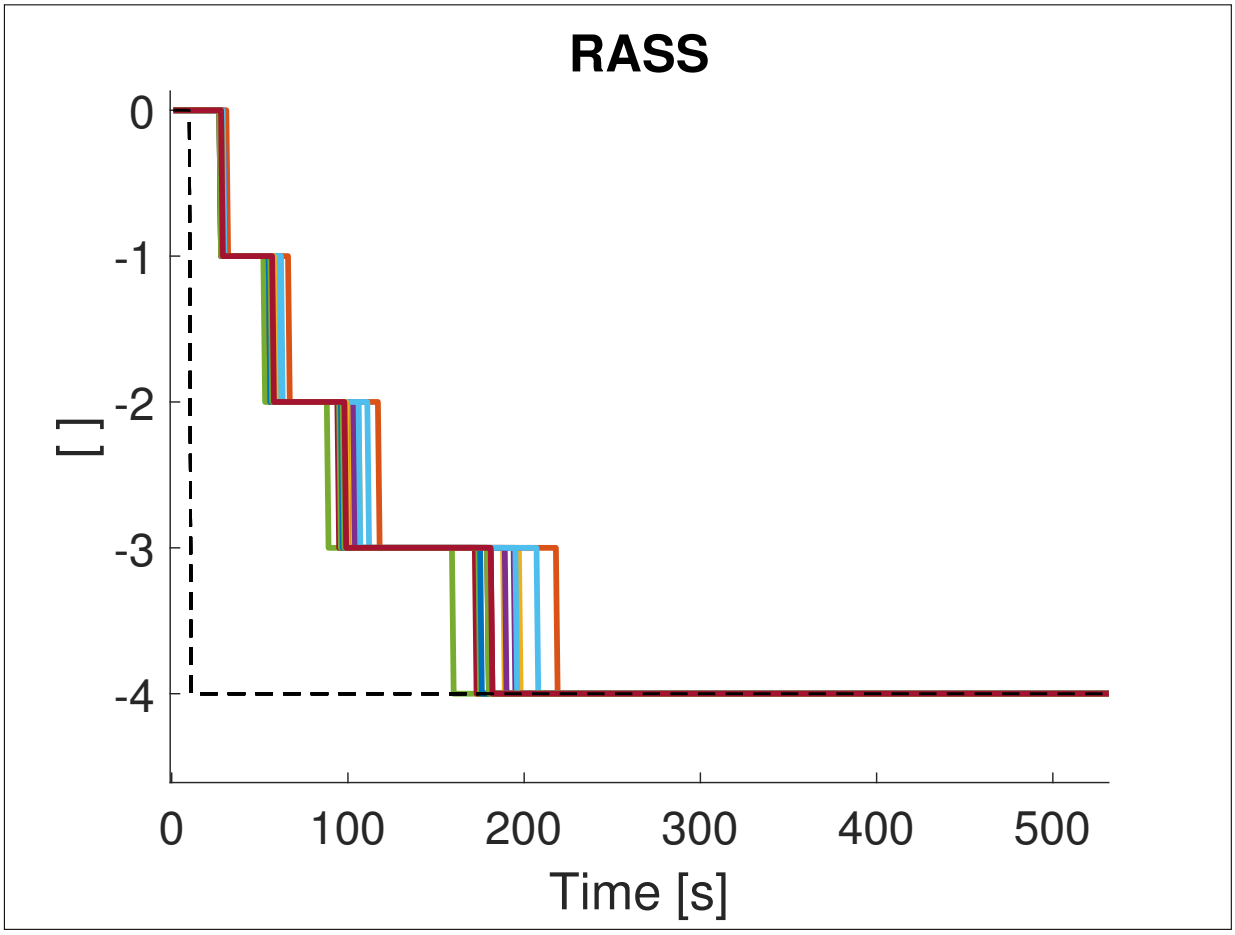

Figure 2.5: PID simulation - Induction phase: RASS

PID performance	
min TT [s]	160
max TT [s]	219
mean TT [s]	170.42
min RASS-NADIR [ ]	-4
max RASS-NADIR [ ]	-4
mean RASS-NADIR [ ]	-4
min ST [s]	160
max ST [s]	219
mean ST [s]	170.42
min US [%]	0
max US [%]	0
mean US [%]	0
min PE [%]	0
max PE [%]	100
mean PE [%]	10.35

Table 2.3: Induction phase: PID performance for Remifentanil administration

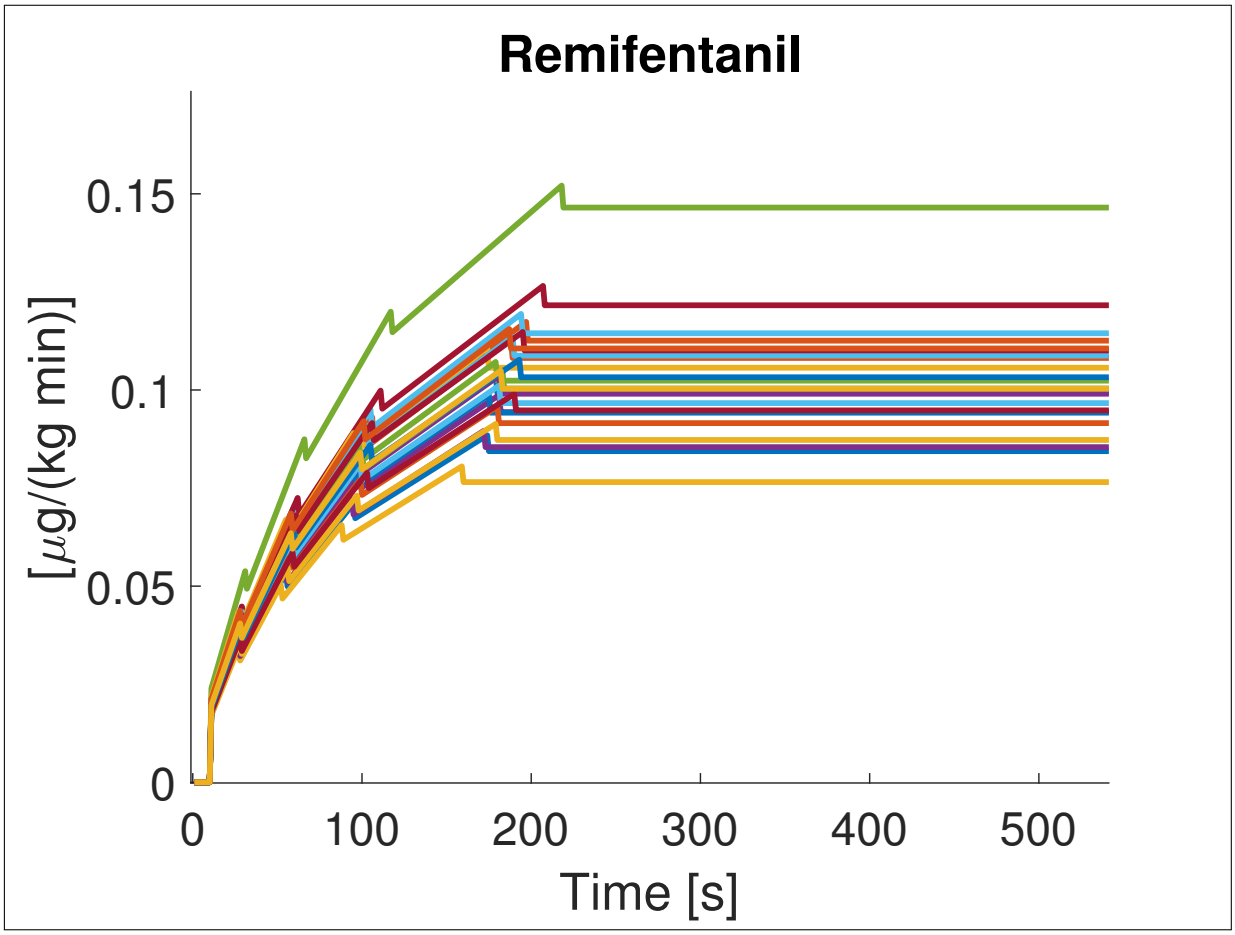

Figure 2.6: PID simulation - Induction phase: Remifentanil

Table 2.3 lists the performance of the PID controller for Remifentanil administration during the induction phase: as even shown in Figure 2.5, the observed time to target (TT) of the RASS follows the indicated timing and the settling time (ST) is equal to the TT since there is no undershoot. Figure 2.6 reports the infusion rates of Remifentanil.

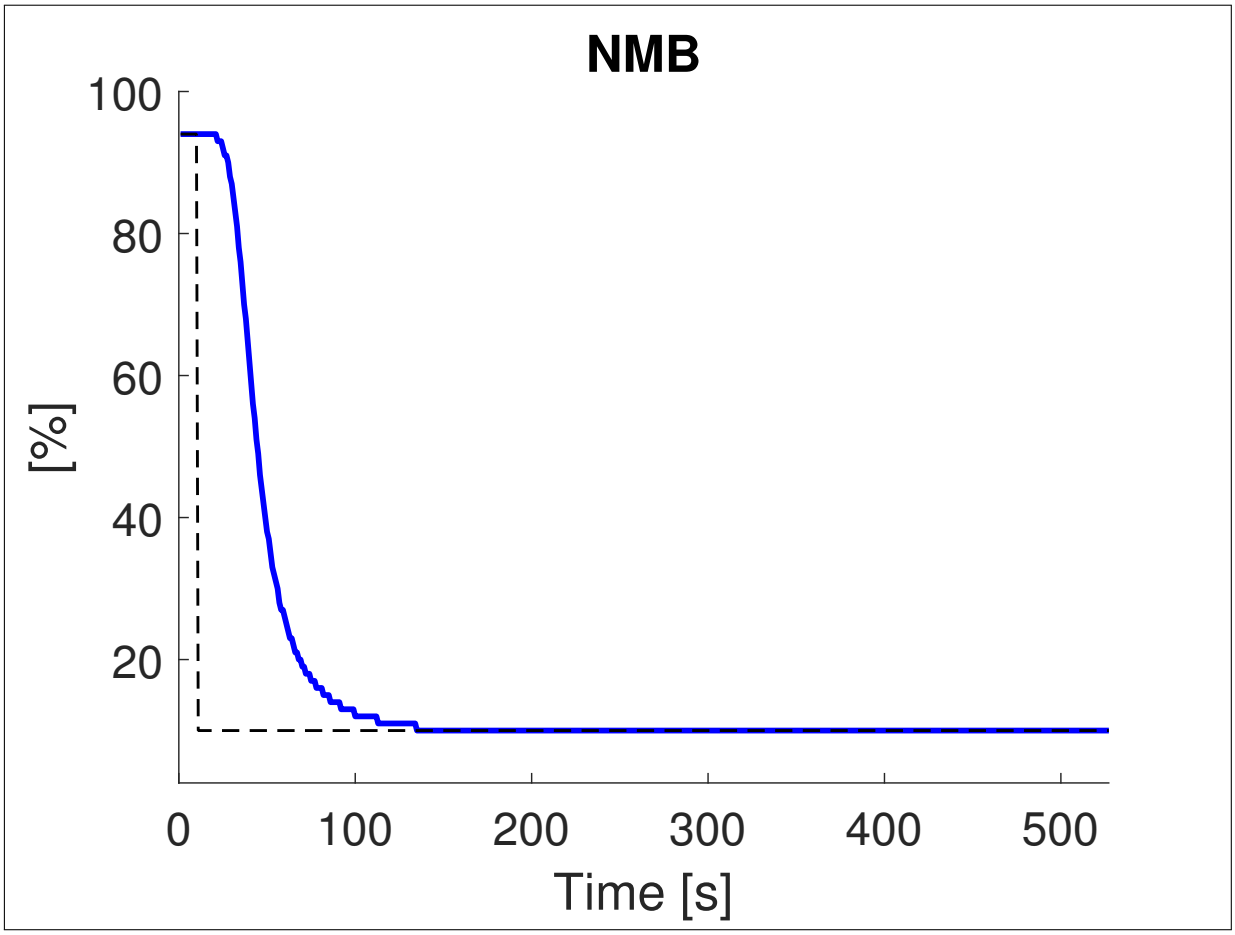

Figure 2.7: PID simulation - Induction phase: NMB

PID performance	
min TT [s]	68
max TT [s]	68
mean TT [s]	68
min NMB-NADIR [%]	10
max NMB-NADIR [%]	10
mean NMB-NADIR [%]	10
min ST [s]	68
max ST [s]	68
mean ST [s]	68
min US [%]	0
max US [%]	0
mean US [%]	0
min PE [%]	0
max PE [%]	840
mean PE [%]	39.83

Table 2.4: Induction phase: PID performance for Atracurium administration

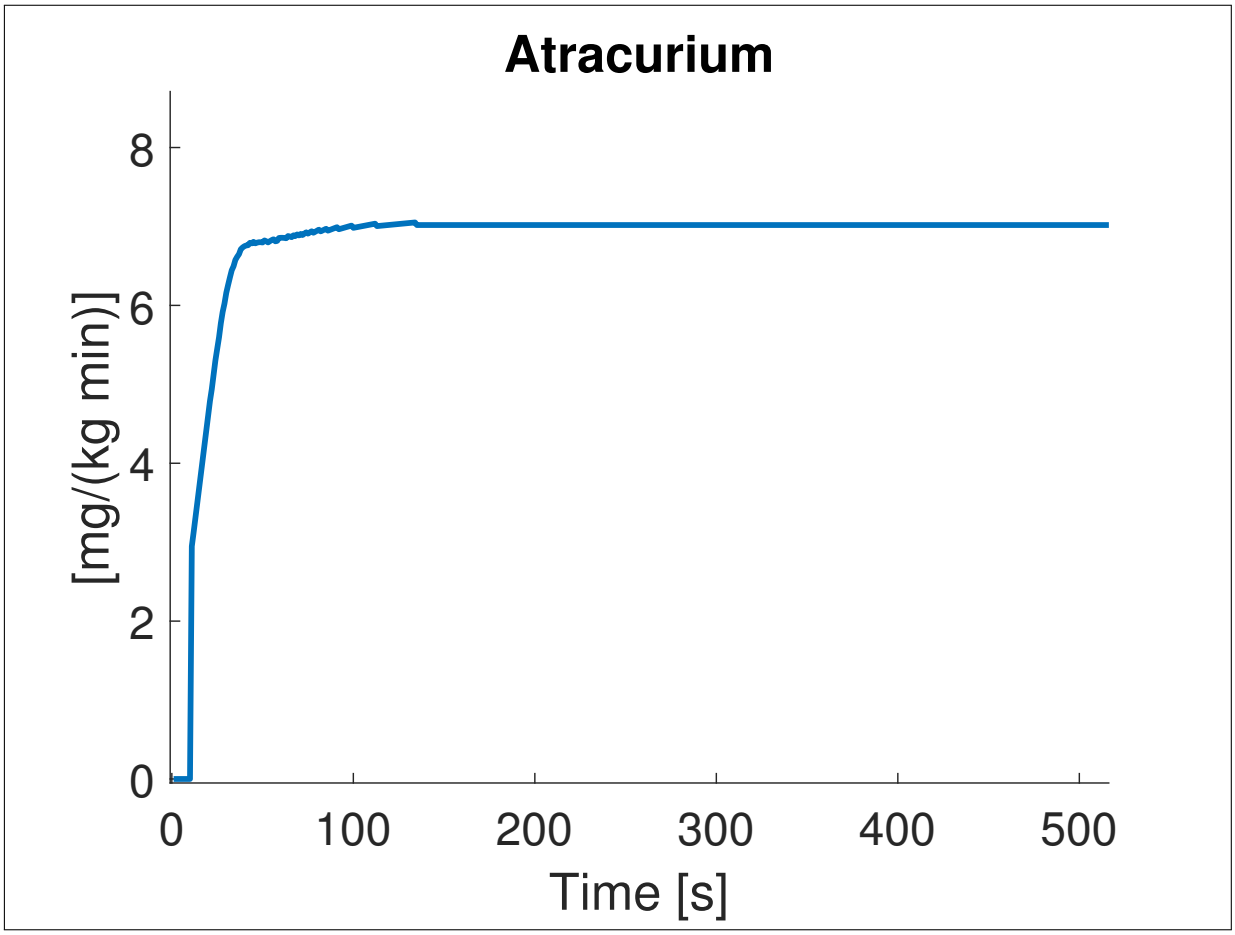

Figure 2.8: PID simulation for comparison with MPC - Induction phase: Atracurium

Table 2.4 lists the performance of the PID controller for Atracurium administration during the induction phase: as even shown in Figure 2.7, the observed time to target (TT) of the RASS follows the indicated timing and the settling time (ST) is equal to the TT since there is no undershoot. The NMB response is equal for all the patients since the Atracurium to NMB model does not include the interpatient variability. Figure 2.8 reports the infusion rates of Atracurium.

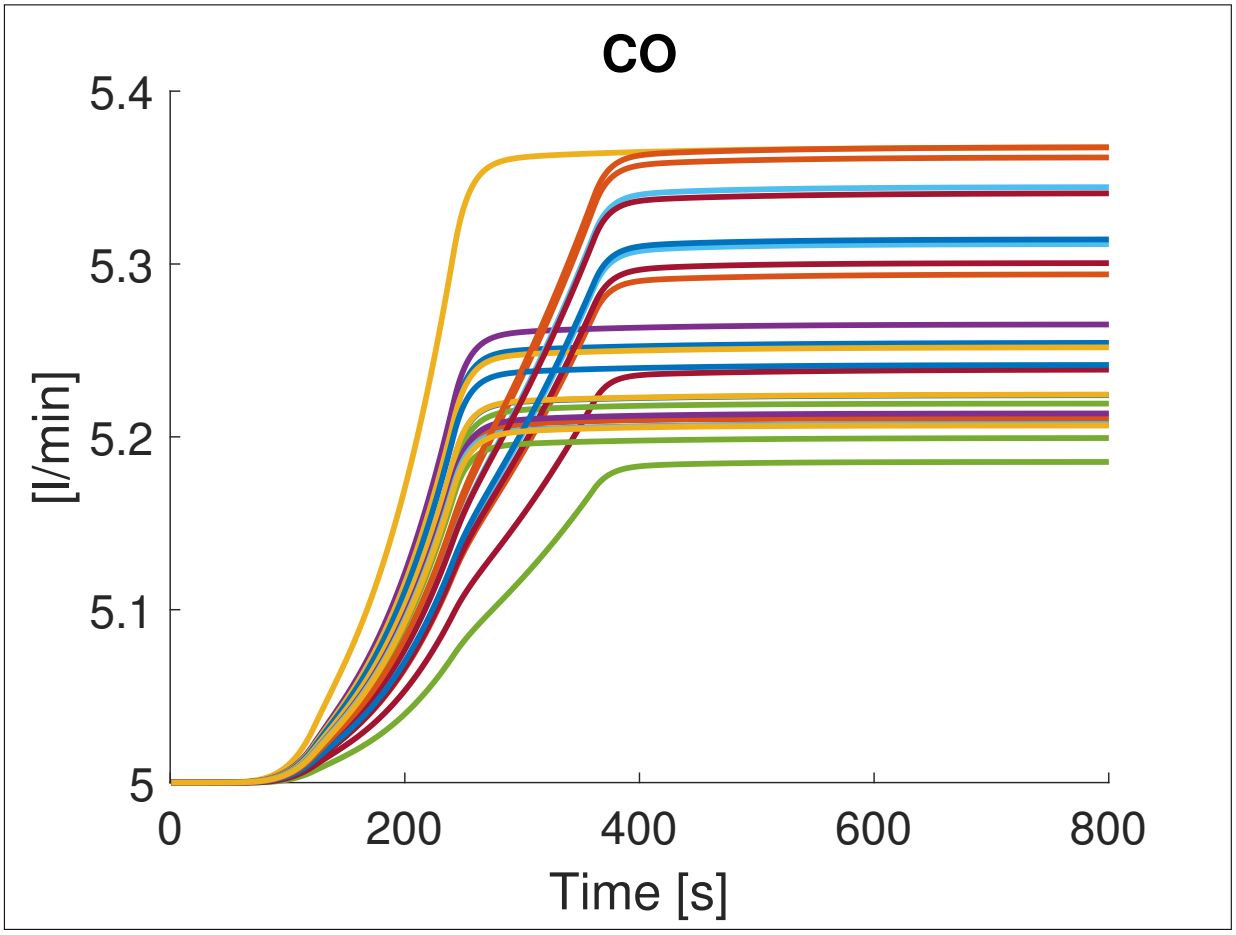

Figure 2.9: PID simulation - Induction phase: CO

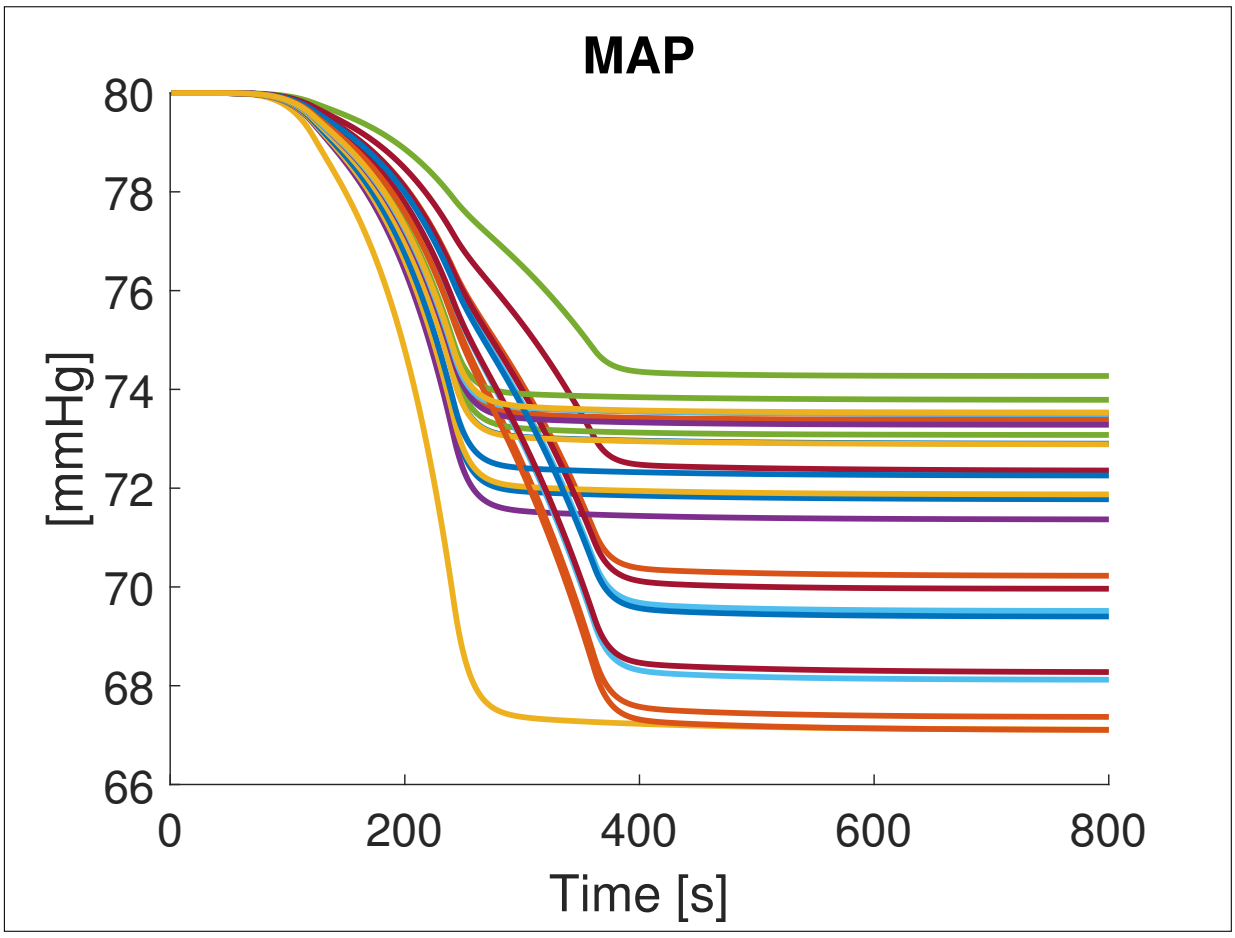

Figure 2.10: PID simulation - Induction phase: MAP

Regarding the hemodynamic system, Figure 2.9 displays the Cardiac output (CO) response to drugs administation, while Figure 2.10 shows the Mean arterial pressure (MAP) outcome. For all the patients, both CO and MAP remain withing the safe intervals indicated in Table 1.8.

2.3 Maintenance phase

Feedback controllers in anesthesia primarily address the disturbance attenuation problem. As explained in Section 1.2.2, the disturbances are due to surgical stimulations. In order to assist the controller in the disturbance rejection task, an additional Propofol dose administered by the anesthesiologist can be included in the simulation. Since the system dynamics is very fast, it was not considered necessary to anticipate the anesthesiologist's action with respect to the beginning of the surgical stimulation. As previously explained, the disturbances act only on the BIS index, thus in this section RASS and NMB are not considered.

As mentioned in Section 2.2, a gain scheduling technique has been performed. Two different controllers have been designed for the two examined phases of anesthesia: initially a PID controller with parameters optimized for the set-point following task has been employed, then, once the target BIS has been achieved, the control has been switched to

another PID with parameters optimized for the disturbance rejection task. As mentioned in [26], by analyzing the results of the optimal tuning methodology it can be observed that the use of a gain scheduling technique may be beneficial.

	$\mathbf{K_p}$ [mg/(kg min)]	$\mathbf{K_i}$ [mg/(kg min^2)]	$\mathbf{K_d}$ [mg/kg]
Propofol - **SP**	0.05	0.0002	0.001
Propofol - **DR**	0.02	0.0001	0.01

Table 2.5: Tuning of PID parameters for SP and DR

Table 2.5 reports the values of the PID gains for the control of Propofol administration during induction phase and maintenance phase. Compared to the tuning for the set-point following task, the proportional gain K_p of the PID controller for the disturbance rejection task has been decreased to avoid oscillatory behaviours in response to the surgical stimulation step; in order to obtain a better disturbance rejection, the derivative gain K_d has been increased and the integral gain K_i has been decreased.
Regarding the performance of the PID control during the maintenance phase, only the TT and the BIS-NADIR indices are meaningful, and they are calculated separately for the positive and for the negative step signals [7]. The indices of the positive step are denoted with the subscript p, those of the negative step with the subscript n.

Simulation results

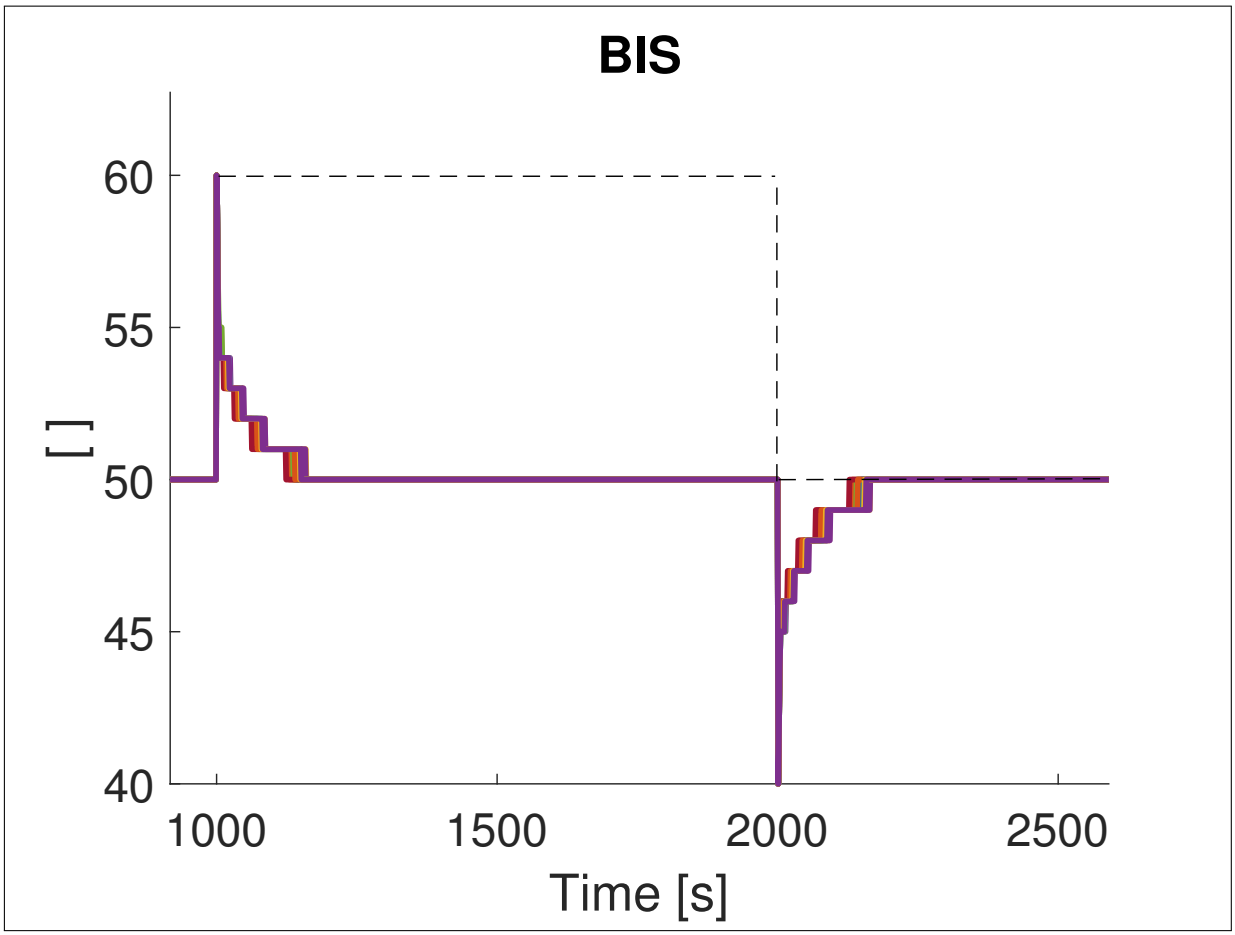

Figure 2.11: PID simulation - Disturbance rejection: BIS response to surgical stimulation

PID performance	
min TT_p [s]	3
max TT_p [s]	4
mean TT_p [s]	3.12
min BIS-$NADIR_p$ [ ]	50
max BIS-$NADIR_p$ [ ]	50
mean BIS-$NADIR_p$ [ ]	50
min TT_n [s]	4
max TT_n [s]	9
mean TT_n [s]	4.87
min BIS-$NADIR_n$ [ ]	50
max BIS-$NADIR_n$ [ ]	50
mean BIS-$NADIR_n$ [ ]	50

Table 2.6: Disturbance rejection: PID performance for Propofol administration - surgical stimulation

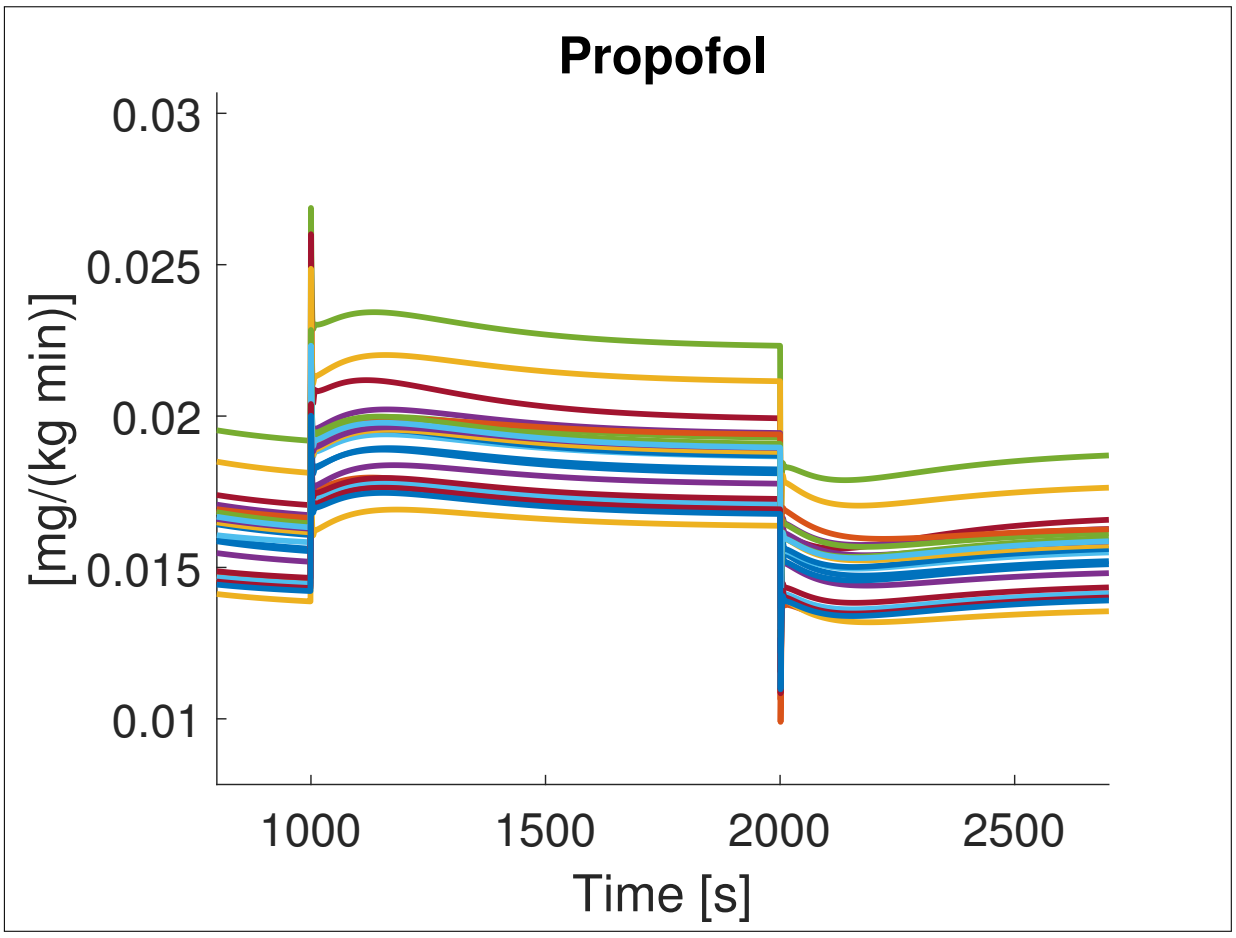

Figure 2.12: PID simulation - Disturbance rejection: Propofol infusion rate in response to surgical stimulation

The performance of the PID controller for Propofol infusion in dealing with the disturbance rejection task is reported in Table 2.6. Figure 2.11 displays the BIS response to the disturbance: after the start of the surgical stimulation, the BIS is rapidly reduced by a bolus of Propofol and is returned to the safe range of [45-55]. After this fast initial reduction of the BIS, the decrease to the target 50 is slightly slower. The patient with the quickest response is patient 7, whose BIS level after the positive step of the disturbance returns to 50 in 124 s, while the slowest is patient 16, whose BIS level returns to 50 in 181 s. Regarding the end of the disturbance, i.e. the negative step, the patient with the quickest response is patient 7 again, whose BIS level returns to 50 in 128 s, while the slowest is patient 16, whose BIS level returns to 50 in 187 s. Figure 2.12 shows the Propofol infusion rates in response to the surgical stimulation. As soon as the disturbance starts, the controller promptly reacts by administering a bolus of Propofol. When the disturbance ends, the BIS instantaneously decreases by 10 %, and the Propofol dose decreases in order to re-establish the reference BIS value.

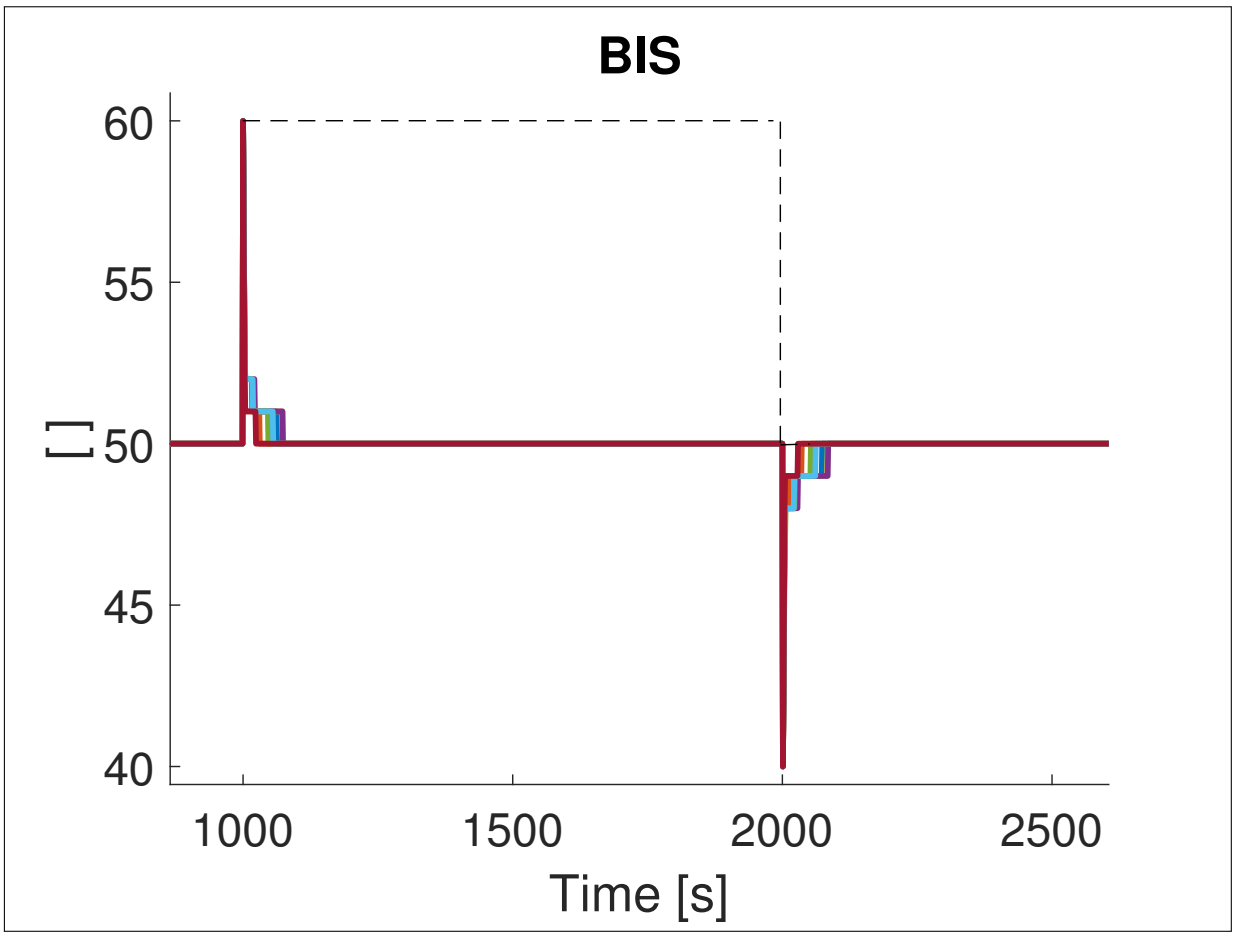

Figure 2.13: PID simulation - Disturbance rejection: BIS response to surgical stimulation and anesthesiologist's action

PID performance	
min TT_p [s]	2
max TT_p [s]	2
mean TT_p [s]	2
min BIS-$NADIR_p$ [ ]	50
max BIS-$NADIR_p$ [ ]	50
mean BIS-$NADIR_p$ [ ]	50
min TT_n [s]	3
max TT_n [s]	4
mean TT_n [s]	3.16
min BIS-$NADIR_n$ [ ]	50
max BIS-$NADIR_n$ [ ]	50
mean BIS-$NADIR_n$ [ ]	50

Table 2.7: Disturbance rejection: PID performance for Propofol administration - surgical stimulation and anesthesiologist's action

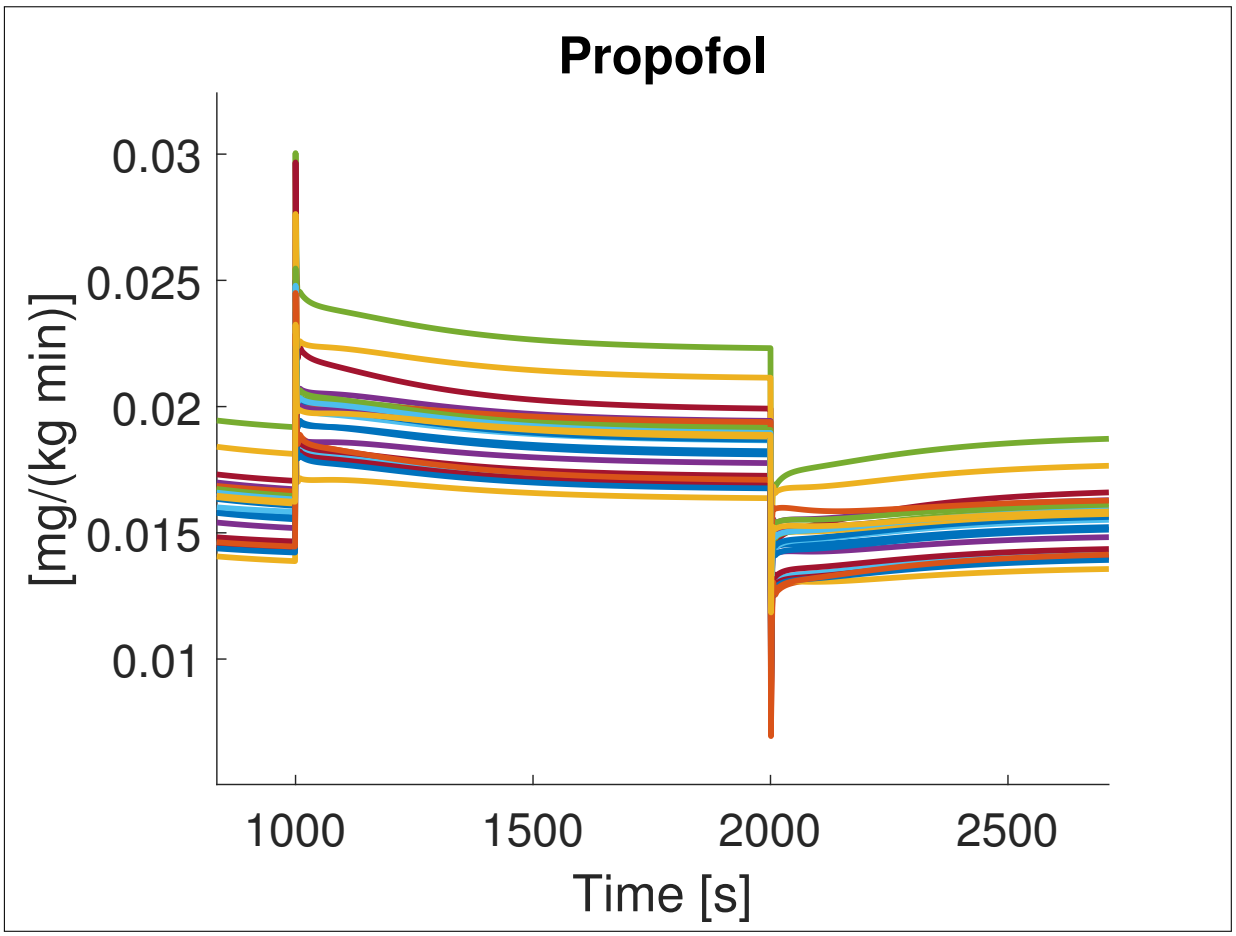

Figure 2.14: PID simulation - Disturbance rejection: Propofol infusion rate in response to surgical stimulation and anesthesiologist's action

If the action of the anesthesiologist is included in the simulation, the performance of the PID controller (see Table 2.7) is better than the case where the Propofol administration is controlled only by the PID (see Table 2.6). As it is possible to verify also from Figure 2.13, the obsereved TT are lower, both for the positive and the negative step. The response of patient 7 is also quicker: its BIS index returns to 50 in 24 s, significantly faster than the previous case. The patient with the slower response is patient 16, whose BIS returns to the target is 107 s. Regarding the negative step, the patient with the quickest response is patient 7 again, whose BIS level returns to 50 in 29 s, while the slowest is patient 16 again, whose BIS level returns to 50 in 119 s. Even in this case, the disturbance rejection task performs better with respect to the simulation without the anesthesiologist's action. Figure 2.14 shows the Propofol infusion rates determined by the PID controller in response to the surgical stimulation, when also the additional Propofol dose is administered by the anesthesiologist. The disturbance rejection has been obtained without under- or over-shoots in both cases.

2.4 Noise

As described in Section 2.4, it is possible to include the presence of noise on the BIS index. The presence of this BIS related high amplitude noise is a relevant issue [26], thus a low-pass online filter has been employed in order to reduce it. The considered low-pass filter has the following discrete transfer function:

$$G(z) = K\frac{\frac{T_s}{T}z^{-1}}{1+(\frac{T_s}{T}-1)z^{-1}} \tag{2.7}$$

where K is the filter gain (obviously set to 1), T is the filter time constant and T_s is the sampling time. The pole of the filter is located in $z = 1 - \frac{T_s}{T}$.
In order to ensure a better visualization of the filtering process, the following figures refer only to patient 1.

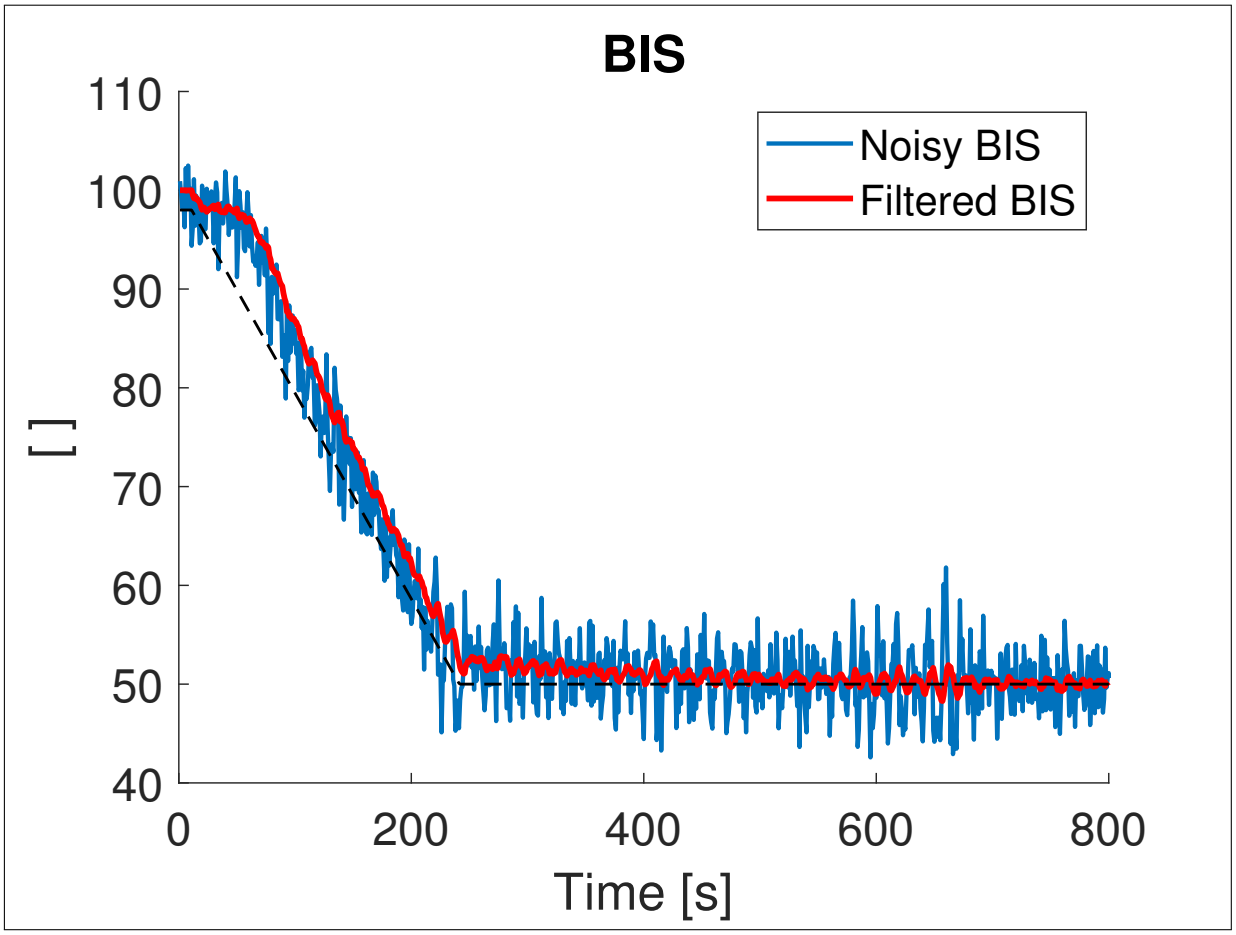

Figure 2.15: PID simulation - Induction phase: noisy and filtered BIS (T = 10)

Regarding the induction phase, the filtered BIS signal shown in Figure 2.15 is obtained by setting the filter time constant T = 10, resulting in a pole located in z = 0.9. By increasing T, the filtered BIS would be smoother, but would also increase the delay with which the signal is estimated, compared to the original (noisy) one.

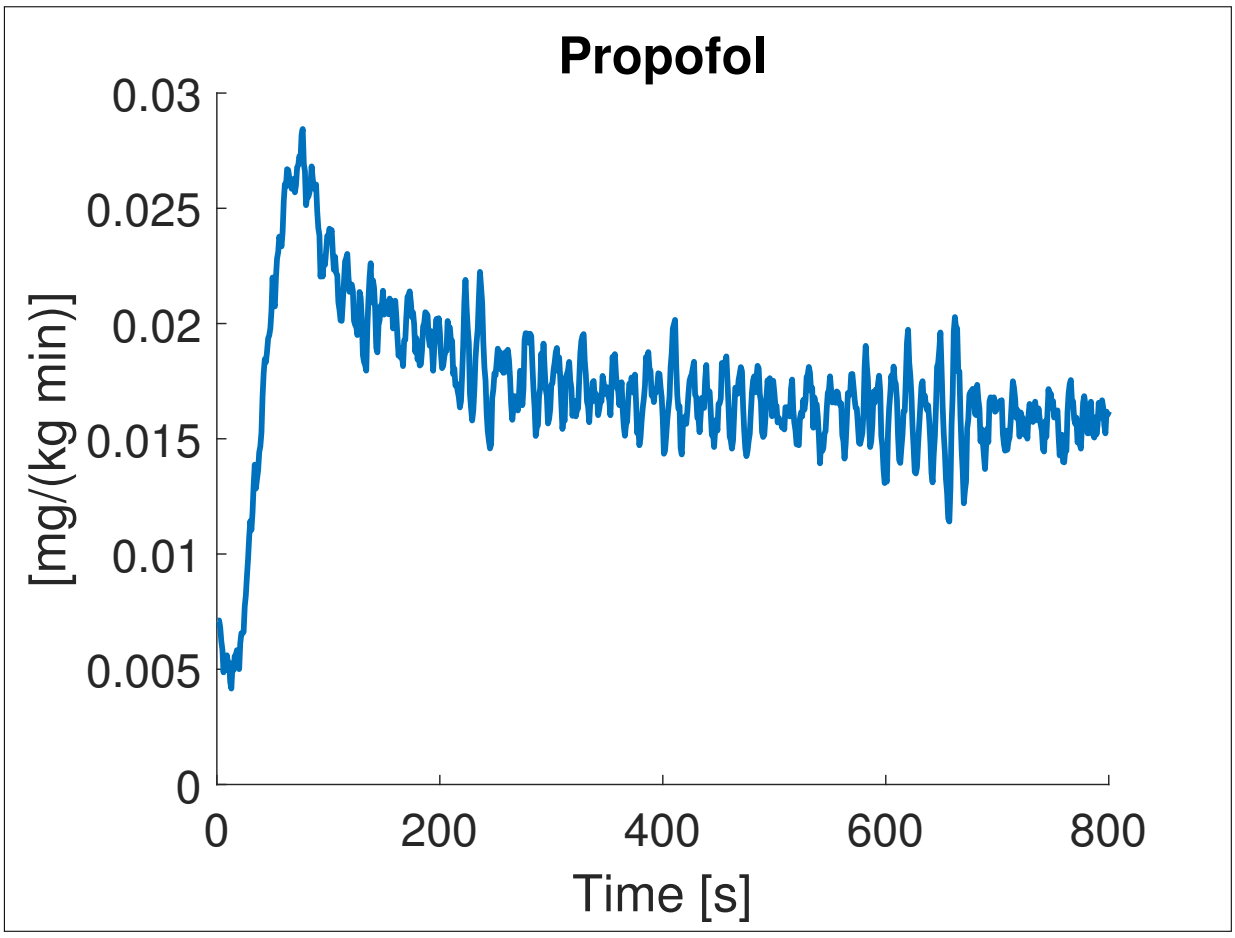

Figure 2.16: PID simulation - Induction phase: Filtered Propofol dose (T = 10)

Figure 2.16 displays the filtered Propofol infusion rate during the induction phase, using a filter time constant of T = 10.

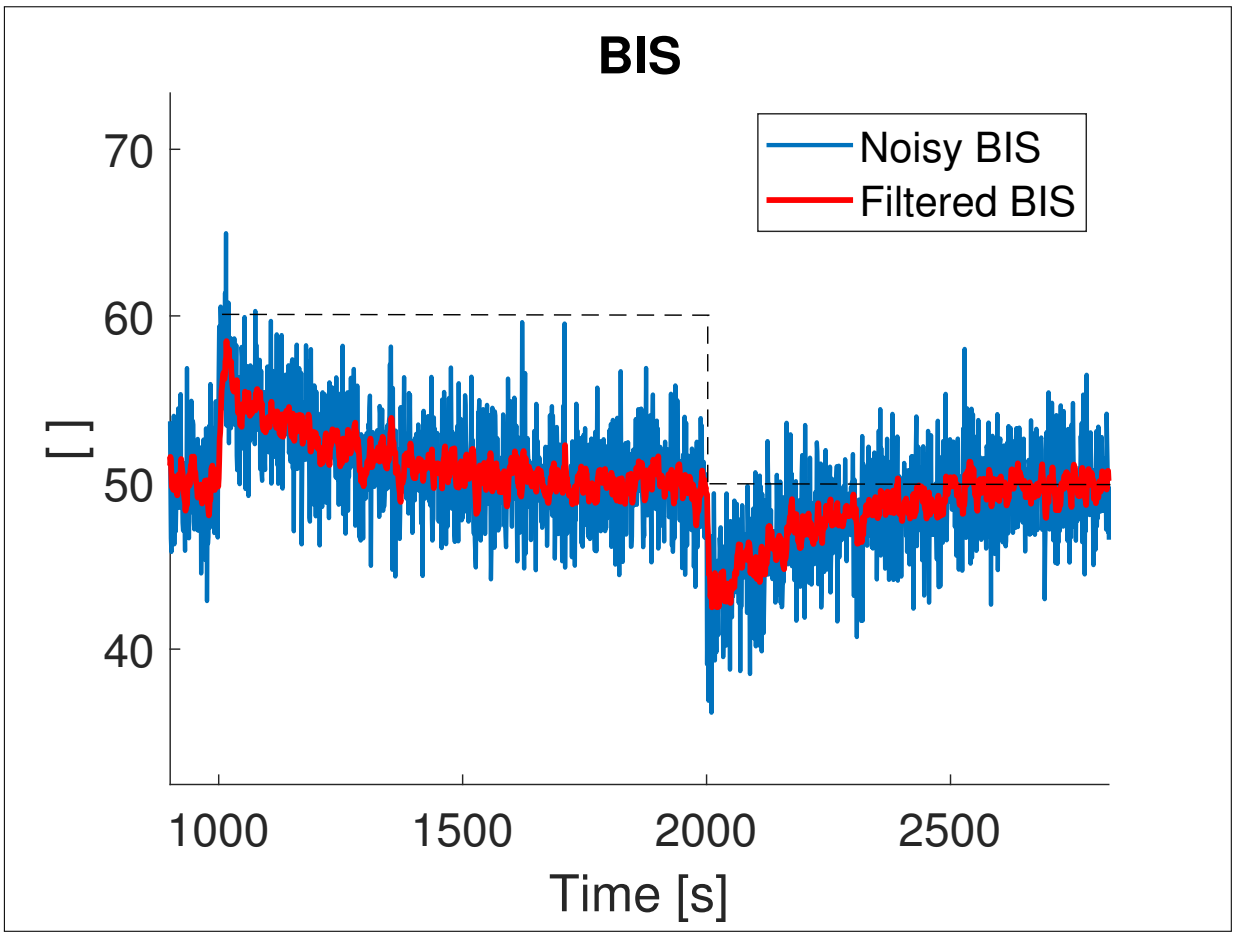

Figure 2.17: PID simulation - Maintenance phase: noisy and filtered BIS (T = 6)

Regarding the maintenance phase, the filtered BIS signal shown in Figure 2.17 has been obtained by setting the filter time constant T = 6, resulting in a pole located in z = 0.83. The BIS is smoother than the original one, but is also distorted by the filter, with respect to the noise free simulation. In fact, the positive step achieves a value of 58 instead of 60, while the negative step a value of 42 instead of 40.

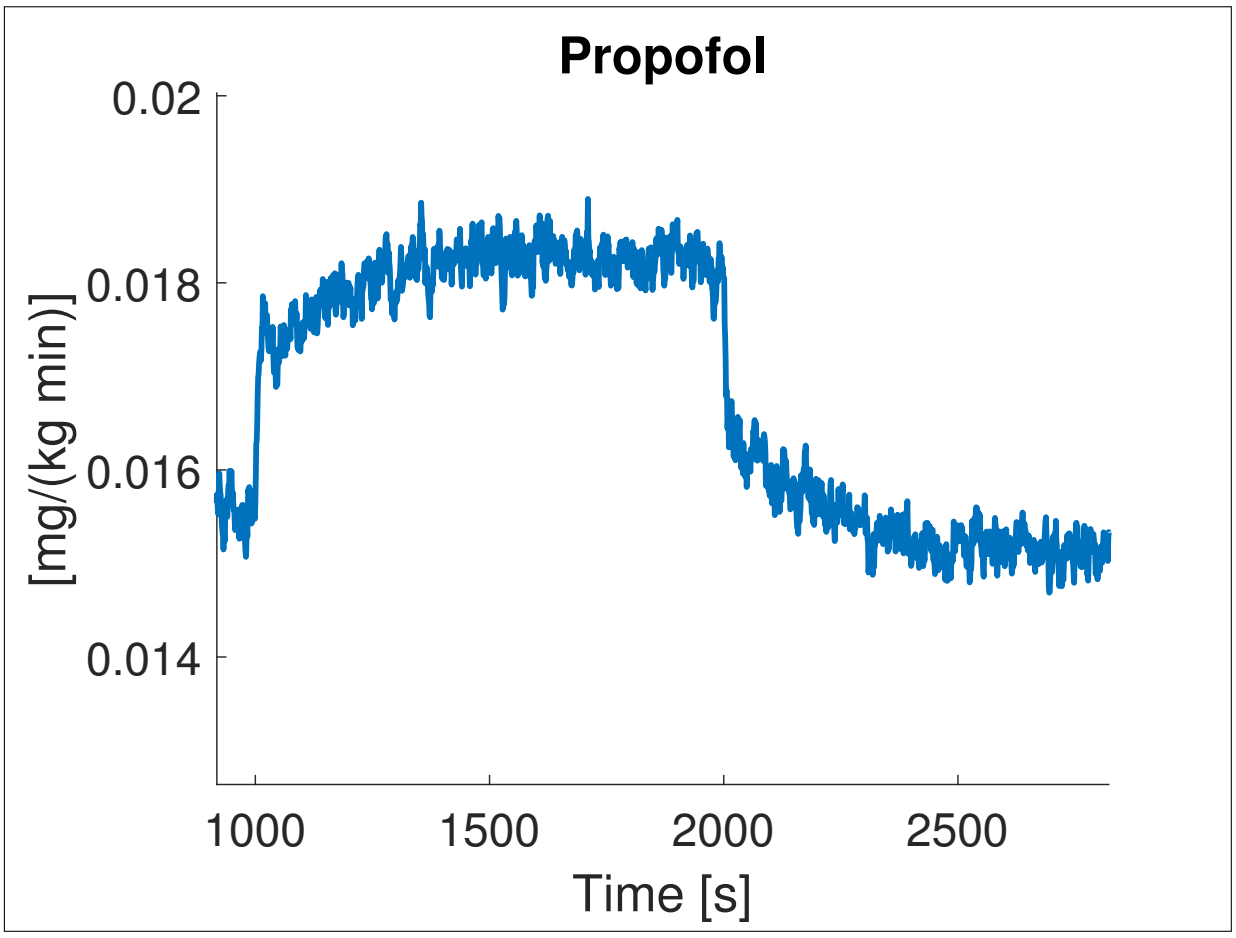

Figure 2.18: PID simulation - Maintenance phase: Filtered Propofol dose (T = 6)

Figure 2.18 shows the filtered Propofol infusion rate during the maintenance phase, concerning the case in which the filter time constant has been set to T = 6. With respect to the noise free case, the PID response to the surgical stimulation is different, especially in the initial instants. In Figure 2.18, the initial bolus is indeed significantly reduced with respect to Figure 2.12, resulting in a slower disturbance rejection, as can be seen in Figure 2.17.

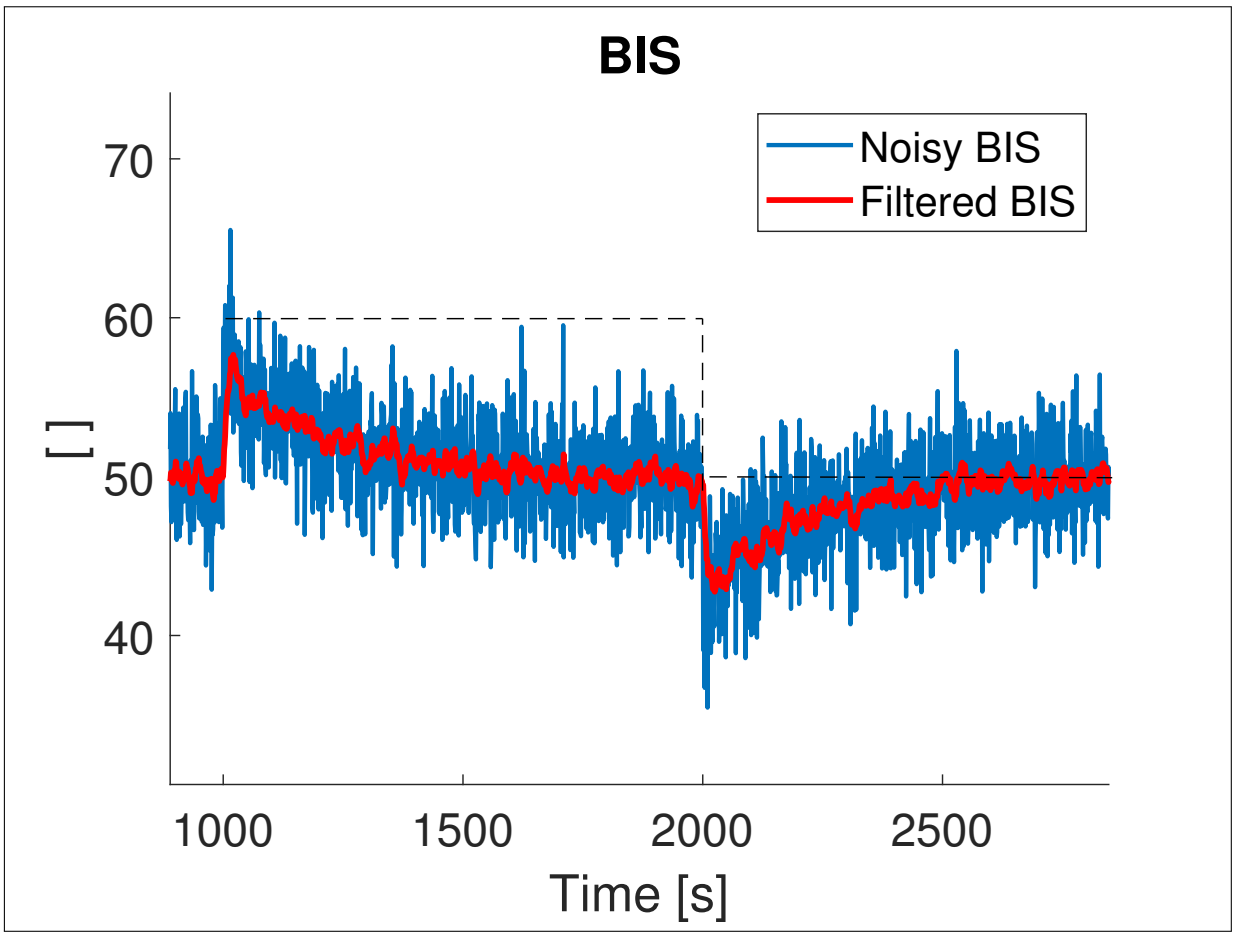

Figure 2.19: PID simulation - Maintenance phase: noisy and filtered BIS (T = 10)

The filtered BIS signal shown in Figure 2.19 has been obtained by setting the filter time constant T = 10, resulting in a pole located in z = 0.9. Compared to the signal filtered with a time constant T = 6, the BIS is smoother, but the distortion is more pronounced. Indeed, the positive step achieves a value of 57 instead of 58 of the previous case, while the negative step a value of 43 instead of 42.

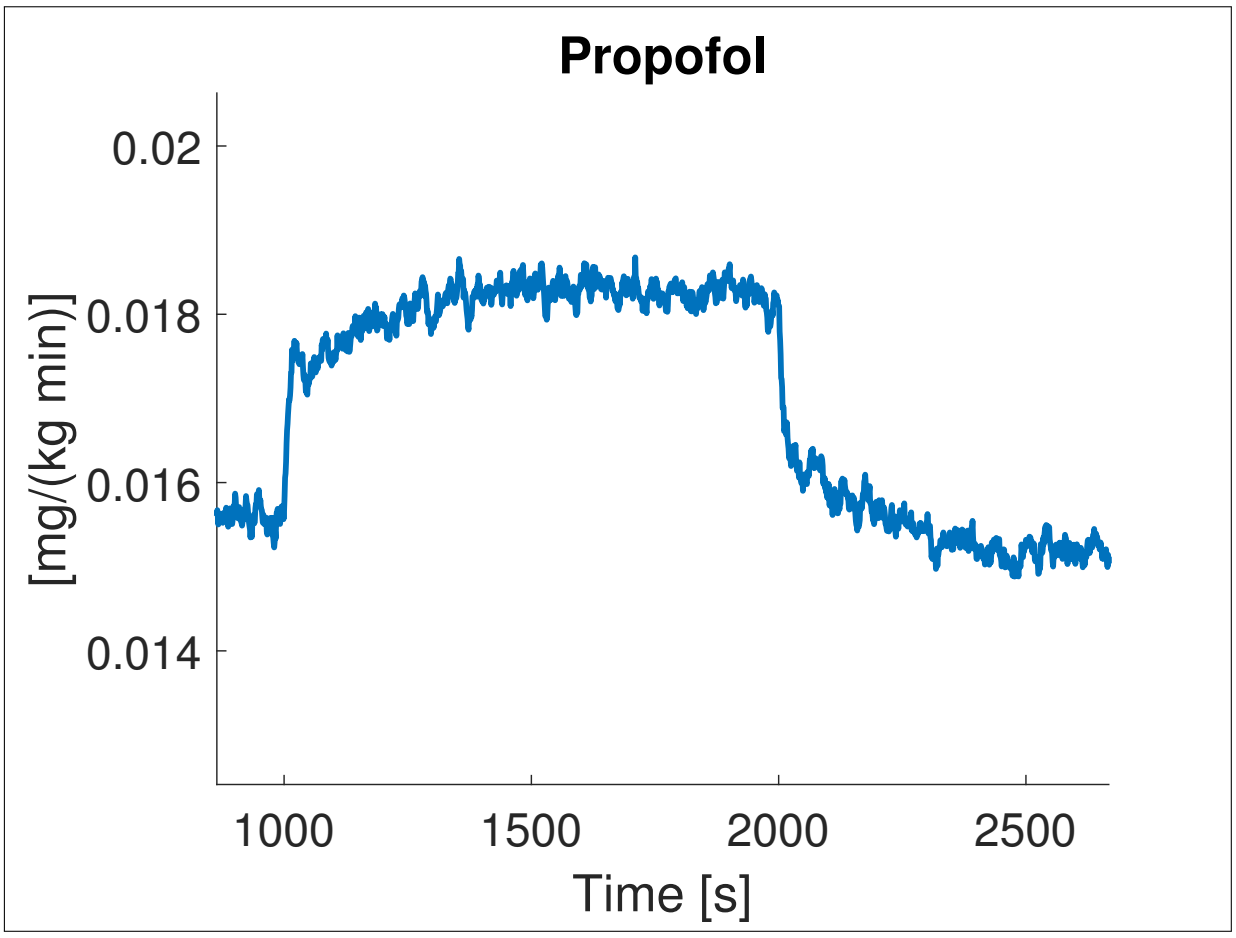

Figure 2.20: PID simulation - Maintenance phase: Filtered Propofol dose (T = 10)

Figure 2.20 shows the filtered Propofol infusion rate during the maintenance phase, concerning the case in which the filter time constant has been set to T = 10. Compared to the Propofol administration with T = 6, the initial Propofol bolus is even more reduced.

2.5 Different set-up

In order to make the simulation more physiological, the parameters of the Hill function of the Propofol to BIS model have been individualized for each patient (see Table 2.8). In this case, the PD sensitivity values vary among the population. Moreover, the sampling time of the simulator is T_s = 1 s, but RASS and NMB need a higher sampling time. Since RASS is measured by clinicians, its sampling time has been set to 120 s, while NMB sampling time has been set to 20 s. BIS sampling time has not been changed. The simulation with this set-up modifications has been performed both for the induction and maintenance phases of anesthesia.

Index	$\mathbf{C_{50}}$	$\boldsymbol{\gamma}$	$\mathbf{E_0}$	$\mathbf{E_{max}}$
-	[mg/ml]	[ ]	[ ]	[ ]
1	2.5	3	98	94
2	4.6	2	98	86
3	5	1.6	91	80
4	1.8	2.5	95	102
5	6.8	1.78	94	85
6	2.7	2.8	90	112
7	2.3	4	92	104
8	7.8	2.9	95	76
9	2.9	1.88	90	63
10	3.9	3.1	90	121
11	2.3	3.1	91	77
12	4.8	2.1	96	90
13	2.5	3	93	96
14	2.5	3	97	78
15	4.3	1.9	98	94
16	2.7	1.6	95	80
17	4.5	1.9	98	82
18	2.7	1.78	92	79
19	6.8	3.1	97	91
20	9.8	1.6	91	103
21	3.2	2.1	92	90
22	5.1	2.51	98	121
23	3.67	3.1	96	85
24	5.8	2.3	93	87

Table 2.8: Patients database: PD model sensitivity values

2.5.1 Induction phase

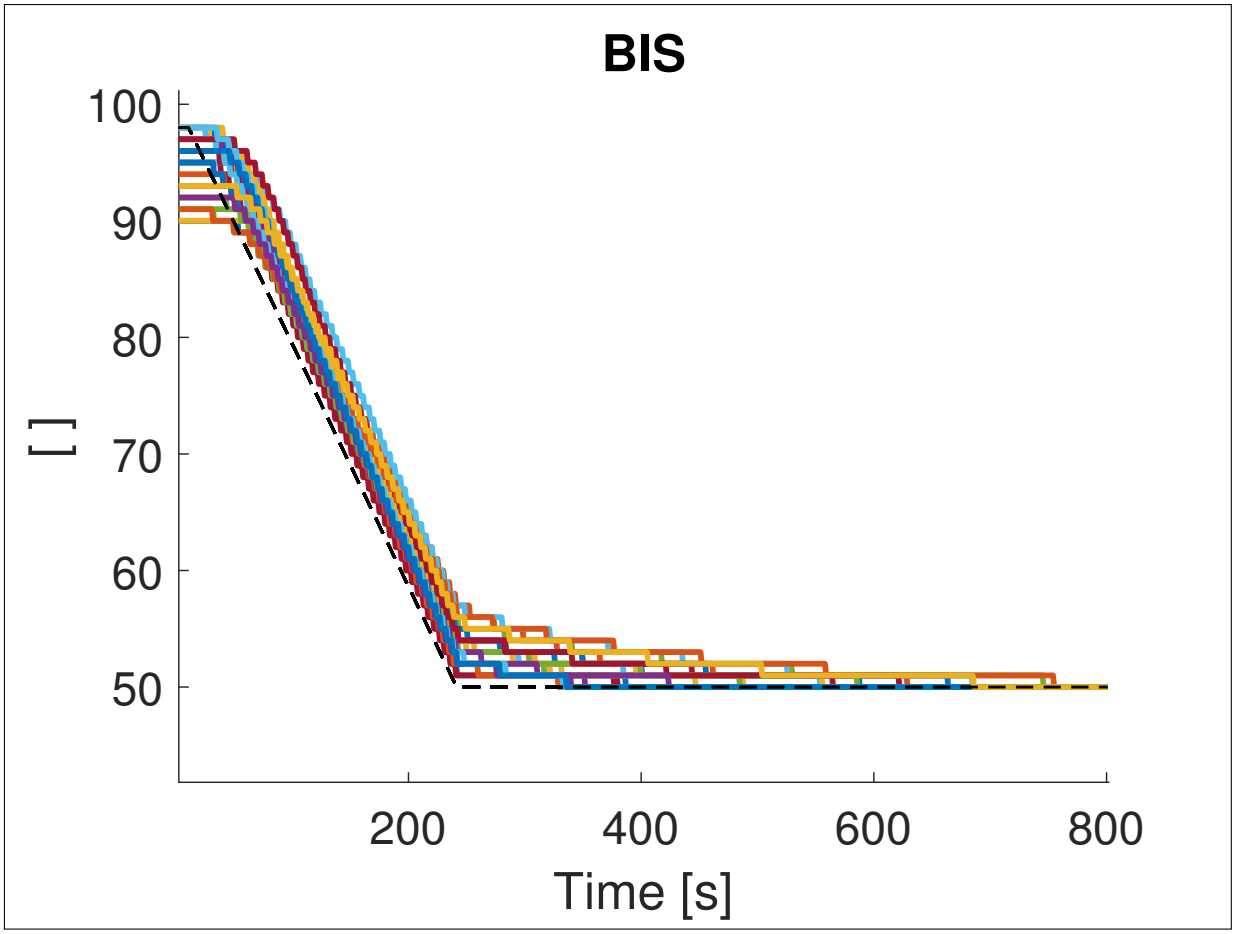

Figure 2.21: PID simulation with different set-up - Induction phase: BIS

PID performance	
min TT [s]	223
max TT [s]	281
mean TT [s]	239.04
min BIS-NADIR [ ]	50
max BIS-NADIR [ ]	50
mean BIS-NADIR [ ]	50
min ST [s]	223
max ST [s]	281
mean ST [s]	239.04
min US [%]	0
max US [%]	0
mean US [%]	0
min PE [%]	0
max PE [%]	7.98
mean PE [%]	2.89

Table 2.9: Induction phase: PID performance for Propofol administration - Simulation with different set-up

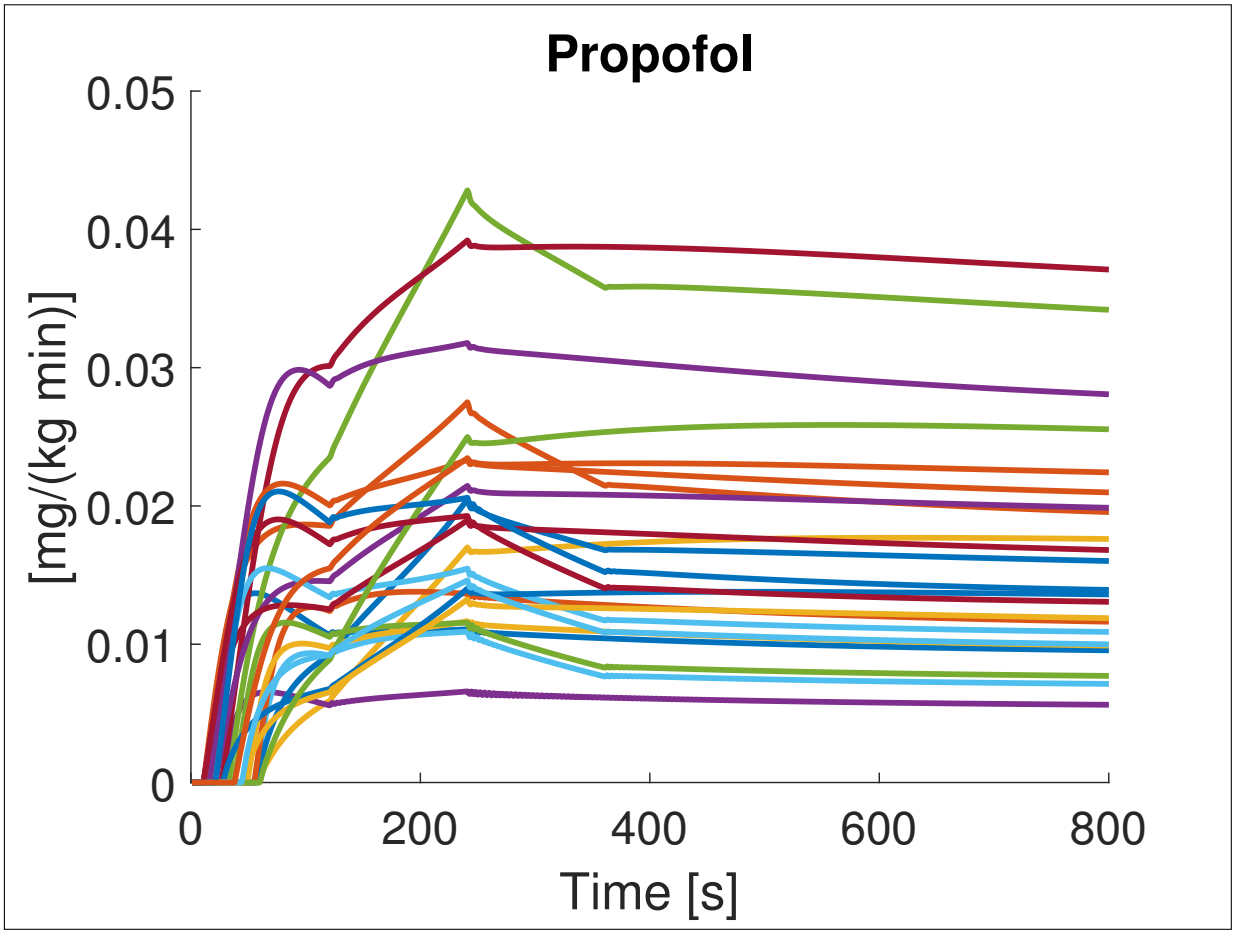

Figure 2.22: PID simulation with different set-up - Induction phase: Propofol

Compared to the case where the interpatient variability on the Propofol PD model has been included (see Figure 2.21), the difference is straightforward: in this case, there is no variation in the baseline value of the patients, and the lack of individualization of the Hill function parameters γ and C_{50} makes the patient responses very similar to each other. The performance (see Table 2.2) is also better in this case: with respect to the case where the interpatient variability on the PD model is considered, the time to target indices are lower, as well as the performance errors. Figure 2.4 shows the Propofol infusion rates concerning the simulation with no interpatient variability on the Propofol PD model. This case is of course less physiological with respect to the case with individualized PD model parameters.

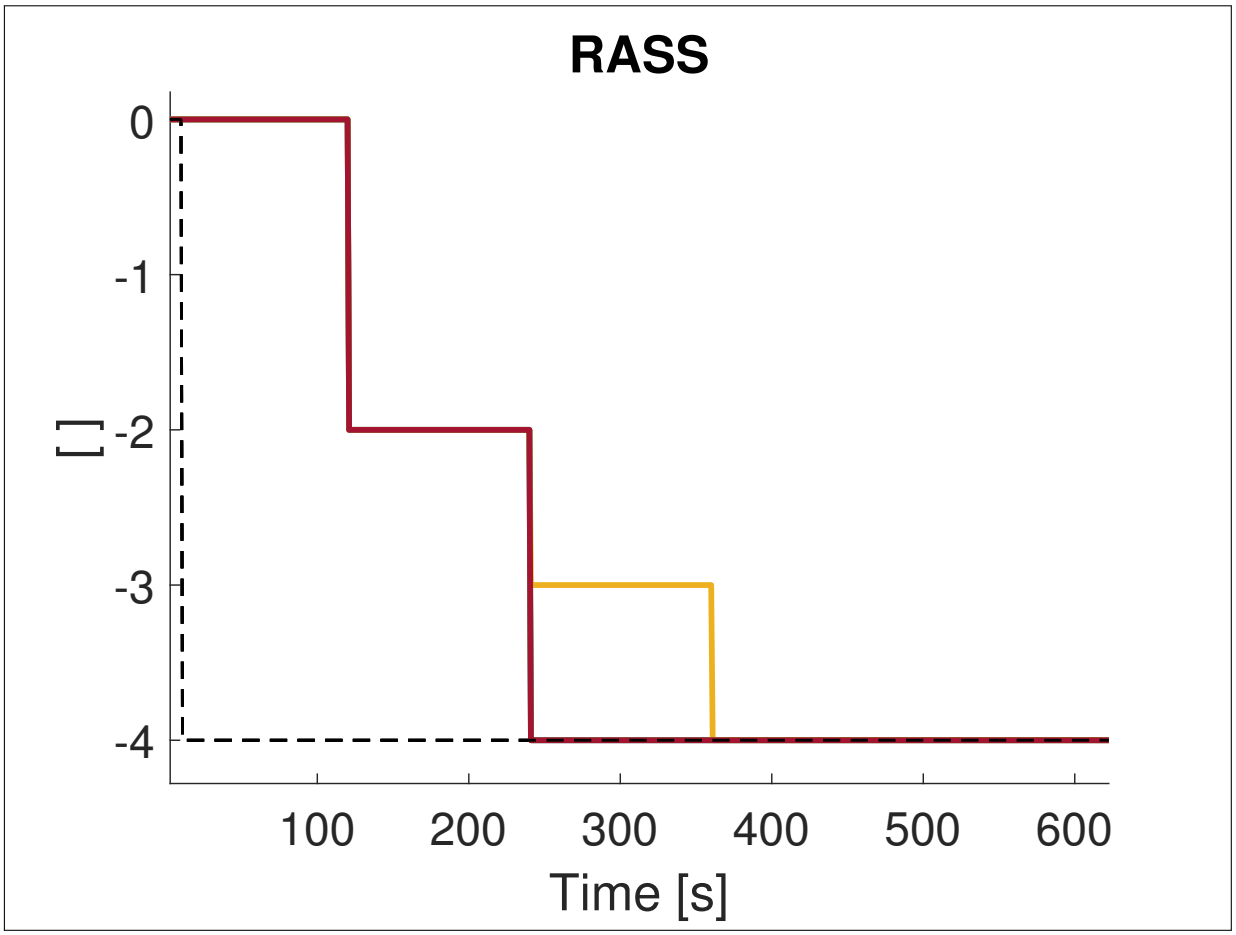

Figure 2.23: PID simulation with different set-up - Induction phase: RASS

PID performance	
min TT [s]	241
max TT [s]	361
mean TT [s]	291
min RASS-NADIR [ ]	-4
max RASS-NADIR [ ]	-4
mean RASS-NADIR [ ]	-4
min ST [s]	241
max ST [s]	361
mean ST [s]	291
min US [%]	0
max US [%]	0
mean US [%]	0
min PE [%]	0
max PE [%]	100
mean PE [%]	18.23

Table 2.10: Induction phase: PID performance for Remifentanil administration - Simulation with different set-up

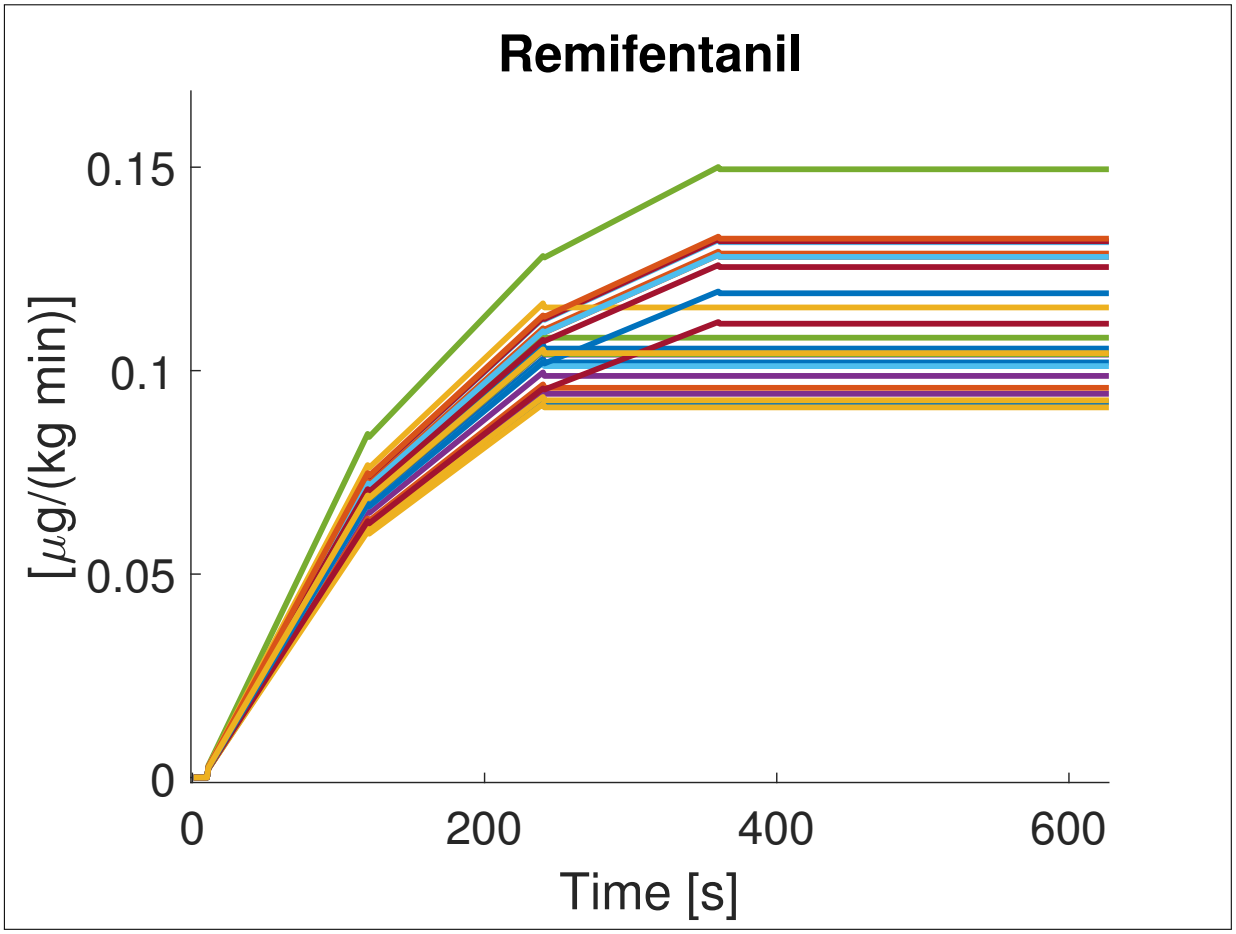

Figure 2.24: PID simulation with different set-up - Induction phase: Remifentanil

Compared to the case with $T_s = 1$ s, the set-point following task for the RASS is slower, as can be seen from Figure 2.23 and Table 2.10. In fact, the minimum, maximum and mean time to target indices are higher, as well as the performance errors. The settling time is equal to the time to target, with 14 patients reaching the target -4 in 241 s ($2T_s$) and the remaining 10 patients in 361 s ($3T_s$). The Remifentanil infusion rates, illustrated in Figure 2.24, clearly show the interpatient variability.

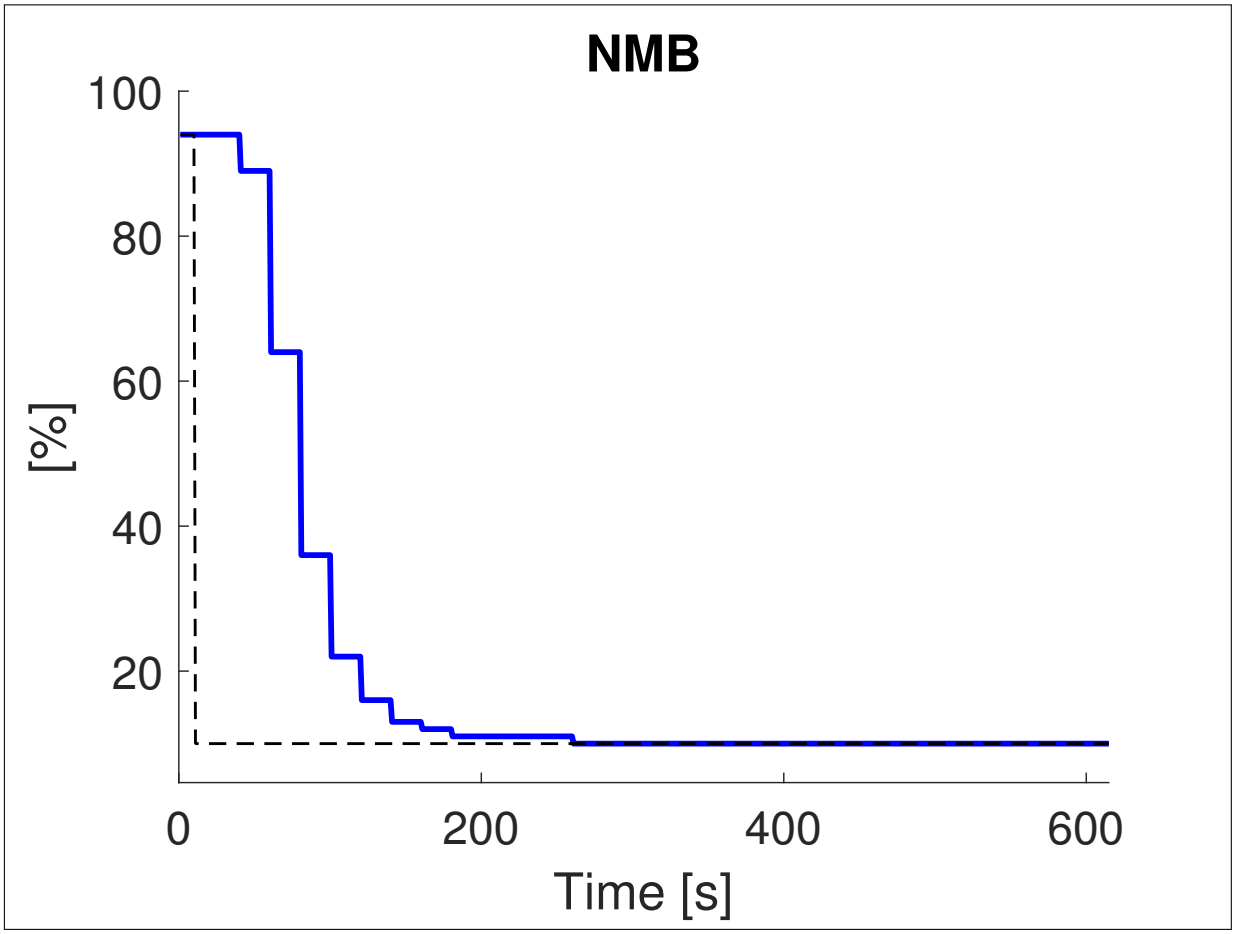

Figure 2.25: PID simulation with different set-up - Induction phase: NMB

PID performance	
min TT [s]	68
max TT [s]	68
mean TT [s]	68
min NMB-NADIR [%]	10
max NMB-NADIR [%]	10
mean NMB-NADIR [%]	10
min ST [s]	121
max ST [s]	121
mean ST [s]	121
min US [%]	0
max US [%]	0
mean US [%]	0
min PE [%]	0
max PE [%]	840
mean PE [%]	62.34

Table 2.11: Induction phase: PID performance for Atracurium administration - Simulation with different set-up

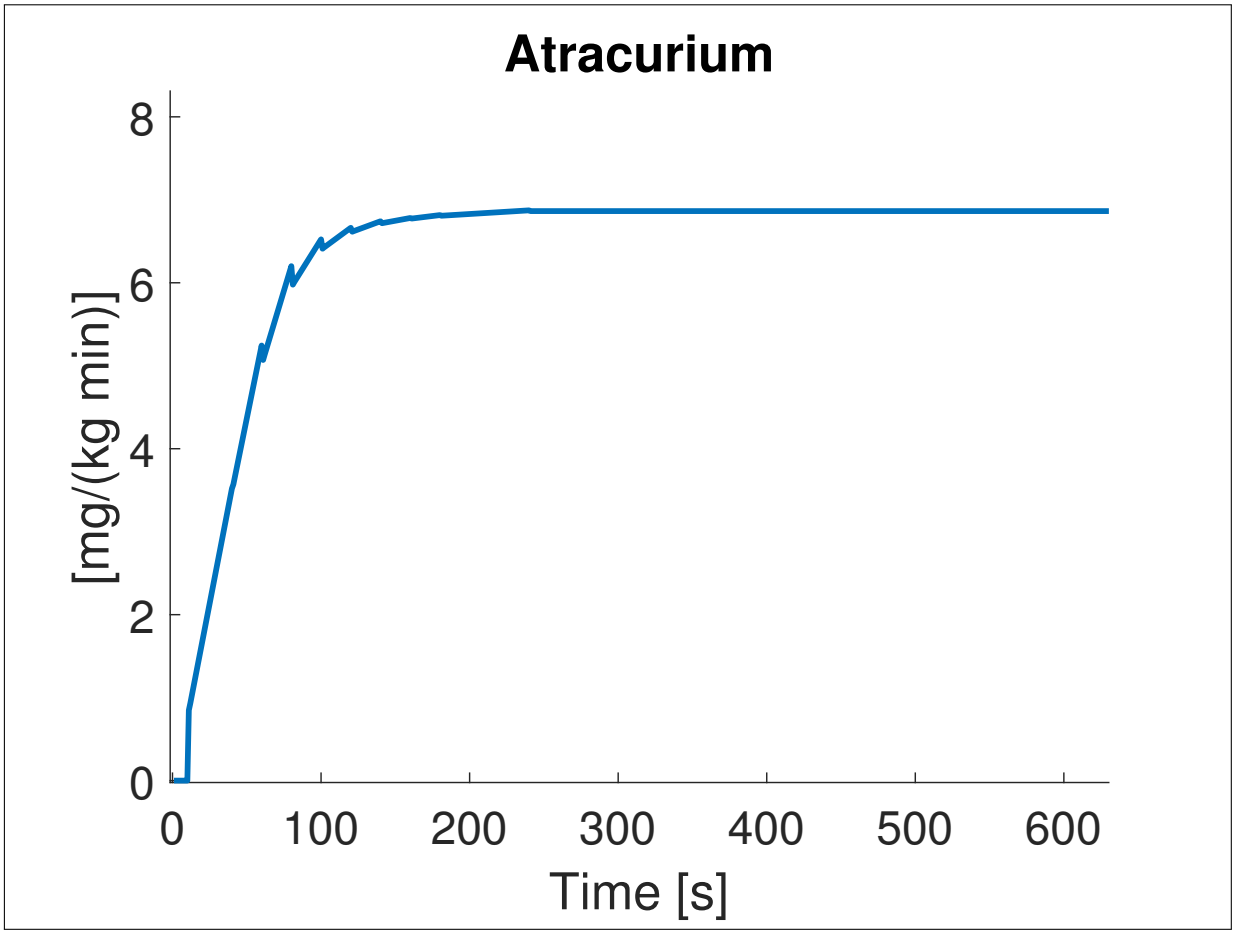

Figure 2.26: PID simulation with different set-up - Induction phase: Atracurium

Compared to the case with $T_s = 1$ s, the set-point following task for the NMB is slower, as can be seen from Figure 2.25 and Table 2.11. Indeed, the minimum, maximum and mean time to target indices are higher, as well as the mean performance errors. The settling time is equal to the time to target since there is no undershoot.

2.5.2 Maintenance phase

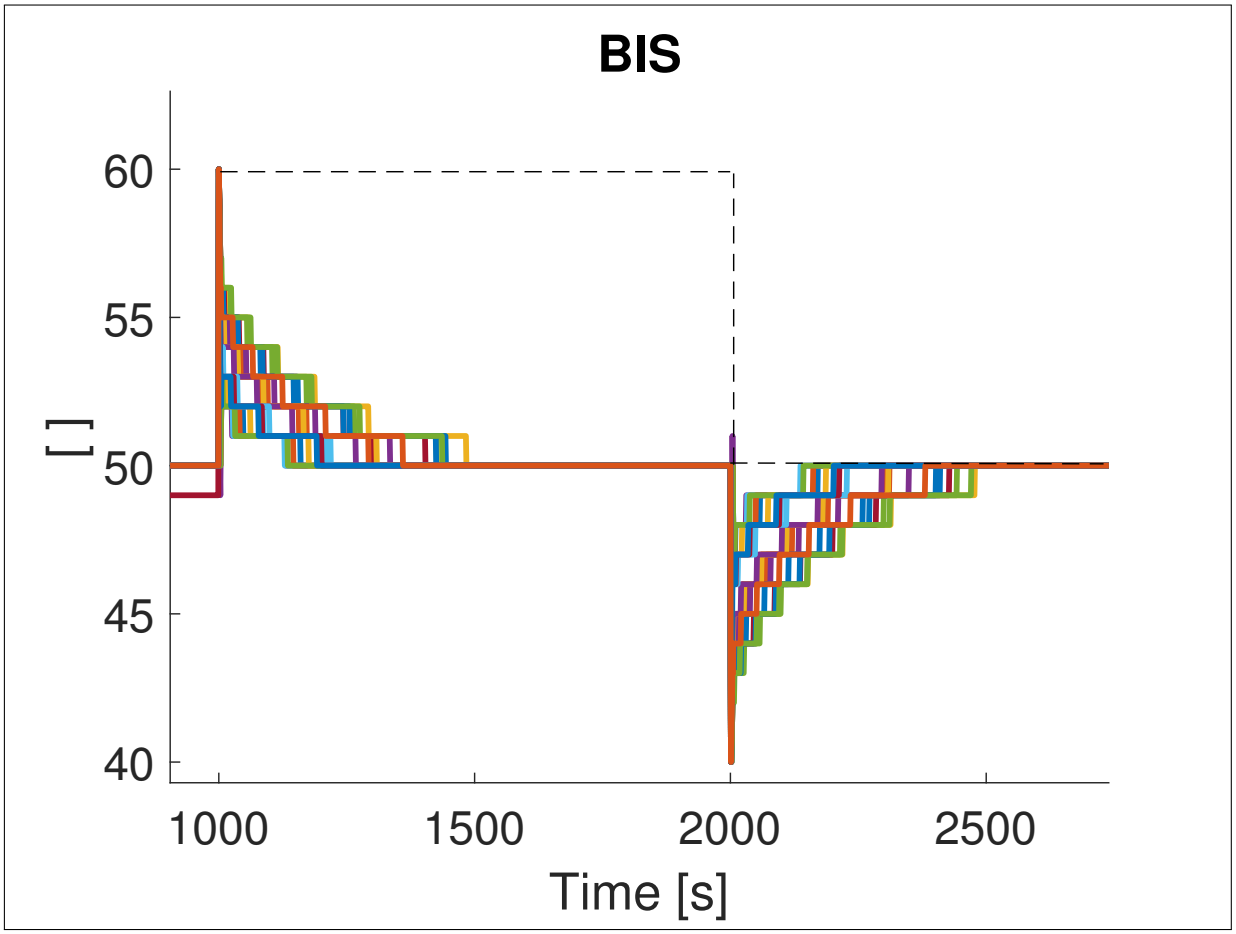

Figure 2.27: PID simulation with different set-up - Disturbance rejection: BIS response to surgical stimulation

PID performance	
min TT_p [s]	2
max TT_p [s]	25
mean TT_p [s]	6.26
min BIS-NADIR$_p$ [ ]	50
max BIS-NADIR$_p$ [ ]	50
mean BIS-NADIR$_p$ [ ]	50
min TT_n [s]	3
max TT_n [s]	58
mean TT_n [s]	16.87
min BIS-NADIR$_n$ [ ]	50
max BIS-NADIR$_n$ [ ]	51
mean BIS-NADIR$_n$ [ ]	50.04

Table 2.12: Disturbance rejection: PID performance for Propofol administration - surgical stimulation - Simulation with different set-up

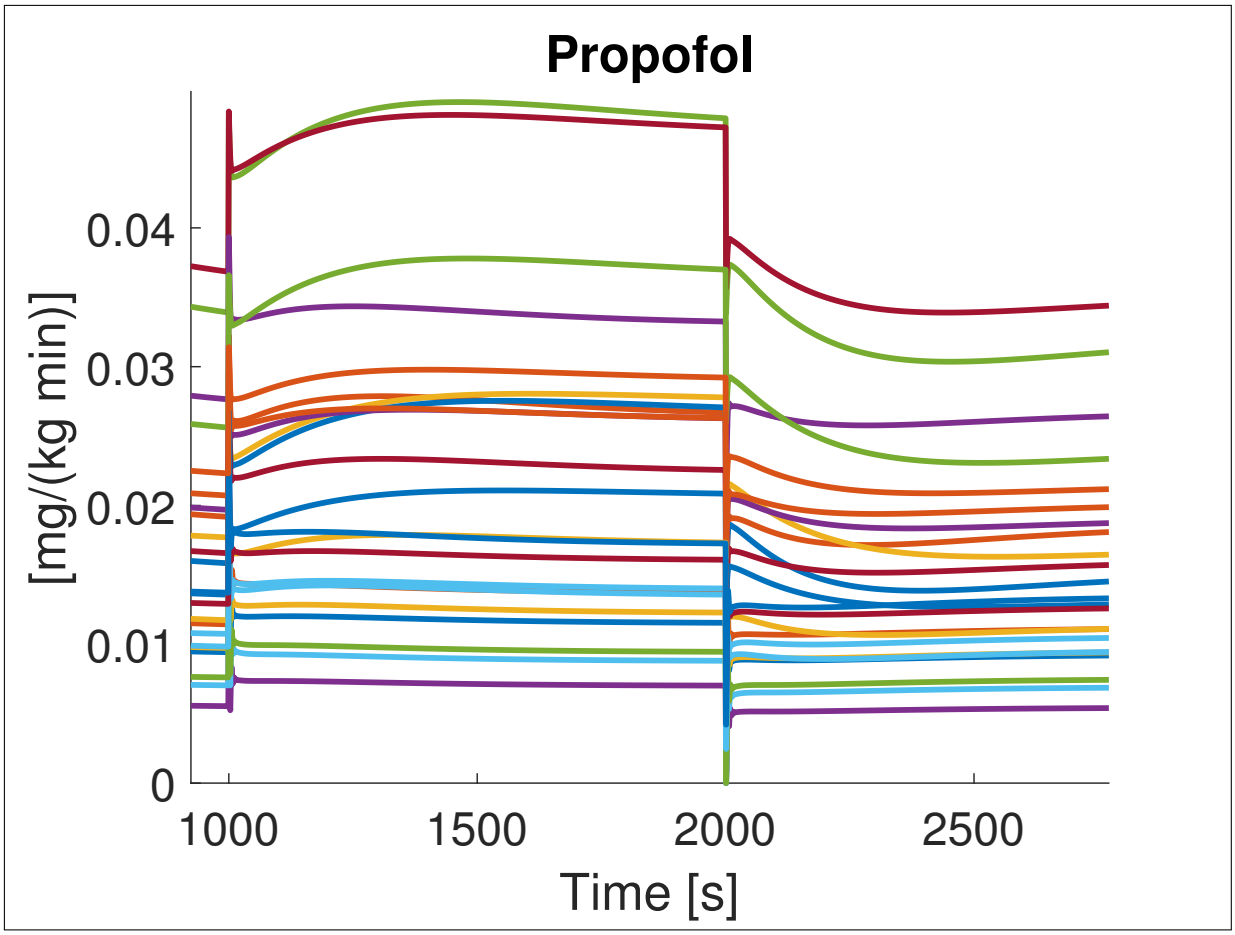

Figure 2.28: PID simulation with different set-up - Disturbance rejection: Propofol infusion rate in response to surgical stimulation

The performance of the PID controller for Propofol infusion in dealing with the disturbance rejection task is reported in Table 2.12. Figure 2.27 displays the BIS response to

the disturbance: after the start of the surgical stimulation, the BIS is rapidly reduced by a bolus of Propofol and is returned to the safe range of [45-55]. After this fast initial reduction of the BIS, the decrease to the target 50 is slightly slower. The patient with the quickest response is patient 6, whose BIS level after the positive step of the disturbance returns to 50 in 129 s, while the slowest is patient 9, whose BIS level returns to 50 in 444 s. Regarding the end of the disturbance, i.e. the negative step, the patient with the quickest response is patient 6 again, whose BIS level returns to 50 in 137 s, while the slowest is patient 3, whose BIS level returns to 50 in 478 s. Figure 2.28 shows the Propofol infusion rates in response to the surgical stimulation, where it is possible to see the increased interindividual variability in the Propofol to BIS model, with respect to the standard simulation (see Figure 2.12). Indeed, the disturbance rejection performes better in the case with less variability, as can be noticed by comparing the performance indices of both cases.

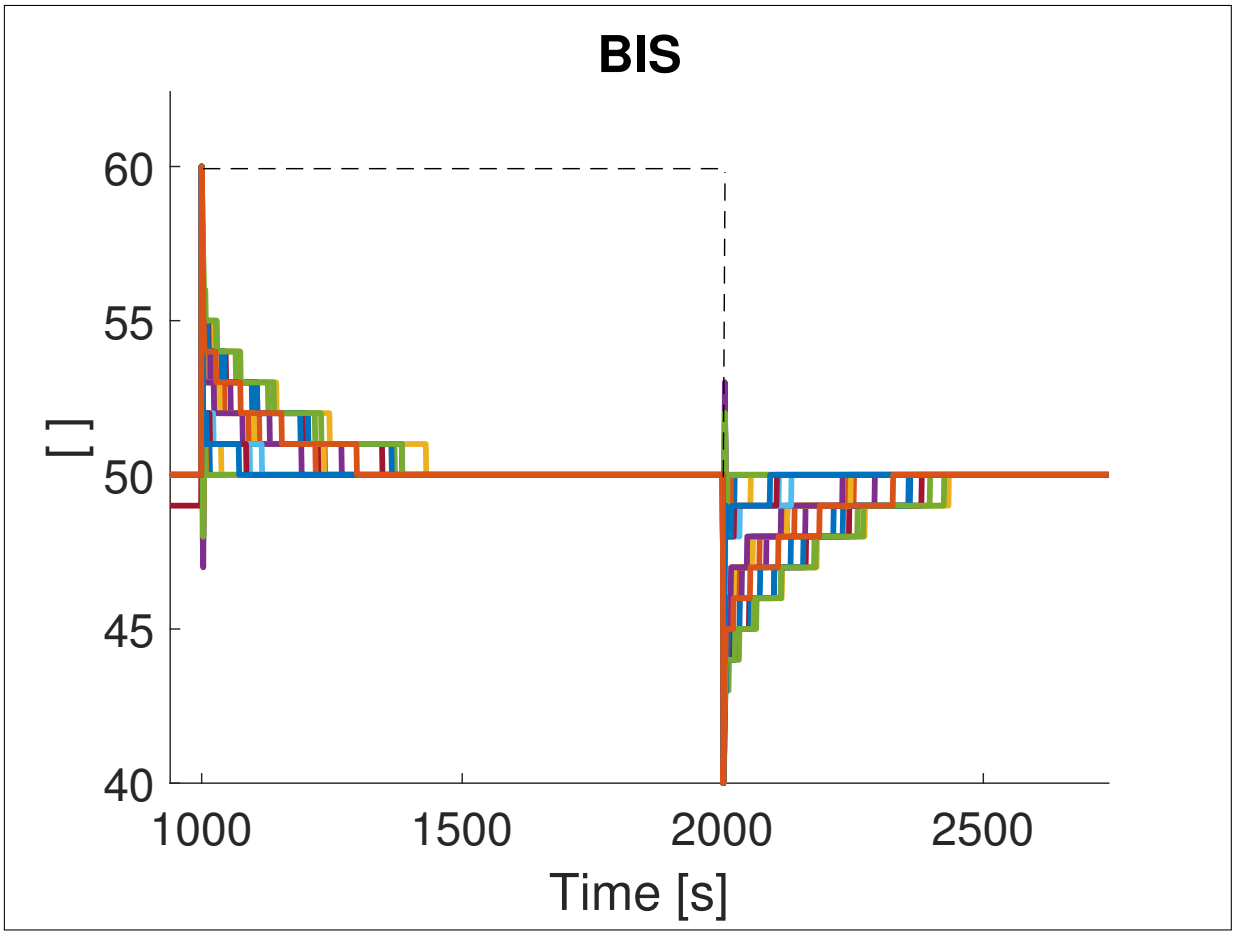

Figure 2.29: PID simulation with different set-up - Disturbance rejection: BIS response to surgical stimulation and anesthesiologist's action

PID performance	
min TT_p [s]	1
max TT_p [s]	8
mean TT_p [s]	2.83
min BIS-NADIR$_p$ [ ]	47
max BIS-NADIR$_p$ [ ]	50
mean BIS-NADIR$_p$ [ ]	49.58
min TT_n [s]	2
max TT_n [s]	24
mean TT_n [s]	7.78
min BIS-NADIR$_n$ [ ]	50
max BIS-NADIR$_n$ [ ]	53
mean BIS-NADIR$_n$ [ ]	50.46

Table 2.13: Disturbance rejection: PID performance for Propofol administration - surgical stimulation and anesthesiologist's action - Simulation with different set-up

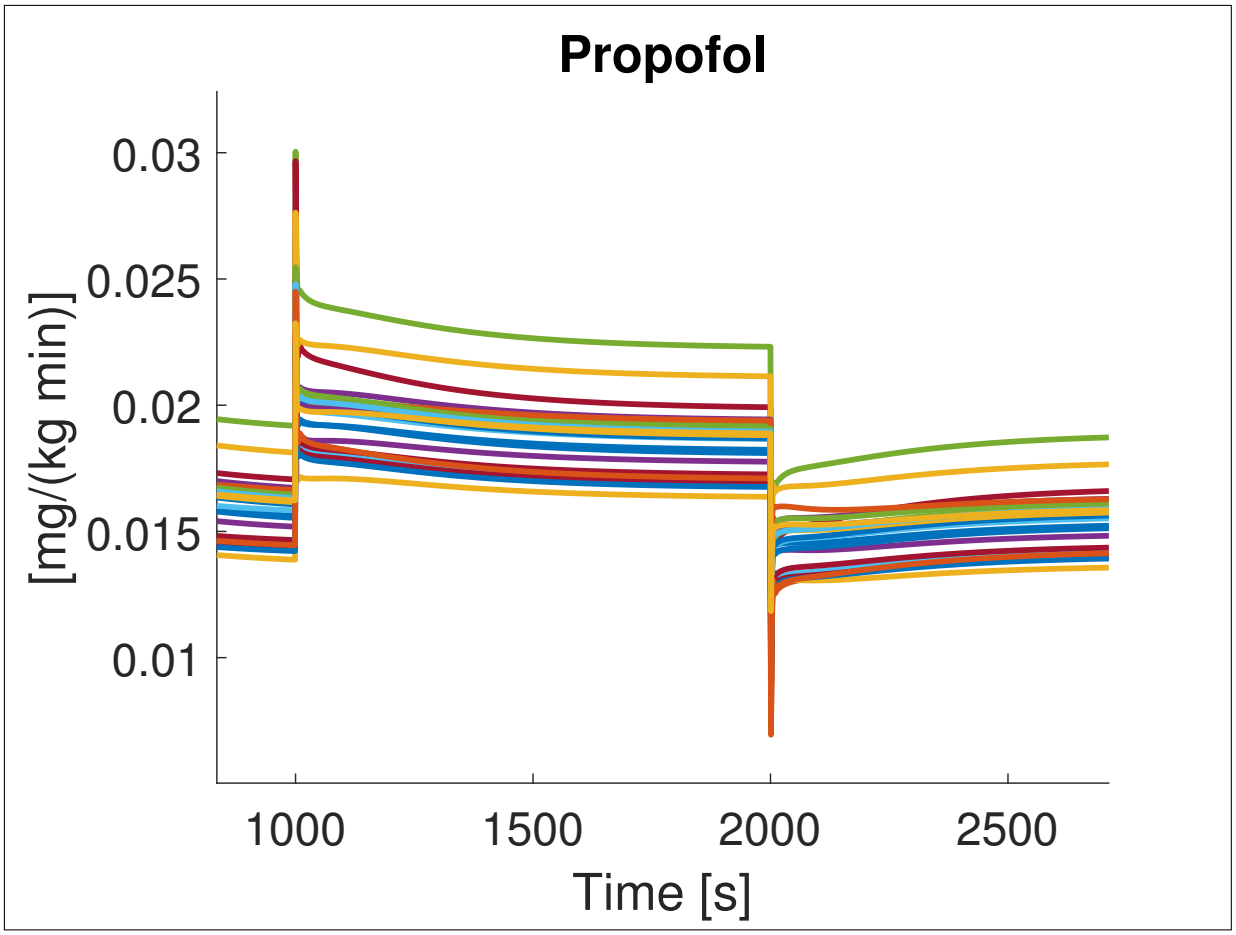

Figure 2.30: PID simulation with different set-up - Disturbance rejection: Propofol infusion rate in response to surgical stimulation and anesthesiologist's action

If the action of the anesthesiologist is included in the simulation, the performance of the PID controller (see Table 2.13) is better than the case where the Propofol admin-

istration is controlled only by the PID (see Table 2.12). As it is possible to verify also from Figure 2.29, the obsereved TT are lower, both for the positive and the negative step. The response of patient 6 is also quicker: its BIS index returns to 50 in 7 s, significantly faster than the previous case. The patient with the slower response is patient 3, whose BIS returns to the target is 431 s. Regarding the negative step, the patient with the quickest response is patient 4, whose BIS level returns to 50 in 7 s, while the slowest is patient 3 again, whose BIS level returns to 50 in 434 s. Even in this case, the disturbance rejection task performs better with respect to the simulation without the anesthesiologist's action. Figure 2.30 shows the Propofol infusion rates determined by the PID controller in response to the surgical stimulation, when also the additional Propofol dose is administered by the anesthesiologist. With respect to the case without the action of the anesthesiologist, some patients experience a slight undershoot after the positive step and an overshoot after the negative step, due to the disturbance rejection. These under- and over-shoots are acceptable since the BIS index never exceeds the limits of the safe interval; the maximum BIS-NADIR values for the positive and the negative steps are indeed 47 and 53, respectively.

Chapter 3

MPC

3.1 Introduction

The term model predictive control (MPC) does not designate a specific control stategy but rather an ample range of control methods, which use a model of the process to obtain the control signal by minimizing an objective function. The basic ideas of model predictive control are the following:

- Explicit use of a model to predict the process output at future time instants;
- Calculation of a control sequence minimizing an objective function;
- Receding strategy, so that at each instant the horizon is moved towards the future, which involves the application of the first control signal of the sequence calculated at each step.

The various MPC algorithms only differ amongst themselves in the model used to represent the process and the cost function to be minimized.
MPC presents the following advantages over other control methods:

- It can be used to control a great variety of processes, from those with relatively simple dynamics to more complex ones;
- It can deal with multivariable cases;
- The resulting controller is an easy-to-implement control law;
- Its extension to the treatment of constraints is conceptually simple, and these can be systematically included during the design process;
- It is very useful when future references are known;
- It is particularly attractive to staff with only limited knowledge of control because the concepts are very intuitive and at the same time the tuning is relatively easy.

On the other hand, its drawbacks are:

- It is necessary for an appropriate model of the process to be available. The design algorithm is based on prior knowledge of the model and is independent of it, but obviously the advantages of this control method will be affected by the discrepancies existing between the real process and the model used;

- Although the resulting control law is easy to implement and requires little computation, its derivation is more complex than that of the classical PID controllers. If the process dynamic does not change, the derivation of the controller can be done beforehead, but in the adaptive control case all the computation has to be carried out at every sampling time. When constraints are considered, the amount of computation required is even higher.

The methodology of all the controllers belonging to the MPC family is characterized by the following strategy:

1. The future output for a determined horizon N, called prediction horizon, are predicted at each time instant t using the process model. These predicted outputs y(t+k|t) for k=1...N depend on the known values up to instant t (past inputs and outputs) and on the future control signals u(t+k|t) for k=1...N-1;

2. The set of future control signals is calculated by optimizing a determined criterion in order to maintain the process as close as possible to the reference trajectory r(t+k). This criterion usually takes the form of a quadratic cost function of the errors between the predicted output signal and the predicted reference trajectory. An explicit solution can be obtained if the cost function is quadratic, the model is linear, and there are no constraints. Otherwise, an iterative optimization method has to be used;

3. The first control action of the set of future control signals, u(t|t), is sent to the process while the next control signals calculated are rejected. At the next sampling instant (t+1), the new measurement y(t+1) is aquired, step 1 is repeated with this new value and all the sequences are updated. Thus the next control action u(t+1|t+1) is calculated using the receding horizon concept.

As explained above, a model is used to predict the future control actions, which are calculated by the optimizer taking into account the cost function as well as the constraints. The process model plays, in consequence, a decisive role in the control strategy. The chosen model must be able to capture the process dynamics to precisely predict the future outputs. In the different MPC strategies, different type of models can be employed, such as impulse response, step response, transfer function o state space models. In this thesis, the state space model has been used. An advantage of this model is that it can be easily used for multivariable processes. The control law is simply the feedback of a linear combination of the state vector. The state space description allows for an easier expression of stability and robustness criteria. The optimizer is another fundamental part of the MPC

strategy as it provides the control actions. If the cost function is quadratic, its minimum can be easily obtained as an explicit function (linear) of past inputs and outputs and the future reference trajectory. In the presence of inequality constraints the solution could be obtained by numerical algorithms [5].

3.2 Patient model for MPC

Since with the MPC it is possible to control a multivariable process, a 3×3 state space model of the patient has been created, representing the PK component of the patient model. The inputs are Propofol, Remifentanil and Atracurium, and the outputs are BIS, RASS and NMB. The matrices of this state space representation are the following:

$$A = \begin{bmatrix} -(k_{10p}+k_{12p}+k_{13p}) & k_{21p} & k_{31p} & 0 & 0 & 0 & 0 & 0 & 0 & 0 & 0 \\ k_{12p} & -k_{21p} & 0 & 0 & 0 & 0 & 0 & 0 & 0 & 0 & 0 \\ k_{13p} & 0 & -k_{31p} & 0 & 0 & 0 & 0 & 0 & 0 & 0 & 0 \\ k_{1ep} & 0 & 0 & -k_{e0p} & 0 & 0 & 0 & 0 & 0 & 0 & 0 \\ 0 & 0 & 0 & 0 & -(k_{10r}+k_{12r}+k_{13r}) & k_{21r} & k_{31r} & 0 & 0 & 0 & 0 \\ 0 & 0 & 0 & 0 & k_{12r} & -k_{21r} & 0 & 0 & 0 & 0 & 0 \\ 0 & 0 & 0 & 0 & k_{13r} & 0 & -k_{31r} & 0 & 0 & 0 & 0 \\ 0 & 0 & 0 & 0 & k_{1er} & 0 & 0 & -k_{e0r} & 0 & 0 & 0 \\ 0 & 0 & 0 & 0 & 0 & 0 & 0 & 0 & -0.561 & -0.0755 & -0.0021 \\ 0 & 0 & 0 & 0 & 0 & 0 & 0 & 0 & 1 & 0 & 0 \\ 0 & 0 & 0 & 0 & 0 & 0 & 0 & 0 & 0 & 1 & 0 \end{bmatrix} \tag{3.1}$$

$$B = \begin{bmatrix} 1 & 0 & 0 \\ 0 & 0 & 0 \\ 0 & 0 & 0 \\ 0 & 0 & 0 \\ 0 & 1 & 0 \\ 0 & 0 & 0 \\ 0 & 0 & 0 \\ 0 & 0 & 0 \\ 0 & 0 & 1 \\ 0 & 0 & 0 \\ 0 & 0 & 0 \end{bmatrix} \tag{3.2}$$

$$C = \begin{bmatrix} 0 & 0 & 0 & 1 & 0 & 0 & 0 & 0 & 0 & 0 & 0 \\ 0 & 0 & 0 & 0 & 0 & 0 & 0 & 1 & 0 & 0 & 0 \\ 0 & 0 & 0 & 0 & 0 & 0 & 0 & 0 & 0 & 0 & 0.0021 \end{bmatrix} \tag{3.3}$$

$$D = \begin{bmatrix} 0 & 0 & 0 \\ 0 & 0 & 0 \\ 0 & 0 & 0 \end{bmatrix} \tag{3.4}$$

where k_{ijp} and k_{ijr} (i,j = 1,2,3) are the drug transfer rates from the i-th to the j-th compartment of Propofol and Remifentanil, respectively. This values are taken from the state space representations of the drugs in Section 1.2.1. The state space model obtained by these matrices contains 11 states: 4 for Propofol (x_1 to x_4), 4 for Remifentanil (x_5 to x_8) and 3 for Atracurium (x_9 to x_{11}). The PK models of these drugs are independent of each

other, indeed matrix A consists of three separate submatrices that are the state matrices of the three drugs (see Section 1.2.1). In particular, A(1:4,1:4) consists of the state matrix of Propofol, A(5:8,5:8) consists of the state matrix of Remifentanil and A(9:11,9:11) consists of the state matrix of Atracurium. Since there are no interactions at this stage, all the other entries have been set to 0. The same principle has been used to built the other matrices of the multivariable model.
Subsequently, the state space model has been discretized with a sampling time $T_s = 1$ s. As previously explained in Section 1.2.2, the sampling times of the variables RASS and NMB have been modified to $T_s = 120$ s and $T_s = 20$ s, respectively. In this MPC simulation, since a single state space model has been considered, the sampling time has been kept equal to $T_s = 1$ s for all the variables.

3.2.1 Model linearization

Before going into the details of the MPC design, it is necessary to deal with the issue of the nonlinearity of the process considered in this thesis. There is nothing in the basic concepts of the MPC against the use of a nonlinear model, since the extension of MPC ideas to nonlinear processes is straightforward. However, this is not a trivial matter, and there are many difficulties derived from the use of nonlinear models such as:

- The availability of nonlinear models from experimental data is an open issue, since there is a lack of identification techniques for non linear processes. On the other hand, model attainment from first principles (mass and energy balance) is not always feasible;
- The optimization problem is non convex and its resolution is much more difficult than the quadratic programming problem. Problems relative to local optimum appear, not only influencing control quality but also deriving in stability issues;
- The difficulty of the optimization problem translates into an important increase in computation time. This can constrain the use of this technique to slow processes;
- The study of crucial aspects such as stability and robustness is more complex in the case of nonlinear systems, and it constitutes an open field of great interest for researches [5].

In order to avoid this issues, it is possible to built a linear model that approximates the nonlinear one for small deviations from the equilibria. Regarding the patient model considered in this thesis, its PK component is linear, but its PD component is nonlinear. Thus, the linearization of the model has been performed.
Considering the following generic discrete nonlinear system:

$$\begin{cases} x((k+1)T) = f(x(kT), u(kT)) \\ y(kT) = g(x(kT), u(kT)) \end{cases} \tag{3.5}$$

with g and f sufficiently regular, assuming that (x_{eq}, u_{eq}) is an equilibrium point and introducing the variables $\bar{x} = x - x_{eq}$ and $\bar{u} = u - u_{eq}$, which describe the deviation from the equilibrium, then the linearization of the system is the following linear system:

$$\begin{cases} \bar{x}((k+1)T) = A\bar{x}(kT) + B\bar{u}(kT) \\ \bar{y}(kT) = C\bar{x}(kT) + D\bar{u}(kT) \end{cases} \tag{3.6}$$

with

$$\begin{cases} A = \dfrac{\partial}{\partial x} f(x,u)|_{x_{eq},u_{eq}} \\ B = \dfrac{\partial}{\partial u} f(x,u)|_{x_{eq},u_{eq}} \\ C = \dfrac{\partial}{\partial x} g(x,u)|_{x_{eq},u_{eq}} \\ D = \dfrac{\partial}{\partial u} g(x,u)|_{x_{eq},u_{eq}} \end{cases} \tag{3.7}$$

Theoretical results ensure that for sufficiently small values of $\bar{x}$ and $\bar{u}$ the linear approximation is accurate.

Since the patient model considered in this thesis includes a nonlinear part (the Hill function), the PKPD model of the mean patient has been linearized around the steady state values. To perform the linearization, the Model Linearizer MatlabSimulink tool has been used. With this tool it is possible to trim the model to identify the operating point, based on the desired steady state output values. The values of the operating point are reported in Table 3.1.

Variable	Operating point
x_1	0.664 [mg/ml]
x_2	2.198 [mg/ml]
x_3	37.02 [mg/ml]
x_4	0.664 [mg/ml]
x_5	2.987 [mg/ml]
x_6	5.004 [mg/ml]
x_7	3.203 [mg/ml]
x_8	3.254 [mg/ml]
x_9	7.37e-21 [mg/ml]
x_{10}	0 [mg/ml]
x_{11}	3285.714 [mg/ml]
x_{12}	2.008 [mg/ml]
x_{13}	48.81 [mg/ml]
u_{Propofol}	0.015 [mg/(kg min)]
$u_{\text{Remifentanil}}$	0.113 [μg/(kg min)]
$u_{\text{Atracurium}}$	6.9 [mg/(kg min)]
y_{BIS}	50.09 [ ]
y_{RASS}	-4.017 [ ]
y_{NMB}	10.1 [%]

Table 3.1: Operating point for the mean patient model linearization

Once the trimming of the system is performed, the Model Linearizer tool linearizes the multivariable state space system around the operating point. The result is a 3×3 state space model with 13 states. The addiction of two states is due to the linearization of the transfer function that consists of the PD part of the Remifentanil to RASS model. Below are the matrices of the linearized state space model:

$$A = \begin{bmatrix} -0.8735 & 0.0706 & 0.0035 & 0 & 0 & 0 & 0 & 0 & 0 & 0 & 0 & 0 & 0 \\ 0.2335 & -0.0706 & 0 & 0 & 0 & 0 & 0 & 0 & 0 & 0 & 0 & 0 & 0 \\ 0.1958 & 0 & -0.0035 & 0 & 0 & 0 & 0 & 0 & 0 & 0 & 0 & 0 & 0 \\ 0.456 & 0 & 0 & 0.456 & 0 & 0 & 0 & 0 & 0 & 0 & 0 & 0 & 0 \\ 0 & 0 & 0 & 0 & -0.8843 & 0.1525 & 0.0088 & 0 & 0 & 0 & 0 & 0 & 0 \\ 0 & 0 & 0 & 0 & 0.2555 & -0.1525 & 0 & 0 & 0 & 0 & 0 & 0 & 0 \\ 0 & 0 & 0 & 0 & 0.0094 & 0 & -0.0088 & 0 & 0 & 0 & 0 & 0 & 0 \\ 0 & 0 & 0 & 0 & 0.456 & 0 & 0 & -0.4186 & 0 & 0 & 0 & 0 & 0 \\ 0 & 0 & 0 & 0 & 0 & 0 & 0 & 0 & -0.561 & -0.0755 & -0.0021 & 0 & 0 \\ 0 & 0 & 0 & 0 & 0 & 0 & 0 & 0 & 1 & 0 & 0 & 0 & 0 \\ 0 & 0 & 0 & 0 & 0 & 0 & 0 & 0 & 0 & 1 & 0 & 0 & 0 \\ 0 & 0 & 0 & 0 & 0 & 0 & 0 & 0 & 0 & 0 & 0 & -2 & 0.0823 \\ 0 & 0 & 0 & 0 & 0 & 0 & 0 & 1 & 0 & 0 & 0 & 0 & -0.0667 \end{bmatrix} \tag{3.8}$$

$$B = \begin{bmatrix} 1 & 0 & 0 \\ 0 & 0 & 0 \\ 0 & 0 & 0 \\ 0 & 0 & 0 \\ 0 & 1 & 0 \\ 0 & 0 & 0 \\ 0 & 0 & 0 \\ 0 & 0 & 0 \\ 0 & 0 & 1 \\ 0 & 0 & 0 \\ 0 & 0 & 0 \\ 0 & 0 & 0 \\ 0 & 0 & 0 \end{bmatrix} \tag{3.9}$$

$$C = \begin{bmatrix} 0 & 0 & 0 & -89.8962 & 0 & 0 & 0 & -24.3121 & 0 & 0 & 0 & 0 & 0 \\ 0 & 0 & 0 & 0 & 0 & 0 & 0 & 0 & 0 & 0 & 0 & -2 & 0 \\ 0 & 0 & 0 & 0 & 0 & 0 & 0 & -0.2941 & 0 & 0 & -0.0079 & 0 & 0 \end{bmatrix} \tag{3.10}$$

$$D = \begin{bmatrix} 0 & 0 & 0 \\ 0 & 0 & 0 \\ 0 & 0 & 0 \end{bmatrix} \tag{3.11}$$

Since the PK model of the patient for all the drugs is linear, the linearization did not affect it. Indeed, matrix A differs from the one reported in Equation 3.1 only for the two additional states of Remifentanil. Regarding matrix C (see Equation 3.10), the first raw is related to the BIS (that depends on Propofol and Remifentanil, i.e. states 4 and 8), the second raw concerns the RASS (that depends only on Remifentanil), and the third raw is related to the NMB (that depends on Remifentanil and Atracurium). Matrix C substitutes the Hill functions of BIS and NMB and the transfer function of RASS, relating the effect-site concentrations of the drugs directly to their effect at the site of action.
To assess the performance of the linearization step, the outputs of the linearized model have been compared to the outputs of the original nonlinear models, in the presence of sinusoidal perturbations of the equilibrium point inputs. Different amplitudes of the sinusoids have been tested.

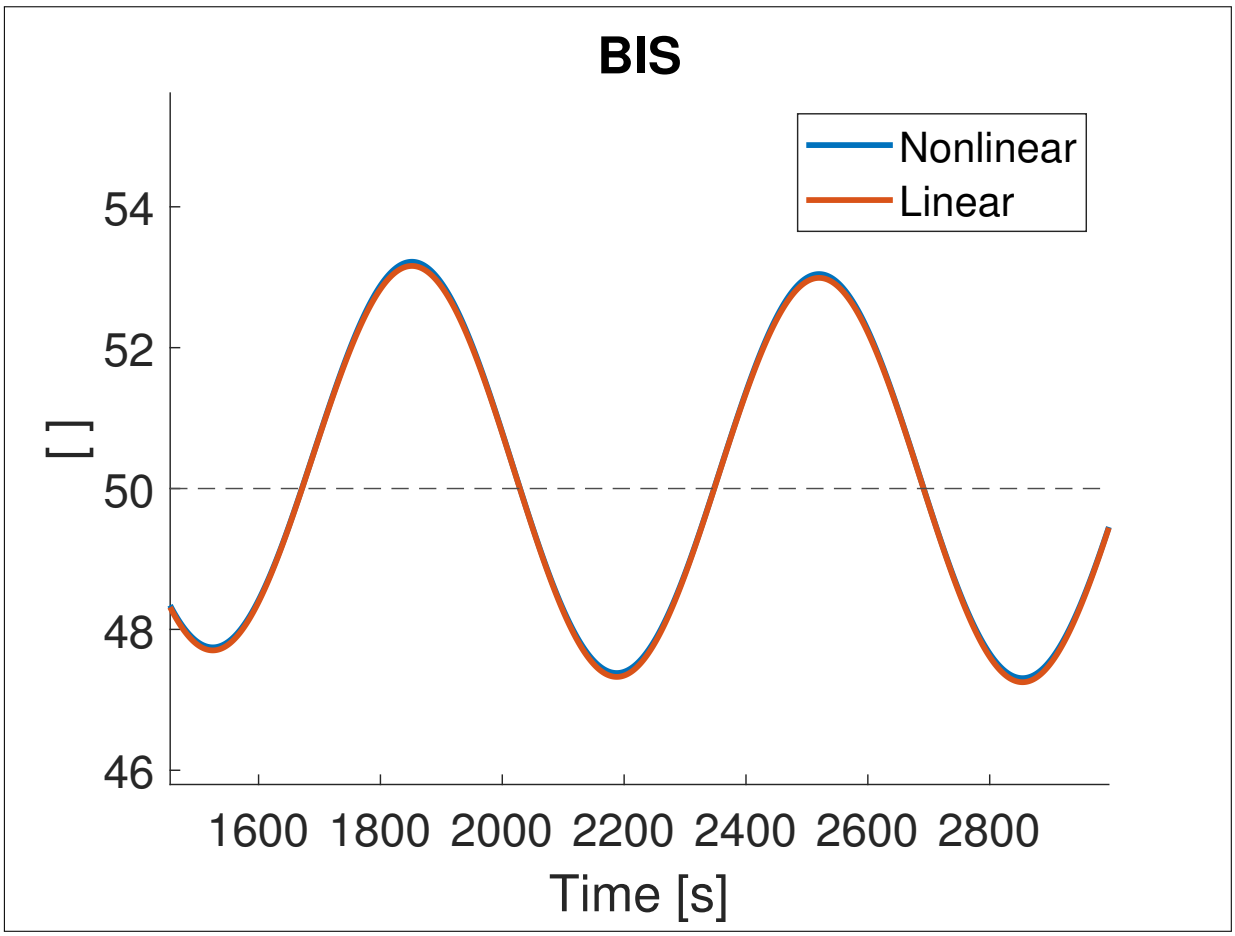

Figure 3.1: Performance of the linearization on BIS: 6% sinusoidal input perturbation

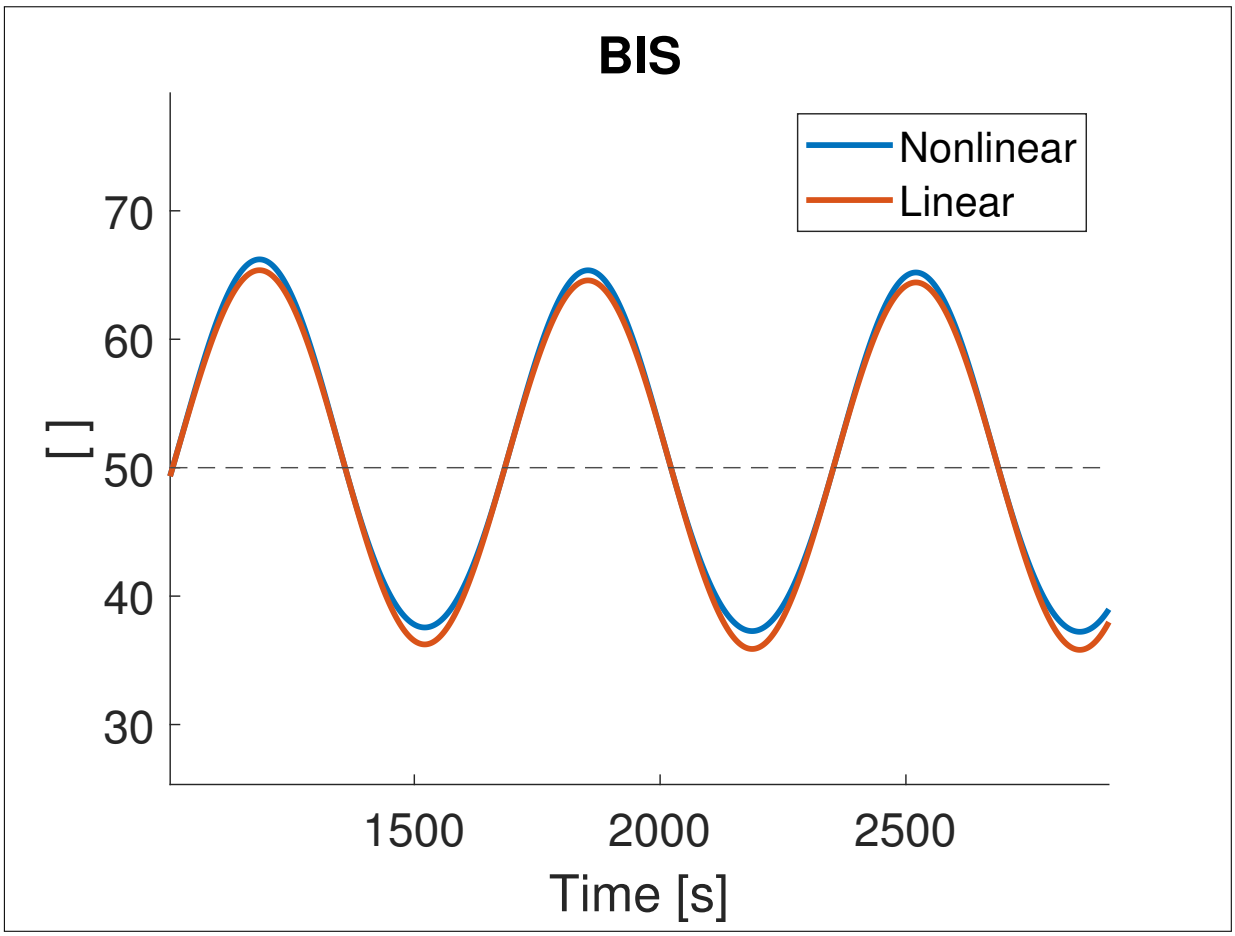

Figure 3.2: Performance of the linearization on BIS: 30% sinusoidal input perturbation

Figure 3.1 shows the BIS index of the linearized Propofol to BIS model and of the original nonlinear model, in response to a 6% sinusoidal perturbation of the equilibrium point input. As expected, for small variations from the equilibrium, the linear approximation coincides with the response of the nonlinear model. Subsenquently, the amplitude of the sine wave has been increased in order to obtain a 30% perturbation: as shown in Figure 3.2, for such variation from the equilibrium the linear approximation no longer coincides with the original signal.

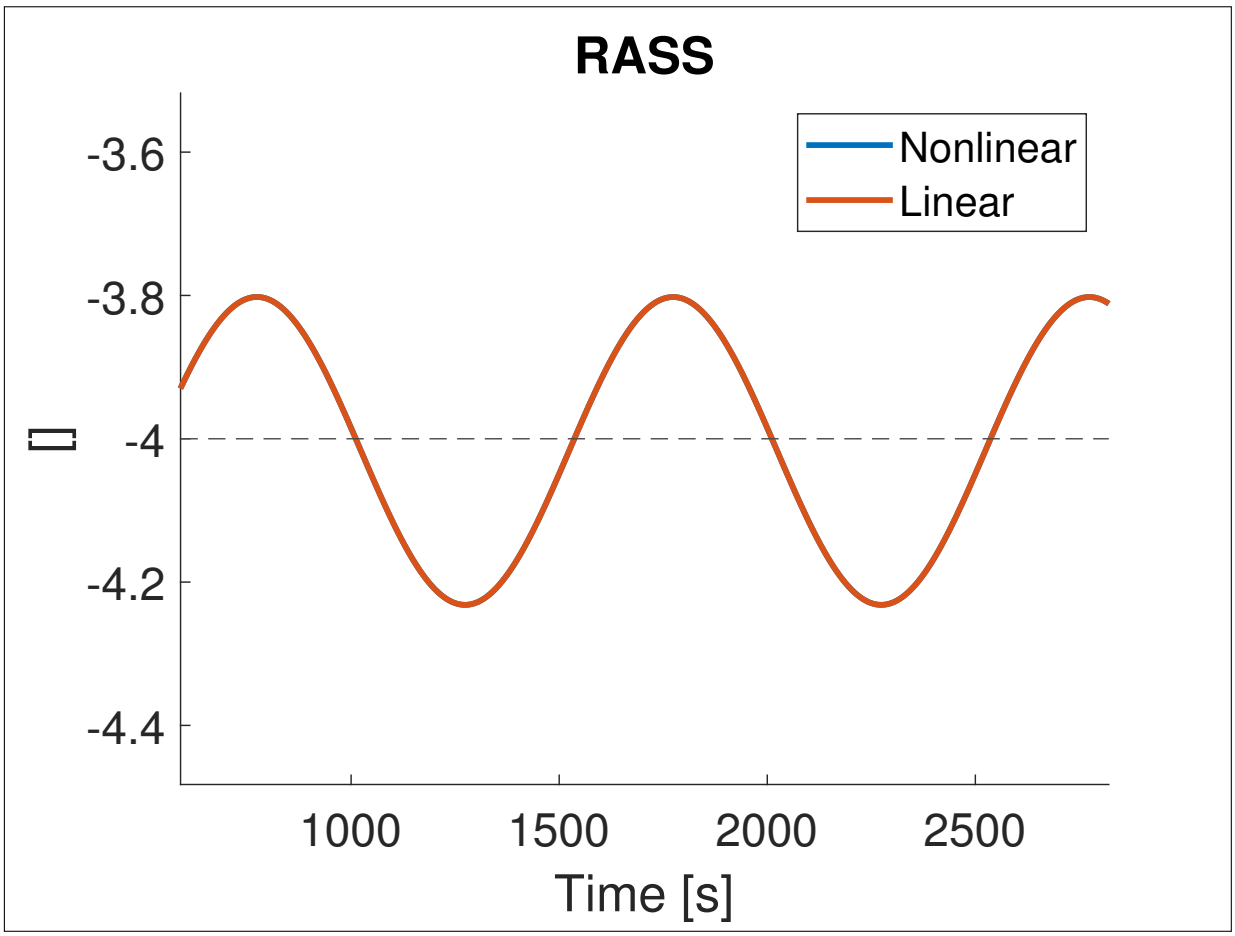

Figure 3.3: Performance of the linearization on RASS: 5% sinusoidal input perturbation

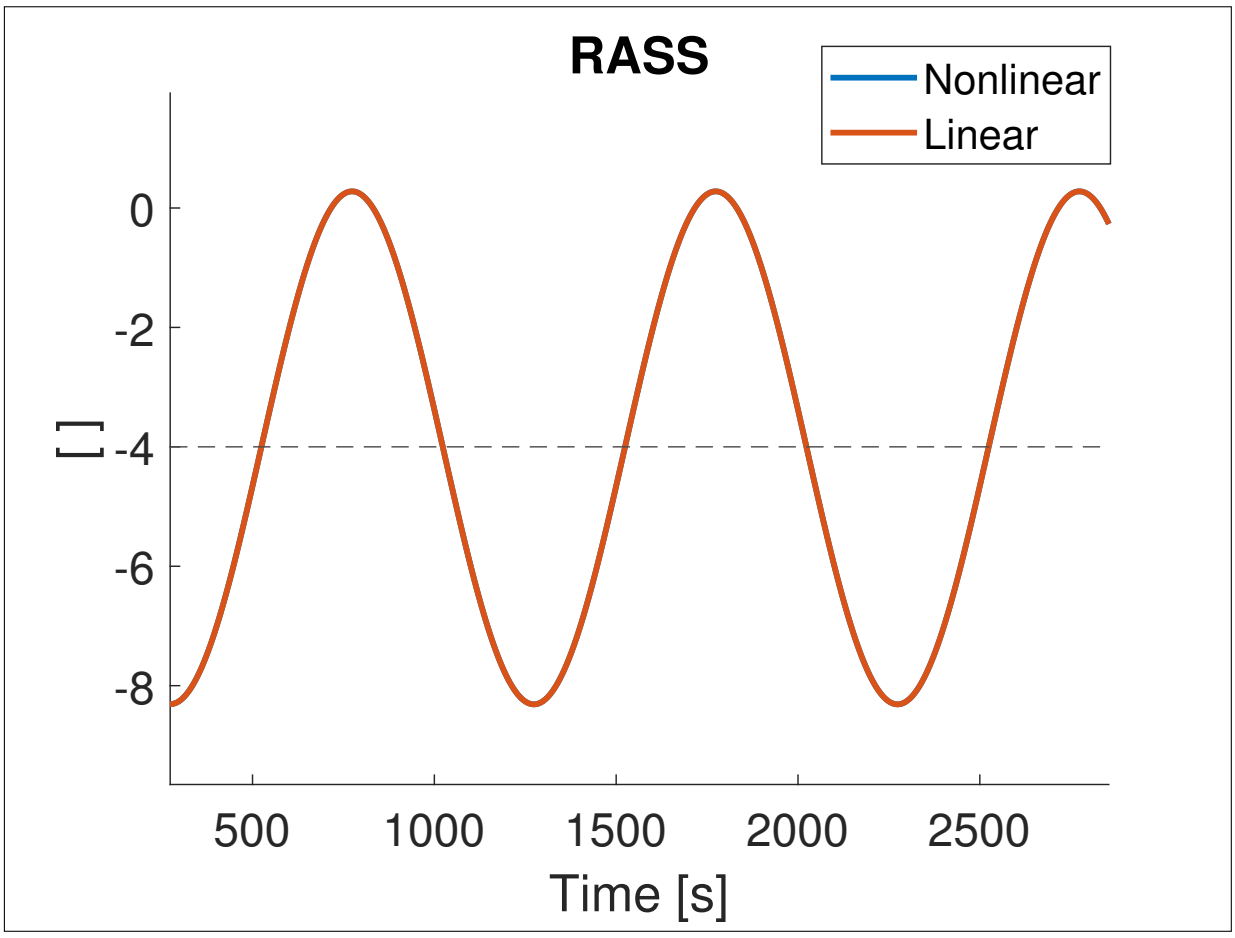

Figure 3.4: Performance of the linearization on RASS: 90% sinusoidal input perturbation

Regarding RASS, initially the sinusoidal input perturbation has been set to 5% (see Figure 3.3), then it has been increased to 90% (see Figure 3.4). For both this sinusoidal inputs, the linear approximation is adequate, since the linearized model output and the nonlinear model output coincide. This procedure has been performed for the sole purpose of verifying if the linear approximation of the model is adequate. Indeed, it is a completely non-physiological approach, since the minimum measurable RASS value is -5, while the output obtained by the input perturbation reaches -8.

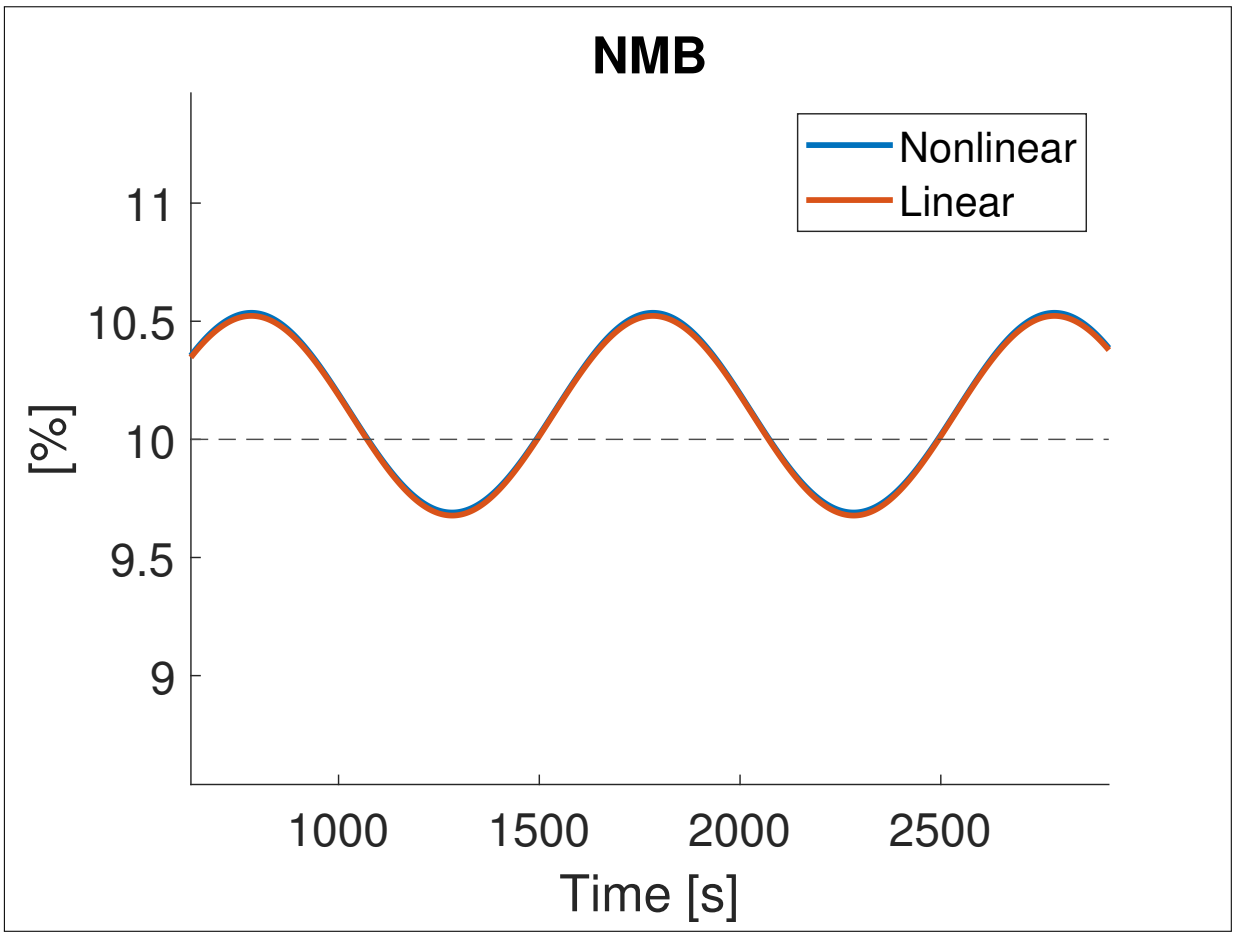

Figure 3.5: Performance of the linearization on NMB: 2% sinusoidal input perturbation

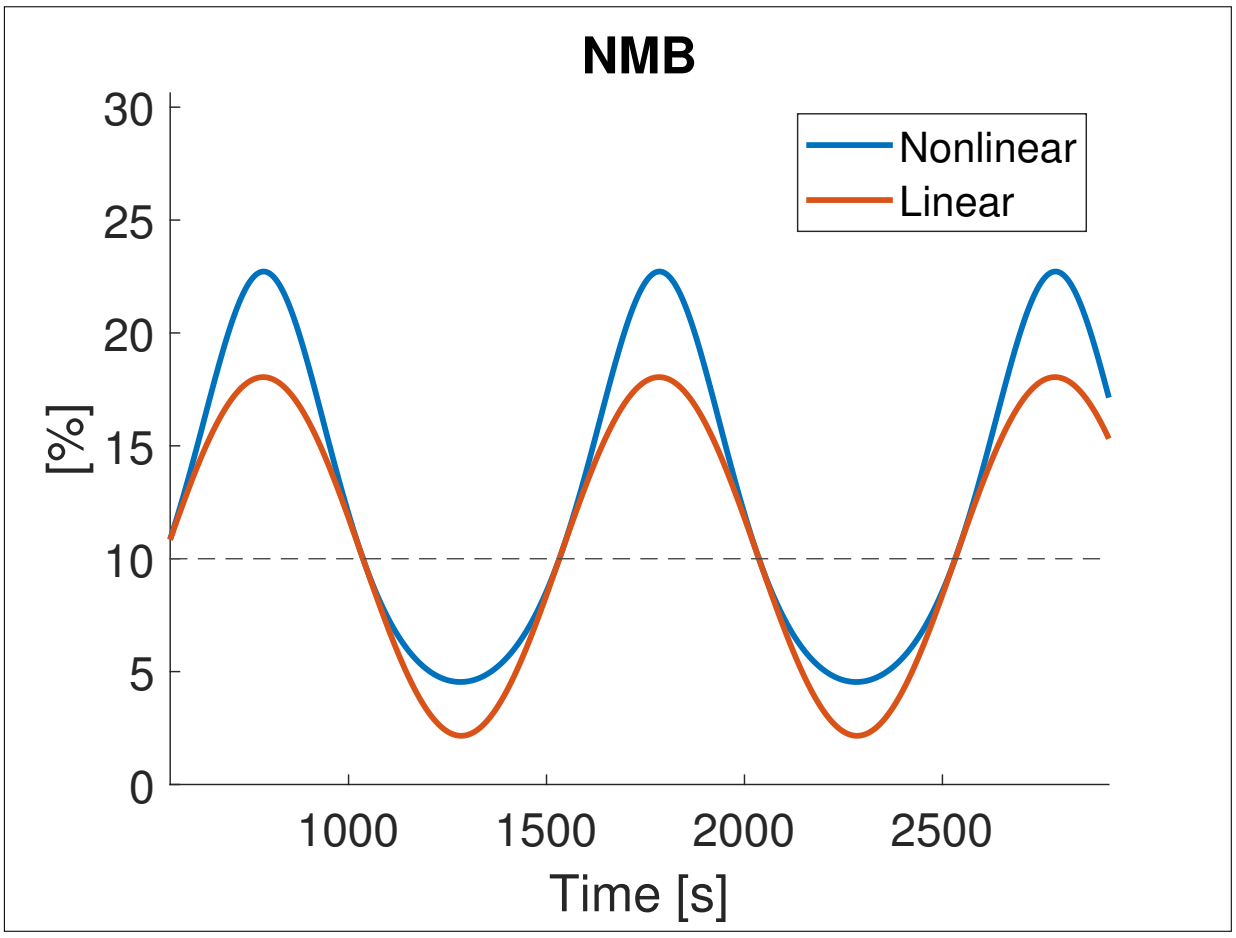

Figure 3.6: Performance of the linearization on NMB: 30% sinusoidal input perturbation

In order to assess the performance of the linearization on the NMB model, initially a sinusoidal input perturbation of 2% has been tested. As can be seen in Figure 3.5, for such a small variation from the equilibrium, the approximation is acceptable, i.e. the linear and nonlinear model outputs coincide. Figure 3.6 shows the NMB response to a sinusoidal input perturbation of 30%, which causes a discrepancy in the linear and nonlinear model responses, meaning that the linear approximation is not acceptable for such large variations from the equilibrium.

3.3 MPC design

Prediction horizon

When designing MPC, an important parameter to choose is the prediction horizon (N). As reported in [7], when only hypnosis is controlled, a prediction horizon of 10 s is often selected. But since the hemodynamic models included in the patient model have larger time constants, the prediction horizon also needs to be larger to guarantee feasibility. Simulations have been performed with a prediction horizon varying between 10 and 500 s. The results indicated that the set-point for the BIS will be reached for all the values of N larger than 10. When analyzing the results for the hemodynamic variables, it has been noticed that small values of N lead to instability of CO and MAP. Furthermore, it

has been observed that the transition from instability to stability is within the range of 50 to 100 s. Hence, the simulation has been repeated with prediction horizons between 50 and 100 s. From the results it is evident that the prediction horizon needs to be at least 60 s to avoid instability in the induction phase. For this reason, in this simulation the prediction horizon has been set to N = 60.

Output prediction

The model of the patient is characterized by the following state space representation:

$$\begin{cases} x((k+1)T) = Ax(kT) + Bu(kT) \\ y(kT) = Cx(kT) + Du(kT) \end{cases} \tag{3.12}$$

where A, B, C and D are the matrices obtained at the linearization step (Equations 3.8 - 3.11). For the Markov property, the update equation states that x((k+1)T) is fully determined by x(kT) and u(kT) at time kT. This means that x(kT) at time kT contains all the past history of the system, therefore all the information needed to compute the evolution of the system is held by x(kT) and the sequence of future inputs [21].
In matrix notation, the state prediction can be expressed as:

$$\underbrace{\begin{bmatrix} \hat{x}(k+1|k) \\ \hat{x}(k+2|k) \\ \hat{x}(k+3|k) \\ \vdots \\ \hat{x}(k+N|k) \end{bmatrix}}_{\hat{\mathcal{X}}} = \underbrace{\begin{bmatrix} A \\ A^2 \\ A^3 \\ \vdots \\ A^N \end{bmatrix}}_{\mathcal{A}_s} \hat{x}(k|k) + \underbrace{\begin{bmatrix} B & 0 & \dots & 0 \\ AB & B & \dots & 0 \\ A^2B & AB & \dots & 0 \\ \vdots & \vdots & \ddots & \\ A^{N-1}B & A^{N-2}B & \dots & B \end{bmatrix}}_{\mathcal{B}_s} \underbrace{\begin{bmatrix} u(k) \\ u(k+1) \\ u(k+2) \\ \vdots \\ u(k+N-1) \end{bmatrix}}_{\mathcal{U}} \tag{3.13}$$

Thus, in compact form:

$$\hat{\mathcal{X}} = \mathcal{A}_s \hat{x}(kT|kT) + \mathcal{B}_s \mathcal{U} \tag{3.14}$$

Since y(kT) = Cx(kT), the output prediction is straightforward to calculate [21]:

$$\underbrace{\begin{bmatrix} \hat{y}(k+1|k) \\ \hat{y}(k+2|k) \\ \hat{y}(k+3|k) \\ \vdots \\ \hat{y}(k+N|k) \end{bmatrix}}_{\hat{\mathcal{Y}}} = \underbrace{\begin{bmatrix} CA \\ CA^2 \\ CA^3 \\ \vdots \\ CA^N \end{bmatrix}}_{\mathcal{A}} \hat{x}(k|k) + \underbrace{\begin{bmatrix} CB & 0 & \dots & 0 \\ CAB & CB & \dots & 0 \\ CA^2B & CAB & \dots & 0 \\ \vdots & \vdots & \ddots & \\ CA^{N-1}B & CA^{N-2}B & \dots & CB \end{bmatrix}}_{\mathcal{B}} \underbrace{\begin{bmatrix} u(k) \\ u(k+1) \\ u(k+2) \\ \vdots \\ u(k+N-1) \end{bmatrix}}_{\mathcal{U}} \tag{3.15}$$

Thus, in compact form:

$$\hat{\mathcal{Y}} = \mathcal{A}\hat{x}(kT|kT) + \mathcal{B}\mathcal{U} \tag{3.16}$$

State estimation

In the calculation of the output prediction, it has been assumed that x(kT) is available at the time kT. In this simulation, the state variable is not accessible from the plant, since the number of states of the nonlinear plant is different from the number of states of the linearized model. Therefore, a state observer is needed in order to estimate the state variable for the feedback. The state observer employed in this thesis is a Kalman filter. The Kalman filter receives the process measurements and the manipulated variables (i.e. the output of the MPC) as inputs, and uses them to estimate the state variable, based on the state space linearized model of the patient. The tuning of the filter has been performed by selecting the process noise covariance matrix (Q_{kf}), the measurement noise covariance matrix (R_{kf}) and the process and measurement noise cross-covariance matrix. Equation 3.17 reports the process noise covariance matrix:

$$Q_{kf} = \begin{bmatrix} 0.0054 & 0 & 0 & 0 & 0 & 0 & 0 & 0 & 0 & 0 & 0 & 0 & 0 \\ 0 & 0.049 & 0 & 0 & 0 & 0 & 0 & 0 & 0 & 0 & 0 & 0 & 0 \\ 0 & 0 & 13.71 & 0 & 0 & 0 & 0 & 0 & 0 & 0 & 0 & 0 & 0 \\ 0 & 0 & 0 & 0.0054 & 0 & 0 & 0 & 0 & 0 & 0 & 0 & 0 & 0 \\ 0 & 0 & 0 & 0 & 0.09 & 0 & 0 & 0 & 0 & 0 & 0 & 0 & 0 \\ 0 & 0 & 0 & 0 & 0 & 0.251 & 0 & 0 & 0 & 0 & 0 & 0 & 0 \\ 0 & 0 & 0 & 0 & 0 & 0 & 0.104 & 0 & 0 & 0 & 0 & 0 & 0 \\ 0 & 0 & 0 & 0 & 0 & 0 & 0 & 0.107 & 0 & 0 & 0 & 0 & 0 \\ 0 & 0 & 0 & 0 & 0 & 0 & 0 & 0 & 0.001 & 0 & 0 & 0 & 0 \\ 0 & 0 & 0 & 0 & 0 & 0 & 0 & 0 & 0 & 0.001 & 0 & 0 & 0 \\ 0 & 0 & 0 & 0 & 0 & 0 & 0 & 0 & 0 & 0 & 0107900 & 0 & 0 \\ 0 & 0 & 0 & 0 & 0 & 0 & 0 & 0 & 0 & 0 & 0 & 0.041 & 0 \\ 0 & 0 & 0 & 0 & 0 & 0 & 0 & 0 & 0 & 0 & 0 & 0 & 23.825 \end{bmatrix} \tag{3.17}$$

Q_{kf} is a diagonal matrix, because the uncertainty that affect the evolution of one state has been assumed to be independent on the uncertainty affecting the other states. The entries of the process noise covariance matrix have been calculated using the following formula:

$$Q_{kfii} = (0.1(\bar{x} + \epsilon))^2 \tag{3.18}$$

where $\epsilon = 0.01$, that has been added to avoid null values of the entries. With this calculation, the standard deviation of the model error has been set to 1/10th of the value of the state at the equilibrium point.

Equation 3.19 represents the measurement noise covariance matrix:

$$R_{kf} = \begin{bmatrix} 1 & 0 & 0 \\ 0 & 6.27 & 0 \\ 0 & 0 & 1 \end{bmatrix} \tag{3.19}$$

R_{kf} is a diagonal matrix, since the error committed in measuring one output is independent of the error committed measuring the others. The entries of the matrix are the values of the variance of the measurement errors of the sensors.

The process and measurement noise cross-covariance matrix has been set to 0, since the

measurement errors and the process errors have been considered uncorrelated.

Constraints

Another aspect to consider in the design of the MPC are the constraints. In this case, the constraints on the amplitude of the manipulated variables must be taken into account, since the infusion rates of the drugs are saturated. For all the drugs, the saturation u(kT) $\in$ [u_{min}, u_{max}] $\forall$k can be expressed as a linear inequality: Au(kT) $\leq$ b, with A = $\begin{bmatrix} 1 \\ -1 \end{bmatrix}$ and b = $\begin{bmatrix} -u_{min} \\ u_{max} \end{bmatrix}$.
The saturation values [u_{min}, u_{max}] are reported in Table 1.6. It is important to notice that u(kT), in output from the MPC, is an incremental variable, not the actual physical variable. The actual physical variable is obtained from the sum of the incremental variable u(kT) and the steady-state value u_{eq}. The controller also requires in input the incremental state variable. Since the Kalman filter estimates the state using the linearized model, its output is already the incremental state variable. In fact, the input of the Kalman filter are the incremental control variables and the incremental outputs of the process, obtained by subtracting the steady-state values to the actual output variables (both for BIS, RASS and NMB) [21]. All the steady-state values are listed in Table 3.1.

Cost function

A fundamental part of the MPC design is the cost function. In this case, a quadratic cost function for reference tracking has been considered. Below, the expression of the cost function in matrix notation [21]:

$$J = (\hat{\mathcal{Y}}(k) - \mathcal{Y}_0(k))^T \mathcal{Q} (\hat{\mathcal{Y}}(k) - \mathcal{Y}_0(k)) + (\mathcal{U}(k))^T \mathcal{R} (\mathcal{U}(k)) \tag{3.20}$$

where

$$\hat{\mathcal{Y}}(k) = [\hat{y}^T(k+1|k) \ \dots \ \hat{y}^T(k+N|kT)]^T$$

$$\mathcal{Y}_0(k) = [y_0^T(k+1|k) \ \dots \ y_0^T(k+N|kT)]^T$$

$$\mathcal{U}(k) = [u^T(k) \ \dots \ u^T(k+N-1)]^T$$

$\mathcal{Y}_0(k)$ is the reference trajectory of the process outputs. The references of BIS, RASS and NMB are the same signals taken into account in the PID simulations (see Section 2.2). Since the future evolution of the reference is known a priori, it is possible to design a lookahead MPC, i.e. the system is able to respond proactively, before the changes in the reference have occurred, avoiding delays in the process responses [5]. More precisely, the reference contains N values for each output.

$\mathcal{Q}$ and $\mathcal{R}$ in Equation 3.20 are the weight matrices:

$$\mathcal{Q} = \begin{bmatrix} 0.0001 & 0 & 0 \\ 0 & 0.01 & 0 \\ 0 & 0 & 0.0001 \end{bmatrix} \tag{3.21}$$

$$\mathcal{R} = \begin{bmatrix} 5 & 0 & 0 \\ 0 & 1 & 0 \\ 0 & 0 & 10 \end{bmatrix} \tag{3.22}$$

The presence of the two terms in the cost function (Equation 3.20) forces the MPC algorithm to find a trade-off between the predicted control error and the cost of a control action. Indeed, the ratio between $\mathcal{Q}$ and $\mathcal{R}$ regulates the controller aggressiveness [21].

Numerical solution using Quadratic Programming

A quadratic programming problem is a problem of this kind:

$$J = \frac{1}{2}x^T Ex + x^T F \tag{3.23}$$

$$Mx \leq \gamma \tag{3.24}$$

where E, F, M and γ are compatible matrices and vectors. Without loss of generality, E is assumed to be symmetric and positive definite. Equation 3.23 reports the cost function while Equation 3.24 presents the constraints. In these equations, x represents the decision variable. A quadratic programming problem it is a convex optimization problem, which means that there is no local minima and the convergence is guaranteed. In the unconstrained case, it is possible to obtain a closed-form solution, while in the constrained case a numerical solution is required [21].
From Equation 3.20, replacing $\hat{\mathcal{Y}}(k)$ with the expression in Equation 3.16, it is possible to obtain:

$$J = 2((\mathcal{A}\hat{x}(kT|kT) - \mathcal{Y}_0(k))^T \mathcal{Q}\mathcal{B})\mathcal{U}(k) + \mathcal{U}^T(k)(\mathcal{B}^T\mathcal{Q}\mathcal{B} + \mathcal{R})\mathcal{U}(k) \tag{3.25}$$

that is a quadratic programming problem.
Several alghoritms that can compute the numerical solution are available. In order to perform the optimization, the Matlab function quadprog with the Active Set algorithm has been employed in this simulation.

3.4 Induction phase

This section reports the results of the simulation of the model predictive control of the induction phase of anesthesia. The simulation includes the same variables of the PID con-

trol simulation, i.e. the anesthestic variables BIS, RASS and NMB and the hemodynamic variables CO and MAP. Even in this case, the simulation has been ran on the set of 24 patients, whose biometric values are reported in Table 1.3.

Simulation results

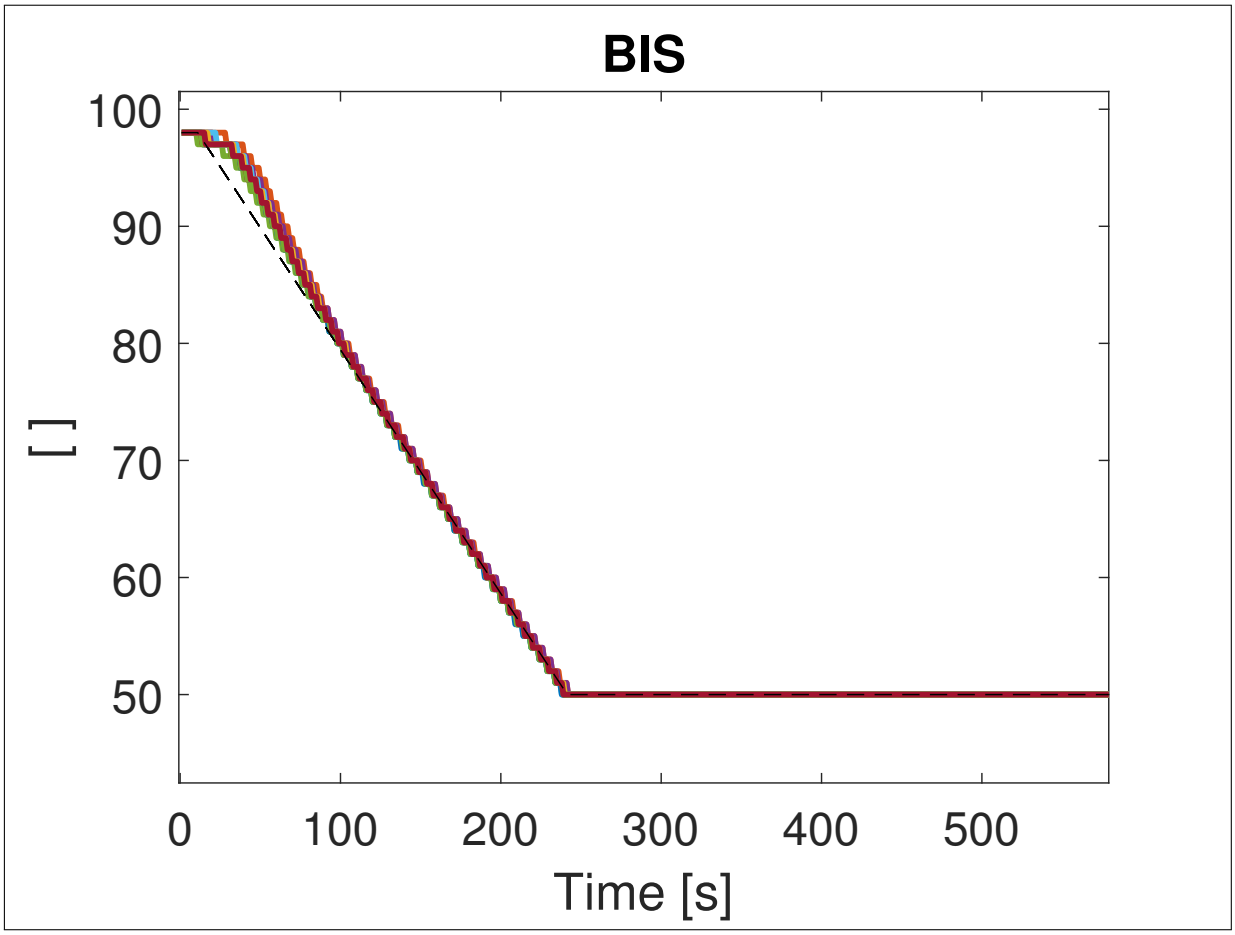

Figure 3.7: MPC simulation - Induction phase: BIS

Figure 3.7 shows the response of the BIS to Propofol and Remifentanil administration. For all the patients, the BIS signal perfectly follows the BIS reference, except in the initial part (i.e. the first 100 s) where there is a slight delay in the response. As reported in Table 3.2, the settling time (ST) is equal to the time to target (TT), since there is no undershoot. Figure 3.8 shows the Propofol infusion rates.

MPC performance	
min TT [s]	214
max TT [s]	217
mean TT [s]	215.4
min BIS-NADIR [ ]	50
max BIS-NADIR [ ]	50
mean BIS-NADIR [ ]	50
min ST [s]	214
max ST [s]	217
mean ST [s]	215.4
min US [%]	0
max US [%]	0
mean US [%]	0
min PE [%]	0
max PE [%]	3.68
mean PE [%]	0.29

Table 3.2: Induction phase: MPC performance for Propofol administration

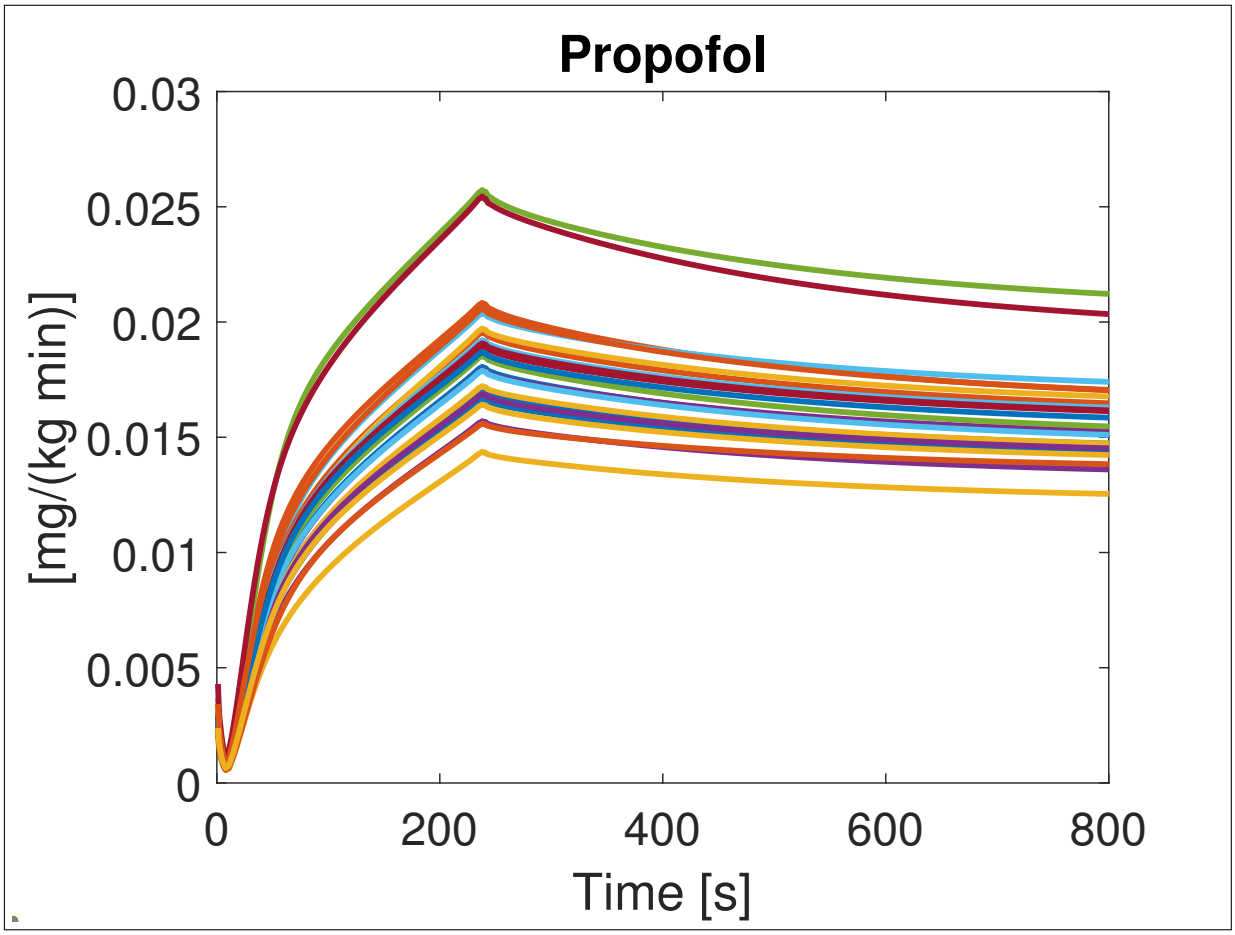

Figure 3.8: MPC simulation - Induction phase: Propofol

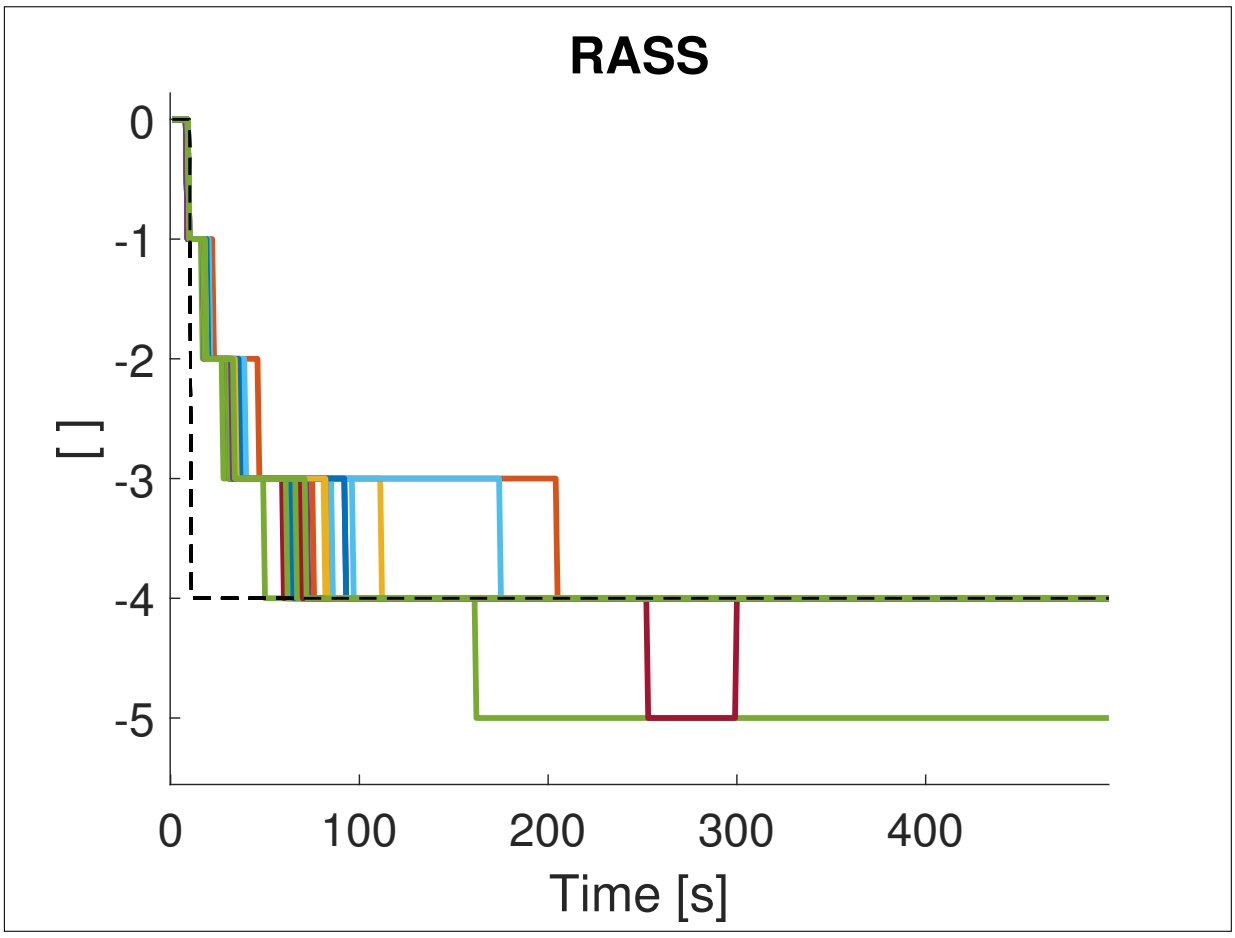

Figure 3.9: MPC simulation - Induction phase: RASS

Figure 3.9 illustrates the response of the RASS to Remifentanil administration. This variable follows the RASS reference for all the patients except for patient 3, whose RASS remains at value -5, which is still within the accepted RASS interval (see Table 1.8), therefore there is no undershoot for any patient. In fact, as can be seen in Table 3.3, the settling time (ST) is equal to the time to target (TT). Figure 3.10 shows the Remifentanil infusion rates.

MPC performance	
min TT [s]	50
max TT [s]	205
mean TT [s]	85.29
min RASS-NADIR [ ]	-4
max RASS-NADIR [ ]	-5
mean RASS-NADIR [ ]	-4.08
min ST [s]	50
max ST [s]	205
mean ST [s]	85.29
min US [%]	0
max US [%]	0
mean US [%]	0
min PE [%]	0
max PE [%]	75
mean PE [%]	3.69

Table 3.3: Induction phase: MPC performance for Remifentanil administration

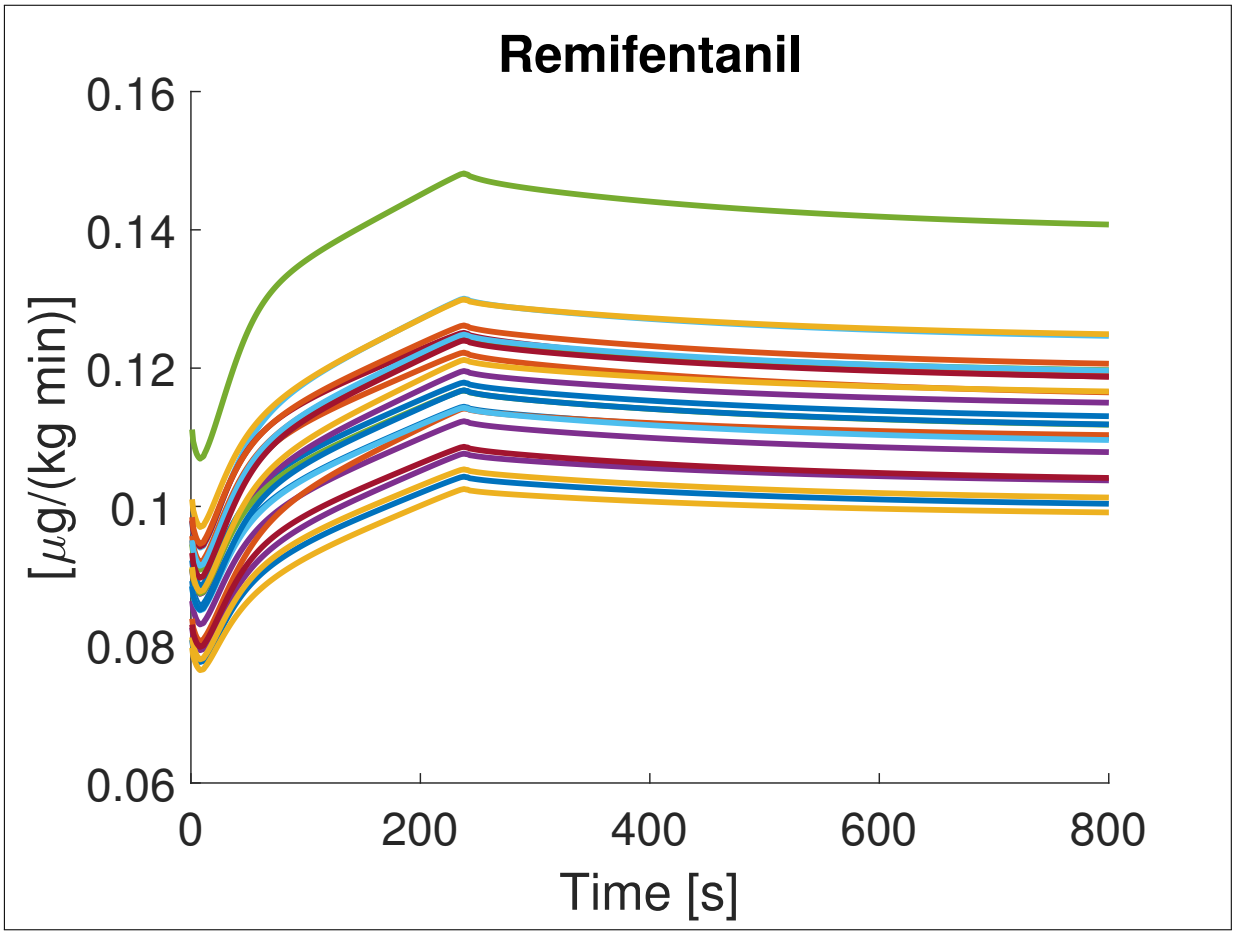

Figure 3.10: MPC simulation - Induction phase: Remifentanil

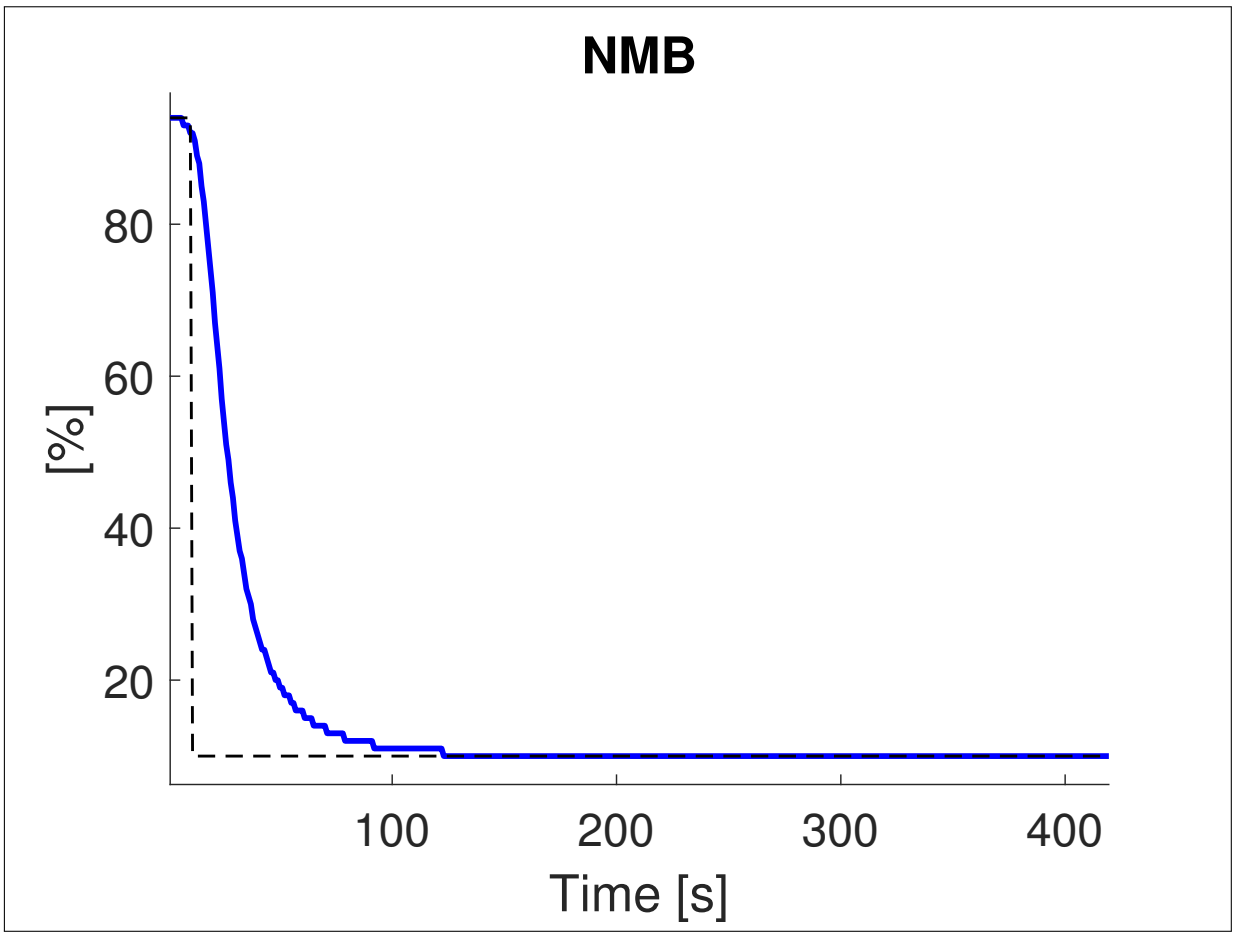

Figure 3.11: MPC simulation - Induction phase: NMB

Figure 3.11 shows the NMB response to Atracurium and Remifentanil administration. The signal is the same for all the subjects since the Atracurium to NMB model does not include the interpatient variability. As reported in Table 3.4, the time to target (TT) is equal to the settling time (ST) since there is no undershoot. Figure 3.12 shows the Atracurium infusion rates.

MPC performance	
min TT [s]	49
max TT [s]	49
mean TT [s]	49
min NMB-NADIR [%]	10
max NMB-NADIR [%]	10
mean NMB-NADIR [%]	10
min ST [s]	49
max ST [s]	49
mean ST [s]	49
min US [%]	0
max US [%]	0
mean US [%]	0
min PE [%]	0
max PE [%]	820
mean PE [%]	21.22

Table 3.4: Induction phase: MPC performance for Atracurium administration

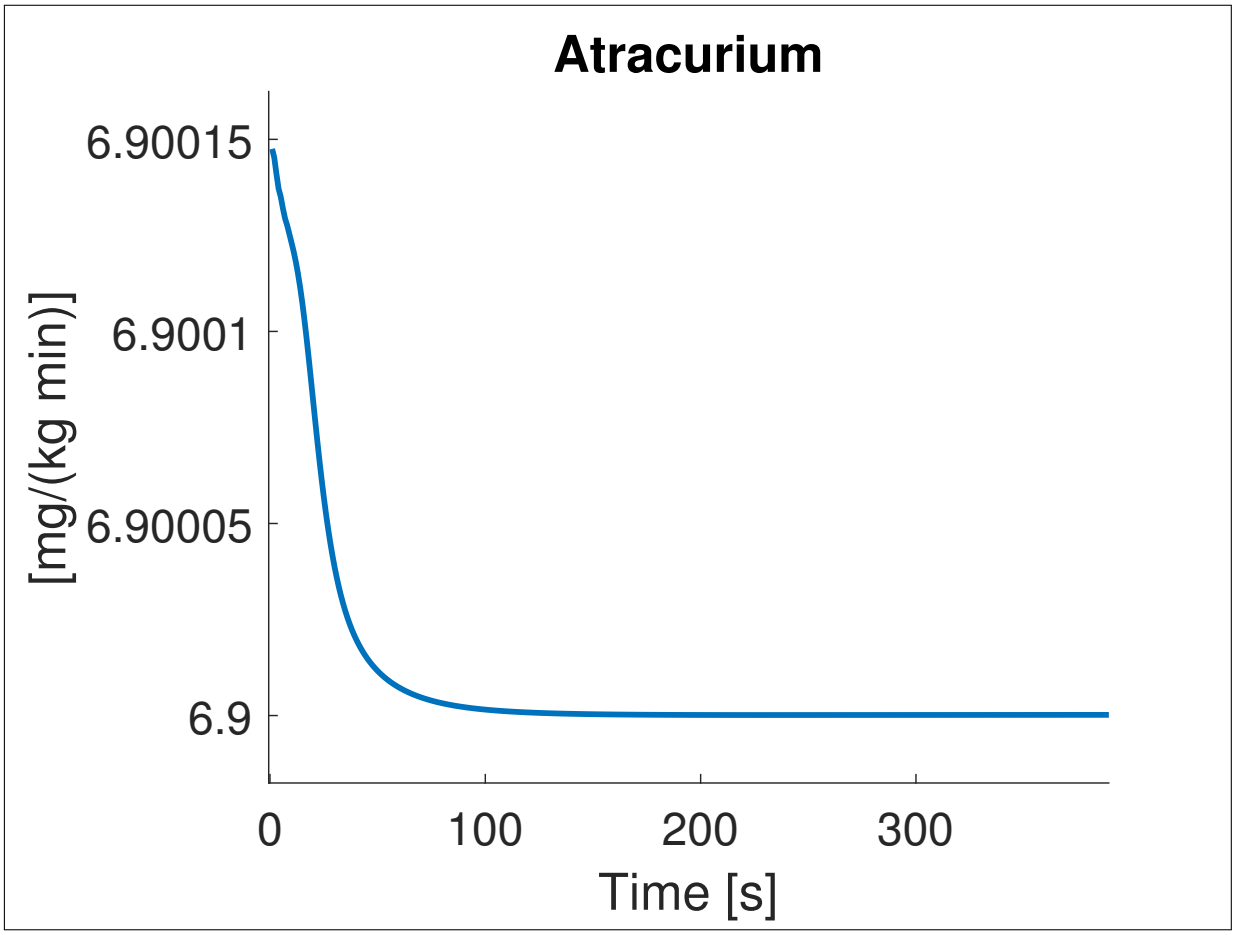

Figure 3.12: MPC simulation - Induction phase: Atracurium

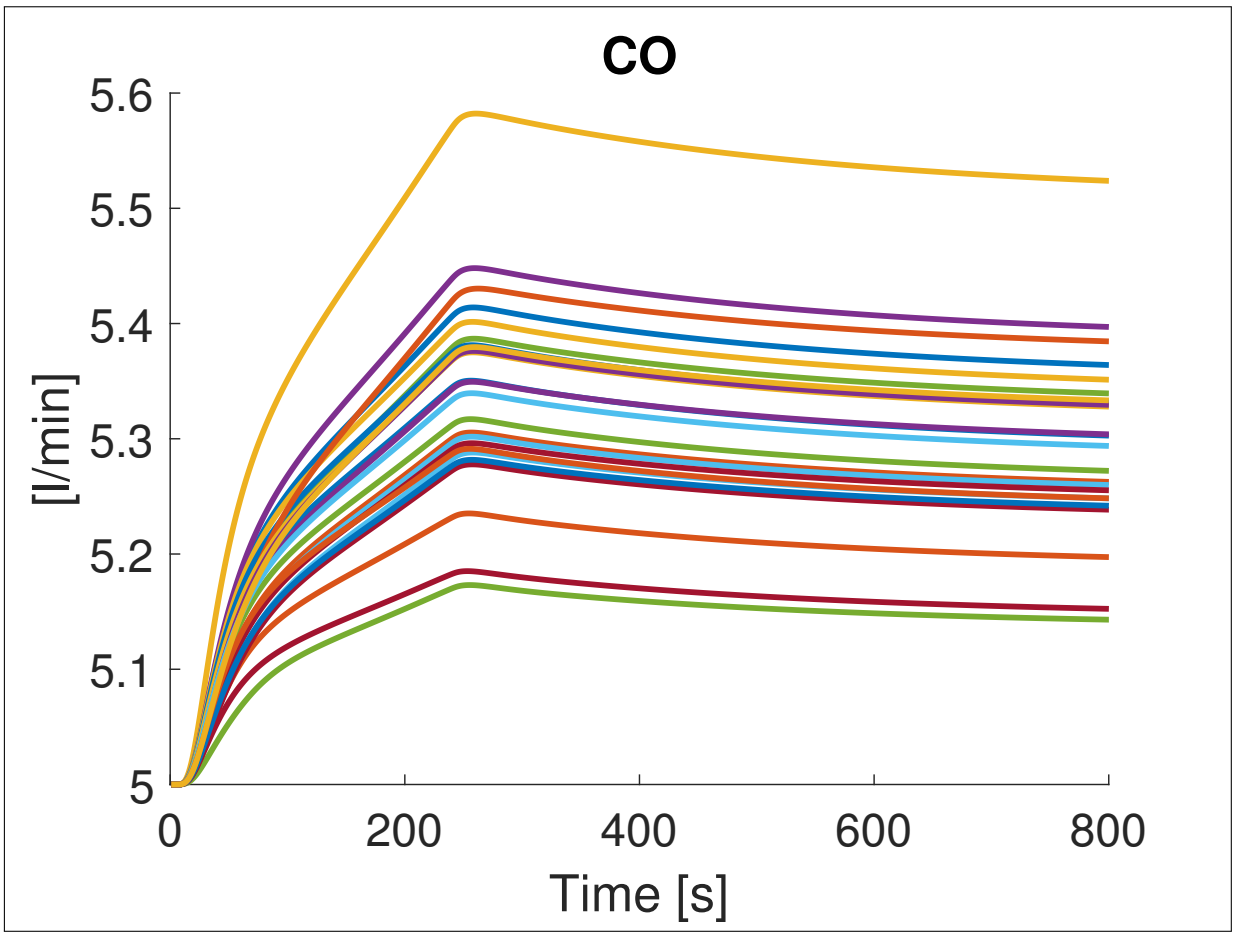

Figure 3.13: MPC simulation - Induction phase: CO

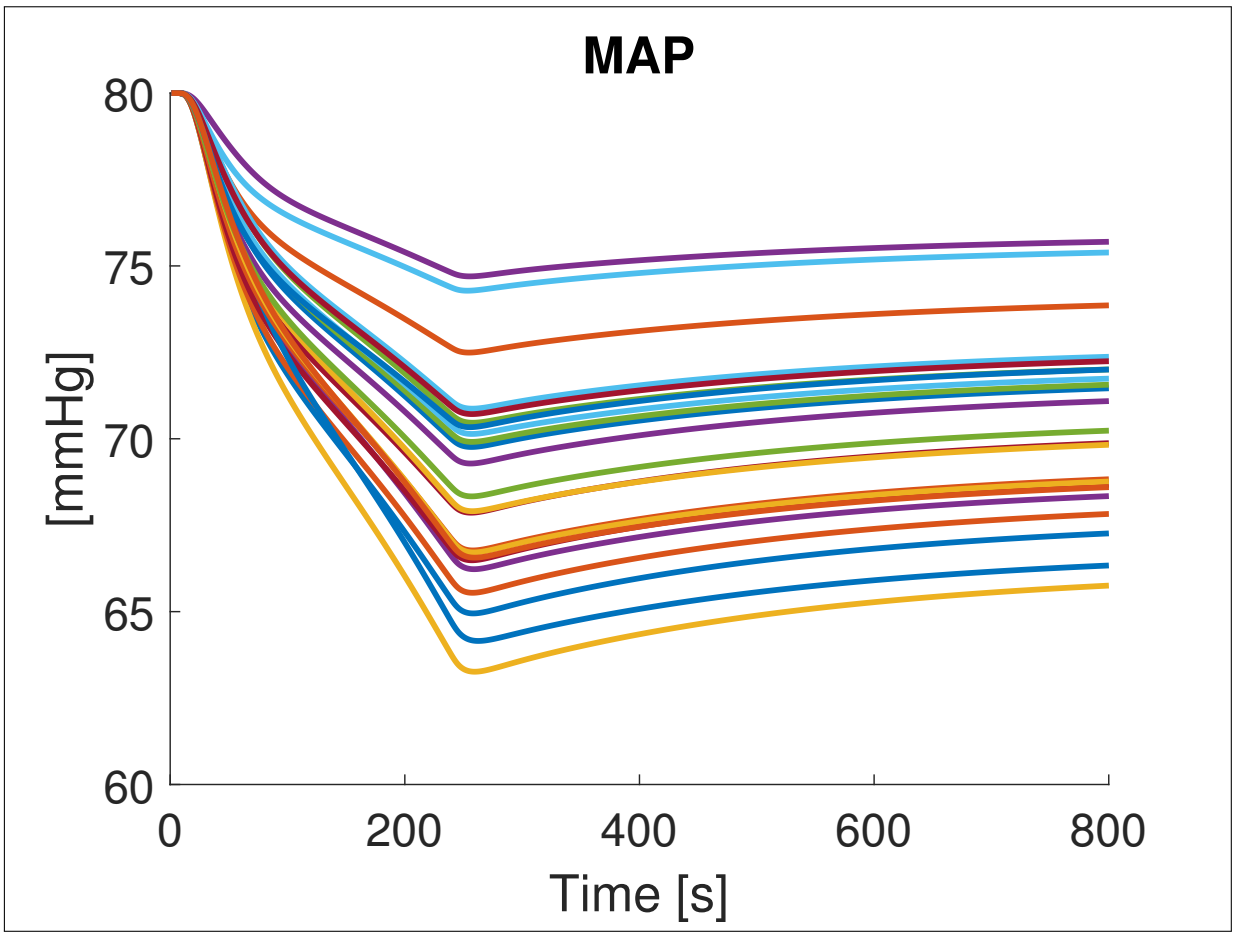

Figure 3.14: MPC simulation - Induction phase: MAP

Regarding the hemodynamic system, both CO and MAP remain within the safe ranges during the induction phase, as can be seen from Figure 3.13 and Figure 3.14.

3.5 Comparison between PID and MPC

In this section the comparison between the results of the simulations of the PID control and the MPC is performed. The comparison has been conducted only for the induction phase, since the maintenance phase in the MPC case has not been investigated. Tables 3.5, 3.6 and 3.7 report the differences between the performance indices of the PID and MPC simulations for Propofol, Remifentanil and Atracurium administration, respectively. For a generic performance index, the term Δindex can be expressed as:
$\Delta\text{index} = \text{index}_{\text{PID}} - \text{index}_{\text{MPC}}$, representing the difference between the value of a performance index for the PID control performance evaluation and the value of the same index for the MPC performance evaluation. As an example, taking into account the minimum time to target of the BIS:
$\Delta\text{min TT} = \text{min TT}_{\text{PID}} - \text{min TT}_{\text{MPC}} = 225 - 214 = 11$ s.
For all the performance indices used in this thesis it is valid that the lower the index, the better the control performance. Therefore:

- if $\Delta\text{index} > 0$, the control performance is better for the MPC with respect to the

PID control;

- if Δindex $= 0$, the control performance is equal for the MPC and the PID control;
- if Δindex < 0, the control performance is better for the PID control with respect to the MPC.

Performance comparison	
Δmin TT [s]	11
Δmax TT [s]	13
Δmean TT [s]	10.4
Δmin BIS-NADIR [ ]	0
Δmax BIS-NADIR [ ]	0
Δmean BIS-NADIR [ ]	0
Δmin ST [s]	11
Δmax ST [s]	13
Δmean ST [s]	10.4
Δmin US [%]	0
Δmax US [%]	0
Δmean US [%]	0
Δmin PE [%]	0
Δmax PE [%]	6.28
Δmean PE [%]	1.86

Table 3.5: Induction phase: Differences between the PID and MPC performance indices for Propofol administration

Regarding the control of Propofol administration, as presented in Table 3.5, the BIS-NADIR is the same for the PID and the MPC simulations, since there is no undershoot in the BIS signal. The ΔTT indices are positive values, both in the minimum, mean and maximum cases, as well as the ΔPE in the mean and maximum cases. Therefore, in this case the MPC controller performs better than the PID controller in carrying out the set-point following task.

Performance comparison	
Δmin TT [s]	110
Δmax TT [s]	14
Δmean TT [s]	85.13
Δmin RASS-NADIR [ ]	-1
Δmax RASS-NADIR [ ]	0
Δmean RASS-NADIR [ ]	-0.08
Δmin ST [s]	110
Δmax ST [s]	14
Δmean ST [s]	85.13
Δmin US [%]	0
Δmax US [%]	0
Δmean US [%]	0
Δmin PE [%]	0
Δmax PE [%]	25
Δmean PE [%]	6.66

Table 3.6: Induction phase: Differences between the PID and MPC performance indices for Remifentanil administration

Regarding the control of Remifentanil administration, as presented in Table 3.6, the ΔTT indices are positive values, therefore the RASS response is quicker in the MPC simulation. The only negative values are the ΔRASS-NADIR in the minimum and mean cases, meaning that the PID controller performs better in tracking the RASS reference. Nevertheless, the ΔPE is positive both for the mean and the maximum cases.

Performance comparison	
Δmin TT [s]	19
Δmax TT [s]	19
Δmean TT [s]	19
Δmin NMB-NADIR [%]	0
Δmax NMB-NADIR [%]	0
Δmean NMB-NADIR [%]	0
Δmin ST [s]	19
Δmax ST [s]	19
Δmean ST [s]	19
Δmin US [%]	0
Δmax US [%]	0
Δmean US [%]	0
Δmin PE [%]	0
Δmax PE [%]	20
Δmean PE [%]	18.61

Table 3.7: Induction phase: Differences between the PID and MPC performance indices for Atracurium administration

Regarding the control of Atracurium administration, Table 3.7 shows that there are no negative Δindex values, therefore the MPC performance is better or equal to the PID control performance. In particular, the ΔTT is positive, meaning that the set-point following task has been carried out quicker with the MPC controller, compared to the PID controller.
Concerning the hemodynamic system, CO and MAP remain within the safe intervals both in the PID and MPC simulations.

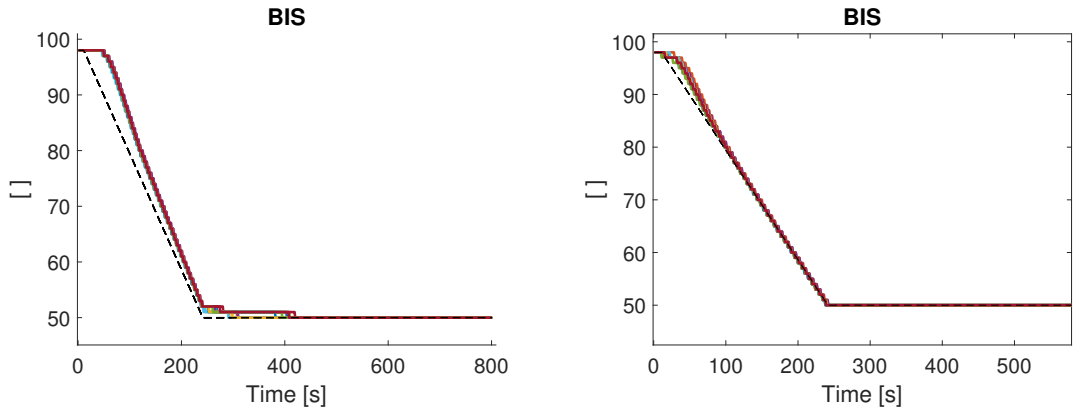

(a) *PID simulation - BIS*

(b) *MPC simulation - BIS*

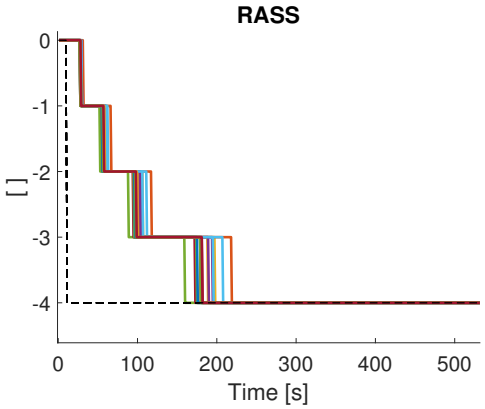

(c) *PID simulation - RASS*

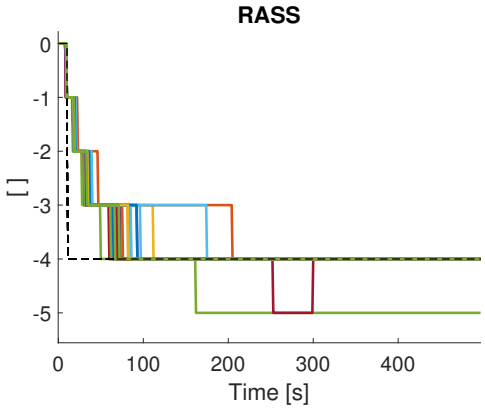

(d) *MPC simulation - RASS*

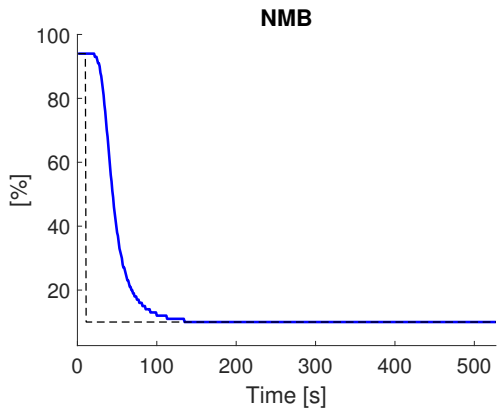

(e) *PID simulation - NMB*

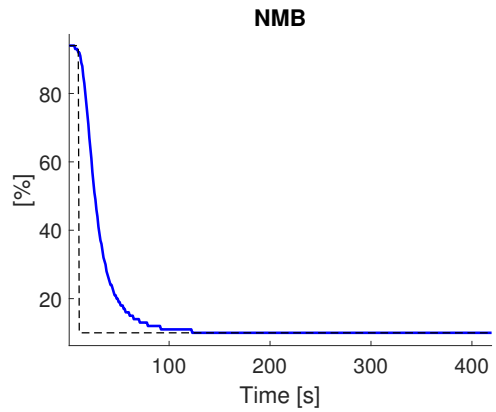

(f) *MPC simulation - NMB*

Figure 3.15: Comparison of the figures of the PID and MPC simulations - Anesthetic variables

In order to provide a better visualization of the comparison between the PID and the MPC simulations of the induction phase of anesthesia, Figure 3.15 shows the charts of the anesthetic variables of the PID simulation (left side of the figure) paired with the charts of the same variables, obtained from the MPC simulation (right side of the figure).

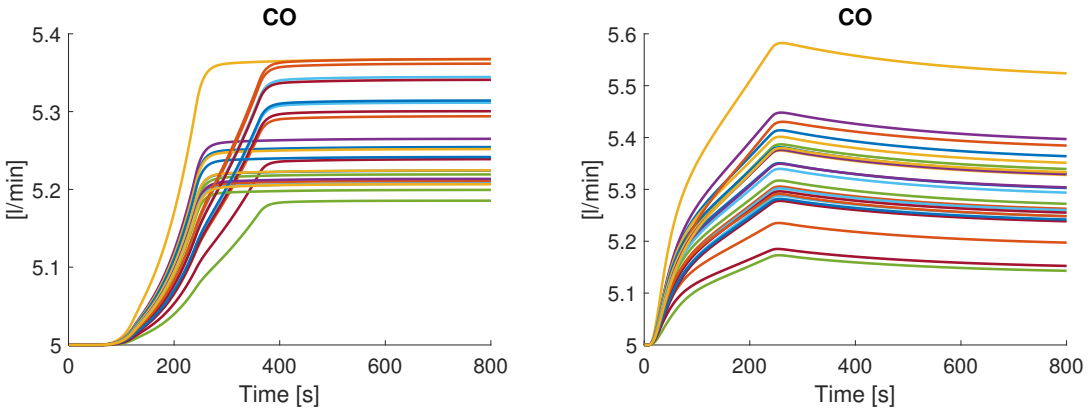

(a) *PID simulation - CO* (b) *MPC simulation - CO*

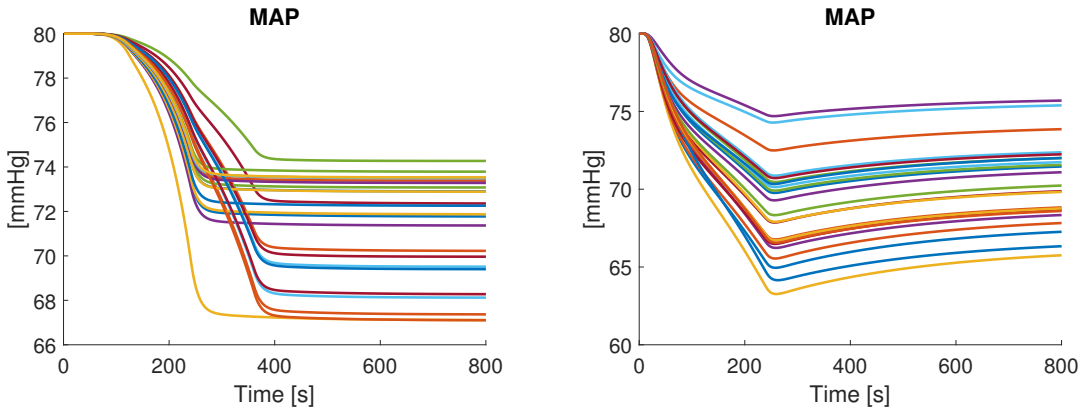

(c) *PID simulation - MAP* (d) *MPC simulation - MAP*

Figure 3.16: Comparison of the figures of the PID and MPC simulations - Hemodynamic variables

A paired visualization has been also attained for the hemodynamic variables: the left side of Figure 3.16 shows the charts of the hemodynamic outcomes of the PID simulation, while the right side presents the charts of the same variables, obtained from the MPC simulation.
To conclude the comparison, the pros and cons of both control strategies are reported.
Advantages of the PID control:

- Easy use and tuning;
- Good performance for simple problems;
- Low computational complexity.

Disadvantages of the PID control:

- It can not deal with multivariable cases;
- Not appropriate for complex systems.

Advantages of the MPC:

- Possibility to manage multivariables cases;

- Good performance even for complex systems;
- Possibility to include the constraints in the controller design;
- Useful if the reference is known in advance.

Disadvantages of the MPC:

- High computational complexity;
- It is necessary to know the model of the system; furthermore, if the model is nonlinear, it is recommended to linearize it, with possible loss of performance if the linear approximation is too rough.

Conclusion

In this thesis the complex task of automated control of anesthesia has been addressed. Different simulations have been ran in order to compare them and discuss their positive aspects and limitations. Initially, an open-loop simulation has been executed: the results obtained are not satisfactory, confirming the need to include a closed-loop approach in the anesthesia delivery. Regarding the closed-loop control of anesthetic drugs administration, two different methods have been tested: the proportional-integral-derivative (PID) control and the model predictive control (MPC). Compared to the open-loop simulation, both closed-loop strategies performed better, showing the ability to manage the interpatient variability in a more effective way. The MPC technique performed better with respect to the PID technique, on the basis of the indices taken into account in the performance assessment.

The PID control method has been extensively tested in this thesis, both for the induction and the maintenance phase of anesthesia, with the addiction of the action of the anesthesiologist. Moreover, for the PID simulation, a different set-up with the addiction of the interpatient variability on the PD model of the BIS and the modification of the sampling time of RASS and NMB has been tested, in order to perform a robustness test. Regarding the MPC technique, the simulation has been ran only for the induction phase, since in this case the addiction of an intergral action for the MPC should be introduced. In order to complete the comparison between the PID and the MPC strategies, the simulation for the maintenance phase of anesthesia could be performed in the MPC simulation, i.e. adding the disturbances (the surgical stimulation) and the anesthesiologist's action, with the addiction of the integral action. Future work could also include the introduction in the MPC simulation of the modifications made to the simulator for the PID control, such as the differentiation of the sampling times for the various anesthetic variables (BIS, RASS and NMB). In the MPC simulation, this could be carried out by appropriately modifying the variance of the Kalman filter, in particular for RASS and NMB.

The patient simulator would also benefit from the introduction of a new pain monitoring system and a PD model for analgesia, as a separate output variable to be controlled [16].

Bibliography

[1] A.R. Absalom and G.M. Kenny. "Closed-loop control of propofol anaesthesia using bispectral index: performance assessment in patients receiving computer controlled propofol and manually controlled remifentanil infusions for minor surgery". In: *Br J Anaesth* (2003).

[2] A. R. Aitkenhead and G. Smith. *Anestesia*. Universo, 1992.

[3] Karl Astrom and Tore Hagglund. *Advanced PID control*. Isa, 2006.

[4] Etrusca Brogi, Shantale Cyr, and Roy Kazan. "Clinical performance and safety of closed-loop systems: A systematic review and meta-analysis of randomized controlled trials". In: *J. Anaesthesiol. Clin. Pharmacol.* (2016).

[5] Eduardo Camacho and Carlos Bordons. *Model Predictive Control*. Springer, 2013.

[6] J Cohen and D Royston. "Remifentanil". In: *Curr. Opin. Crit. Care* (2001).

[7] Dana Copot. *Automated drug delivery in anesthesia*. Academic Press, 2020.

[8] Dana Copot and Clara Ionescu. "Drug delivery system for general anesthesia: where are we?" In: *Proceedings of the IEEE international conference on systems, man and cybernetics* (2014).

[9] Dana Copot, Clara Ionescu, and Robin De Keyser. "Anesthesiologist in the loop and predictive algorithm to maintain hypnosis while mimicking surgical disturbance". In: *IFAC World Congress* (2017).

[10] Hartmut Derendorf and Bernd Meibohm. "Modeling of Pharmacokinetic/Pharmacodynamic (PK/PD) relationships: concepts and perspectives". In: *Pharm Res* (1999).

[11] Guy Dumont and Mark Ansermino. "Closed-loop control of anesthesia: a primer for anesthesiologists". In: *Anesth Analg* (2013).

[12] Mihaela Ghita, Martine Neckebroek, and Cristina Muresan. "Closed-Loop control of anesthesia: survey on actual trends, challenges and perspectives". In: *IEEE Access* (2020).

[13] T.M. Hemmerling and N. Le. "Brief review: neuromuscular monitoring: an update for the clinician". In: *Canadian Journal of Anesthesia* (2007).

[14] Clara Ionescu. "Robust Predictive Control Strategy Applied for Propofol Dosing Using BIS as a Controlled Variable During Anesthesia". In: *IEEE Transactions on Biomedical Engineering* (2008).

[15] Clara Ionescu and Ioana Nascu. "Lessons learned from closed loops in engineering: towards a multivariable approach regulating depth of anaesthesia". In: *J Clin Monit Comput* (2014).

[16] Clara Ionescu et al. "An Open Source Patient Simulator for Design and Evaluation of Computer Based Multiple Drug Dosing Control for Anesthetic and Hemodynamic Variables". In: *IEEE Access* (2021).

[17] Clara Ionescu et al. "Nonlinear dynamics of the patient's response to drug effect during general anesthesia". In: *Commun Nonlinear Sci Numer Simulat* (2015).

[18] Ali Khaqan, Quadeer ul Hasan, and Shahzad M. Malik. "Comparison of two Nonlinear control strategies for hypnosis regulation". In: *Arab J Sci Eng* (2017).

[19] Alexandra Krieger and Efstratios Pistikopoulos. "Model predictive control of anesthesia under uncertainty". In: *Comput Chem Eng* (2014).

[20] Miroslav Krstic and Ioannis Kanellakopoulos. *Non linear and adaptive control design*. New Publisher, 2021.

[21] Wang Liuping. *Model predictive control system design and implementation using Matlab*. Springer, 2009.

[22] C.F. Minto, N. Morton, and G.N. Kenny. "Pharmacokinetics and pharmacodynamics of remifentanil". In: *Anesthesiology* (1997).

[23] Ioana Nascu et al. "Advanced Model-Based Control Studies for the Induction and Maintenance of Intravenous Anaesthesia". In: *Biomed Eng* (2015).

[24] M. Neckebroek, Clara Ionescu, and Robin De Keyser. "A comparison of propofol-to-BIS post-operative intensive care sedation by means of target controlled infusion, Bayesian-based and predictive control methods: an observational, open-label pilot study". In: *J Clin Monit Comput* (2019).

[25] Fabrizio Padula, Clara Ionescu, and N. Latronico. "Inversion-based propofol dosing for intravenous induction of hypnosis". In: *Commun Nonlinear Sci Numer Simulat* (2016).

[26] Fabrizio Padula et al. "Optimized PID control of depth of hypnosis in anesthesia". In: *Comput Methods Programs Biomed* (2017).

[27] L. Paz, M.M Da Silva, and S. Esteves. "Automated total intravenous anesthesia from induction to recovery". In: *IEEE International Symposium on Medical Measurements and Applications* (2014).

[28] Richard Pino. *Clinical Anesthesia Procedures of the Massachusetts General Hospital*. Lippincott Williams and Wilkins, 2010.

[29] Medical Advisory Secretariat. "Bispectral index monitor: an evidence-based analysis". In: *Ont. Health Technol. Assess. Ser.* (2004).

[30] Curtis Sessler and Mark Gosnell. "The Richmond Agitation–Sedation Scale. Validity and Reliability in Adult Intensive Care Unit Patients". In: *Am. J. Respir. Crit. Care Med.* (2001).